Inferring user multimodal trajectories from cellular network metadata in metropolitan areas

Fereshteh Asgari

▶ To cite this version:

HAL Id: tel-01355223
https://tel.archives-ouvertes.fr/tel-01355223

Submitted on 22 Aug 2016

Inférence des déplacements humains sur un réseau de transport multimodal par l'analyse des meta-données d'un réseau mobile

JOINT DOCTORATE OF

TELECOM SUDPARIS AND UNIVERSITY OF PIERRE & MARIE CURIE

Presented by:

Fereshteh ASGARI

For the degree of

DOCTORATE OF TELECOM SUDPARUS

Inferring User Multimodal Trajectories from Cellular Network Metadata in Metropolitan Areas

Thesis Defense Data: 30/03/2016

Mr. Ken CHEN	Université Paris 13	Reviewer
Mr. Marco FIORE	Politecnico of Torino, CNR	Reviewer
Mr. Miguel NUNEZ	Université du Pacifique	Examinator
Mr. Hossam AFIFI	Telecom SudParis	Examinateur
Mr. Nicolas GAUDE	Bouygues Telecom	Examinator
Ms. Monique BECKER	Telecom SudParis	Thesis Director
Mr. Mounim EL-YACOUBI	Telecom SudParis	Thesis Co-director
Mr. Vincent GAUTHIER	Telecom SudParis	Thesis Superviseor

Thesis number: 2016TELE0005

"The science of today is the technology of tomorrow."

Edward Teller

Abstract

Around half of the world's population are living in cities where different transportation networks are cooperating together to provide efficient transportation facilities for individuals. To improve the performance of the multimodal transportation network it is crucial to monitor and analysis the multimodal trajectories. However obtaining the multimodal mobility data is not a trivial task. GPS data with fine accuracy, is extremely expensive to collect; Additionally, GPS is not available in tunnels and underground. Recently, thanks to telecommunication advancement, cellular data used as Call Data Records (CDRs), is great resource of mobility data, nevertheless it is noisy and sparse in time; Subsequently it is not a proper resource for multimodal mobility data in metropolitan areas. The objective the present thesis is to propose a solution to this challenging issue of inferring real trajectory and transportation layer from wholly cellular observations. To achieve these objectives we use Cellular signalization data which is more frequent than CDRs and despite their spatial inaccuracy, they provide a fair source of multimodal trajectory data. We propose 'CT-Mapper' to map cellular signalization data collected from smart phones over the multimodal transportation network. The proposed algorithm uses Hidden Markov Model property and topological properties of different transportation layers to model an unsupervised mapping algorithm which maps sparse cellular trajectories on multilayer transportation network. Later on, we propose LCT-Mapper an algorithm to infer the main mode of trajectories. The area of study in this research work is Paris and its suburbs (Ile-de-France); we have modeled and built the multimodal transportation network database. To evaluate our proposed algorithms we use real trajectories data sets collected from a group of volunteers over a period of one month. Users' cellular signalization data was provided by a french operator to assess the performance of our proposed algorithms using GPS data as ground truth. An extensive set of evaluations has been performed to validate the proposed algorithms. To summarize, it is shown in this work that it is feasible to infer the multimodal trajectory of users in an unsupervised manner. Our achievement makes it possible to investigate the multimodal mobility behavior of people and explore and monitor the population flow over multilayer transportation

network.

Abstract

Dans cette thèse, nous avons étudier une méthode de classification et d'évaluation des modalités de transport utilisées par les porteurs de mobile durant leurs trajets quotidiens. Les informations de mobilité sont collectées par un opérateur au travers des logs du réseau téléphonique mobile qui fournissent des informations sur les stations de base qui ont été utilisées par un mobile durant son trajet. Les signaux (appels/SMS/3G/4G) émis par les téléphones sont une source dinformation pertinente pour l'analyse de la mobilité humaine, mais au-delà de ça, ces données représentent surtout un moyen de caractériser les habitudes et les comportements humains. Bien que l'analyse des metadata permette dacquérir des informations spatio-temporelles à une échelle sans précédent, ces données présentent aussi de nombreuses problématiques à traiter afin den extraire une information pertinente.

Notre objectif dans cette thèse est de proposer une solution au problème de déduire la trajectoire réelle sur des réseaux de transport à partir dobservations de position obtenues grâce à l'analyse de la signalisation sur les réseaux cellulaires. Nous proposons "CT-Mapper" pour projecter les données de signalisation cellulaires recueillies auprès de smartphone sur le réseau de transport multimodal. Notre algorithme utilise un modèle de Markov caché et les propriétés topologiques des différentes couches de transport. Ensuite, nous proposons "LCT-Mapper" un algorithme qui permet de déduire le mode de transport utilisé.

Pour évaluer nos algorithmes, nous avons reconstruit les réseaux de transport de Paris et de la région (Ile-de-France). Puis nous avons collecté un jeu de données de trajectoires réelles recueillies auprès dun groupe de volontaires pendant une période de 1 mois. Les données de signalisation cellulaire de l'utilisateur ont été fournies par un opérateur français pour évaluer les performances de nos algorithmes à l'aide de données GPS.

Pour conclure, nous avons montré dans ce travail qu'il est possible d'en déduire la trajectoire multimodale des utilisateurs d'une manière non supervisée. Notre réalisation

permet d'étudier le comportement de mobilité multimodale de personnes et d'explorer et de contrôler le flux de la population sur le réseau de transport multicouche.

Mots-clés : trajectoires multimodal - données de signalisation cellulaire - cartographie trajectoire- Trajectoire cellulaire - transport multicouche de mode Inférence.

Acknowledgements

I would like to thank my two supervisors: Vincent Gauthier and Mounim El Yacoubi whom without their help and guidance this thesis would have not been possible. Vincent helped me through this PhD work and updated me with new studies and works. I also thank him for providing me the possibility to experience a research visit during my PhD work. I thank Mounim for his help and constructive comments and guidance during this work. His clear detailed critics always helped me improve my work and look for solutions in the right place. He provided many suggestions to improve the readability of different versions of the present.

I would then like to thank Prof. Monique Becker for her scientific guidance and support, but also for her kindness. I thank her for the trust she had in me to do this research. I have learnt to improve my work from her and her feedback and patience have always helped all along this journey.

I wish to thank Prof. Marco Fiore, Prof. Ken Chen, Prof. Harvé Debar, Dr. Miguel Nunez and Mr. Nicolas Gaude for having served as my committee members.

My special thanks to Prof. Hakima Chauchi, EIT Digital Paris coordinator for her helps and supports for the research visit during my PhD study. I would like to thank Prof. Alex Arenas to host me in his lab, as well as Alberto Sole for his time and advise during our fruitful discussions and talks.

Then I wish to thank each and every one of my friends and colleagues who helped me with their participation in data collection.

Then I tend to thank my friends whom their friendship makes the world a better place for me. Some I have known for many years, some have entered my life more recently. Some are geographically far but always present and some others have become my Parisian family.

Last but not least, I am grateful to my family, whose continuous support has encouraged me to get this far and to be who I am here present. In the end, my sincere thanks to the one who stood by me along the last year of this roller coaster ride and who always embrased me with his love.

Fereshteh Asgari

Contents

List of Figures

List of Tables

Abbreviations

Abbreviation	Expanion
HMM	Hidden Markov Model
GSM	Global System for Mobile Communications
GPRS	General Packet Radio Service
GTP	GPRS Tunneling Protocol
PDP	Packet Data Protocol
IGN	Institut Geographique National
OSM	Open Street Map
CDR	Call Data Record
OD	Origin Destination
RMSE	Root Mean Square Error
EM	Expectation Maximization
KF	Kalman Filter
NRT	Near Real Time
JSON	JavaScript Object Notation
XML	Extensible Markup Language

To my parents.

Chapter 1

Introduction

Currently, more than half of the world population is living in cities and urban areas, in which different transportation systems are cooperating with each other to provide quick and efficient transportation facilities for the inhabitants. Evidently, developing such systems requires to have a clear comprehension of current underlying systems and mobility models. Understanding mobility behaviors of individuals enables us to build mobility models, to predict traffic flow and thus to improve urban transportation facilities for minimizing congestion in urban areas. However, individuals' mobility cannot be reliably investigated without considering an integrated transportation system containing different transportation modes. Considering a multimodal transportation network, however, increases the network complexity in different aspects. One of the major challenges is modeling and analyzing navigation on different transportation layers. People's daily trajectories often consist of a combination of sub-trajectories on different transportation modes. Thus, the objective of mobility study in multimodal transportation networks is not only finding the optimum path, but also understanding and modeling the way that different layers cooperate in generating optimum paths for mobility in urban areas.

Over the recent years, cell phones have become ubiquitous thanks to major advancements in telecommunication technology. Cellular phones have turned out to be a great resource of data to analyze mobility behavior of people in metropolitan areas, as they overcome the limitations of other resources that fail to collect mobility data in a large scale. GPS, for example, provides accurate spatial data, but has two main disadvantages: device battery usage and the limitation of data collection for a certain

group of people (e.g. drivers). The latter, in particular, makes the multimodal mobility study almost impossible. Cellular data on the other hand, appears to be a proper solution for the aforementioned drawbacks as it is inexpensive to collect for large scale population with no excess of energy consumption of device. The problem with cellular phones compared to GPS is that they provide only coarse-grained mobility data at antenna level, with a varying localization error of hundred meters in densely populated cities, and within several kilometers in rural areas. In order to investigate the mobility behavior of users in choosing a transportation mode among different alternatives or even a combination of modes, the first requirement is to infer the real trajectory of users from their cellular data. In this PhD thesis, we propose a solution to this problem by designing and developing an approach that exploits cellular data for multimodal mobility study. We propose an unsupervised mapping algorithm that maps a sparse cellular trajectory[1] over a multimodal transportation network to :

I) Infer the most likely path an individual has taken given his/her cellular data.

II) Detect the transportation mode associated to the same cellular trajectory.

The results enable us, first, to analyze the multimodal mobility behavior of people in transportation network usage and to model them. Secondly, the results help to detect mode changing hubs in the multimodal transportation network and to improve mode changing facilities (e.g. escalator, car and bike parking, etc.) in case of demand. In addition, if the proposed mapping algorithm be adapted to process mobility data of large scale population in near real time, it can be used for traffic monitoring, anomaly detection and congestion prediction.

For our mobility analysis, a platform to collect and filter streaming cellular data is required. The area of current study is Paris and vicinity (Ile-de-France). The public transport network in Paris Region is now one of the densest in the world. Different transportation networks (subway, train, tramway, bus, bike) cooperate to ensure the traffic. To these public transportation systems, we could add personal cars and taxis in the city which transport hundreds of thousands of individuals per day. In order to improve the collaboration of different transportation systems, the current situation, existing challenges and demands need to be clearly understood. Studying real trajectories of people is one of the best strategies to obtain this perception. In addition to investigate real traffic in the urban area, it also helps to detect anomalies and deficiencies such as congestion.

---

[1]In the rest of this study, the term "cellular trajectory" and "sparse cellular trajectory" will be used interchangeably.

1.1 Motivations and Challenges

Urban mobility analysis is known as one of the main challenges that cities encounter. With the growth of urban areas and metropolitan cities, the demands for efficient monitoring of the mobility of individuals keep increasing. As different transportation systems are involved in metropolitan areas, researchers are motivated to work with a transportation network which not only considers one single layer but rather examines the whole transportation system and the relationships between the layers. In order to investigate the multimodal mobility of individuals, it is extremely important to employ realistic data which is another challenge in mobility studies. Thanks to the ubiquity of mobile phones everywhere, recently network operators have been providing large scale datasets of mobility data in form of Call Data Records (CDRs) which are automatically generated for billing purpose. CDRs, despite being an invaluable resource to extract insights about human mobility, are temporally sparse. Therefore, CDRs cannot be treated as proper data for multimodal transportation studies in cities and metropolitan areas.

A broad study of related literature, recent challenges and motivations in multimodal mobility studies bring us to the conclusion that there is a gap between current ongoing studies and a comprehensive approach to study multimodal mobility using cellular data in urban and metropolitan areas. In this PhD work, we propose an approach to infer multimodal trajectories of smartphone users from their sparse cellular data.

1.2 Thesis Contributions

The main contributions of this work are:

- We propose to study the problem of mapping cellular trajectories to the *multimodal* transportation network, in order to infer the real mobility of the users. To the best of our knowledge, this is the first attempt addressing the multimodal mapping issue. This novelty is subject to the following:
  - The objective is multimodal transportation network rather than single layer.
  - Our proposed algorithm is developed to process cellular signalization data consisting of sparse cellular mobility trajectories (frequency of 15 minutes). Consequently it has the potential to be performed on a large population as the data collection system is inexpensive and secure.

- In our proposed approach, rather than mapping cellular trajectories using supervised mapping algorithms with labeled mobility data, we use an unsupervised mapping algorithm leveraging the topological properties of the transportation network, thus eliminating the tedious human labeling efforts in building the mobility model.

- We modeled and built the multimodal transportation network database using open data collected from different references of geospatial resources. The area of coverage is Paris and vicinity (Ile-de-France) and it contains different transportation layers (road, train, subway, tramway). This database enables us to study multimodal paths through the network. Building a multilayer network was mandatory to study multimodal mobility in metropolitan areas, rather than an uni-modal mobility on a single transportation layer as considered by traditional approaches.

- We propose an unsupervised trajectory mapping algorithm, namely *CT-Mapper*, which maps cellular location data over the multimodal transportation network. The mapping algorithm is modeled by an HMM where the observations correspond to user cellular trajectories and the hidden states are associated with nodes of the multilayer graph. Transition probability and emission score were modeled based on topological properties of the transportation network and the spatial distribution of antenna base stations. The Viterbi decoding algorithm efficiently computes the best match which might enable us to deploy our unsupervised mapping algorithm on large scale mobility data sets in order to estimate multimodal traffic in metropolitan areas.

- We collect real cellular trajectories of a group of users in Paris metropolitan area with the help of a French telecom operator. For the sake of comprehensive evaluation we collect GPS trajectories of corresponding cellular trajectories in parallel. This is then used to evaluate our mapping algorithm. Through the extensive evaluation with cellular trajectories covering more than 2500 intersection nodes and 3 physical layers, 1000 metro and subway stations, we show that our algorithm maps the cellular trajectory onto the multimodal transportation network of Paris metropolitan area with good accuracy given the sparsity of user cellular trajectories. *CT-Mapper* also achieves up to 20% higher accuracy compared to a baseline approach, that exploits, for an unsupervised HMM parameter estimation, the topology of the multilayer network, without considering the transportation properties of network edges.
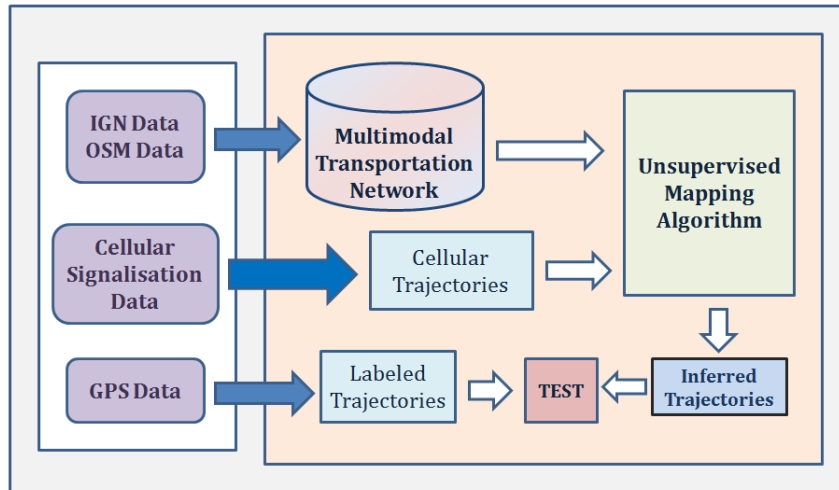
FIGURE 1.1: An overview of the framework of the solution proposed in this thesis, three data types used in this study are located in the white box; they will be served as the input of the system. Geospatial data were used to build the Database. Cellular data and GPS data are used to test and validate the mapping algorithm.

- We propose *LCT-Mapper* which not only maps the cellular trajectories over the multimodal transportation network, but also infer the transportation mode with an accuracy of 85%. In this approach, the multimodal transportation network is represented as a two class-layer network namely *Road* and *Rail* class-layers. The cellular sparse trajectories are mapped over both class-layers and a classifier in *LCT-Mapper* is designed to choose the best match between two likely paths.

1.3 Thesis Organization

Following this introductory chapter, chapter 2 presents state of the art on the related works and studies. The purpose of this chapter is to bring together all the theoretical background and the studies related to the challenges discussed in the previous section. Chapter 2 proposes the state of the art in different aspects of human mobility studies, mobility data and mapping algorithms. The reason of this choice, is to provide an overview of existing findings with a clear comprehension of actual challenges (such as micro studies using cellular data). This chapter also provides the required content for the main contribution of this dissertation by bringing together materials from different fields of studies: (namely: mobility studies, mapping algorithm to complex network). The second chapter ends with a discussion on the detected gaps and claims that in the literature, there is no mapping algorithm dealing with both multimodal
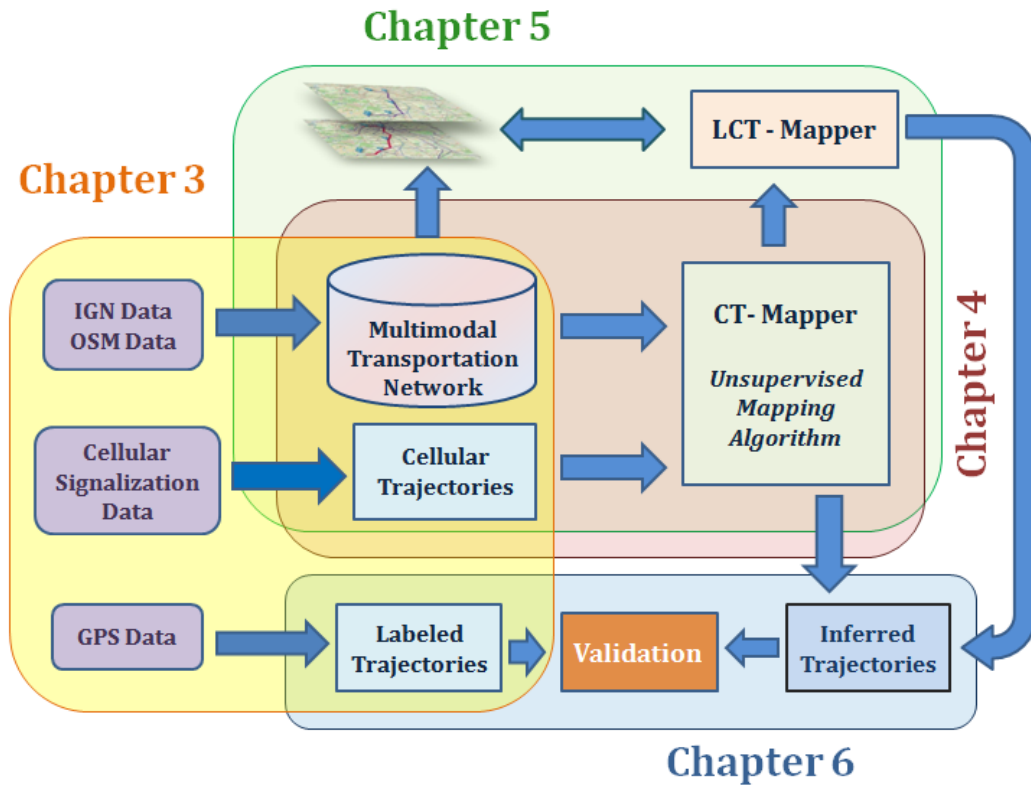
FIGURE 1.2: The overall framework of the research illustrated as chapters organization

transportation network (in fine grain resolution) and also with the scalability of using mobility data (to be scalable for a large number of population) in urban and metropolitan areas.

Three types of data are used in this study. These types, illustrated in a white box in the left side of the framework presented in Fig. 1.1, are geo-spatial data to build multimodal transportation network dataset, sparse cellular trajectory data, and GPS trajectory data. Chapter 3 elaborates on modeling and building the multimodal transportation network dataset containing road, train and metro lines. This chapter also covers a technical description of data extraction and database building. Next, cellular trajectory extraction via cellular signalization data and then GPS trajectory extraction are described.

In chapter 4, we present *CT-Mapper*, our proposed unsupervised inference algorithm developed to map sparse cellular data of smart phone users over the multimodal transportation network. This chapter outlines how we use the HMM framework to model and build the mapping algorithm based on the Viterbi decoding algorithm to

find the most likely path of users on multimodal transportation network given their sparse cellular trajectories only.

Inferring the mobility modes of individuals in daily commutes is a fundamental question in human mobility studies that from one side leads to defining mobility models and from another side provides valuable information for traffic monitoring and congestion prediction. In Chapter 5, we address this issue by proposing *LCT-Mapper*, an ameliorated mapping algorithm that aims to map the cellular trajectories over multimodal transportation network, while detecting the transportation mode of the user. The mode inference is conducted by a classifier that, after comparing two most likely paths of the user on the two class-layers, namely rail and road, selects the correct class-layer based on a set of factors.

Chapter 6 is dedicated to the evaluation and validation of the proposed mapping algorithms. Since this work is the first attempt to map cellular mobility data over a multimodal transportation network in a metropolitan area, it was also required to derive a baseline model for the sake of evaluation. In this chapter, we describe a baseline algorithm and provide a set of metrics for evaluation purposes such as recall, precision and similarity scores. We use cellular data of real trajectories and their corresponding GPS trajectories as ground truth. These two datasets, described in chapter 3, were collected from 10 volunteer users during one month (Aug-Sept 2014). We validate *CT-Mapper* by performing mapping experiments using the sparse cellular trajectory data set and compute the accuracy of the results using GPS data set as ground truth. Conducting the same experiments using baseline algorithm, we show that *CT-Mapper* achieves up to 20% better accuracy compared to the baseline model. *LCT-Mapper* is validated by the aforementioned metrics and surprisingly we observe that along with a fair inference of the main mode of a trajectory it can provide, it also shows better results on performance metrics compared to *CT-Mapper*.

In chapter 7, we recapitulate the main discussions of the thesis and provide a summary of contributions. The chapter points out the limitations as well as the opportunities that our research creates for further works.

Chapter 2

State Of The Art

2.1 Introduction

In this chapter an overview of various concepts related to this PhD work is presented and literature on related work is reviewed. As described in chapter 1 and illustrated in figure 1.1, the overview of this PhD contribution is related to different lines of study and accordingly the state of the art is separated into distinct sections. First of all, studies related to general Human Mobility (Section 2.2) are reviewed. Then we present related works in the fields of network science for traffic analysis, mobility studies and more important complex network studies (section 2.3.2). Next, Section 2.4 (Mobility Data) presents an outline of different data types used in mobility studies. Trajectory Mapping studies (Section 2.5) summarize previous works on mapping algorithms with related concepts that are necessary to describe in this dissertation.

It is important to notice that there are some parts that might not be directly related to the contribution of this thesis. However they are needful for obtaining an overall comprehension about the scope of the study, the gaps and main concerns, and accordingly for perceiving the problematic and limitations of human mobility studies that motivate the contributions of this thesis.
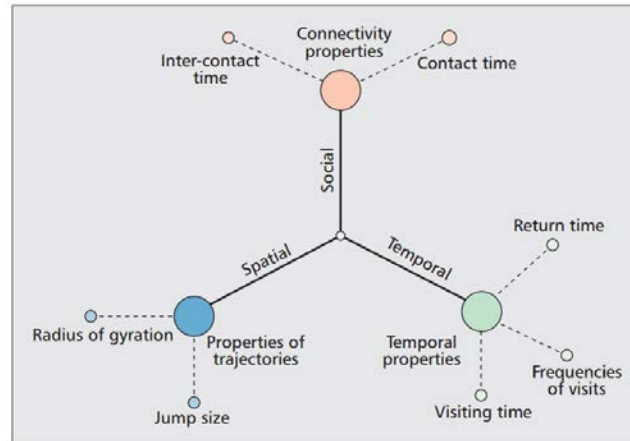
FIGURE 2.1: Human mobility properties [12] [27]

2.2 General Human Mobility Models

Investigating the flows of individuals from one point to the other in cities or within the country provides insights for modeling Human Mobility behaviors and characteristics which are exploited from different aspects. The main significance is that Human Mobility is related to the fundamental problem in traffic systems: Analyzing huge amount of mobility data, one purpose is to study and model traffic flow in road networks and public transportation networks. Another example is urban planning, where knowing how people come and go can help determine where to deploy infrastructure and how to reduce traffic congestion. Consequently, predicting the flow in these networks and possibly predicting the future position of moving objects (either individuals or vehicles) is another purpose of human mobility studies. Furthermore, evaluating the impact of human travel on the environment depends on knowing how large populations move in their daily lives. Similarly, understanding the spread of a disease hinges on a clear picture of the ways that humans themselves move and interact [13]. In addition, statistics about individual movements are interesting for commercial applications such as geomarketing. For instance, finding the hot spot to place the advertisements depends on the number of people going through different locations and thus implies to know the flows. Recommendation systems relying on region of interest [87] of population is another example [11][35]. Nevertheless, the history of Human Mobility studies goes far prior to these recent topics and applications.

As Basol discusses in [12], the value of mobility reaches far beyond mere geographical movement of humans, and provides a complete new mindset on human interactions

which could be considered from spatial, temporal, and contextual aspects. Different dimensions of Human mobility also have been explored by Kakihara and Sorensen in [49]. They describe that the importance of "being mobile" is not just a matter of people traveling but is also related to the interaction they perform – the way in which they interact with each other in their social lives. Considering this observation, they have expanded the concept of mobility by looking at three distinct dimensions; namely, spatial, temporal and contextual mobility. Subsequently, they elaborated on the issues of *virtual community* or *cyber community* [49] which today is known as social network. Karamshuk et al [27] have developed the idea of different aspects of Human Mobility introduced in [12] and presented the properties of Human Mobility in three main different dimensions: ***spatial, temporal and social*** aspects that have been illustrated in figure 2.1. Each of these aspects also has been studied at different scales. The following sections summarize studies related to each of these main aspects. It is worth noting that these aspects cannot be totally separated in the studies and the aim is only to highlight the important issues from each dimension's point of view.

2.2.1 Spatial Dimension

A considerable amount of Human Mobility studies are trajectory-based studies in which individuals trajectories are traced and their behavior is analyzed. These studies are trying to answer the following questions: How far do people travel every day? [16] What are the main measures in Human Mobility studies? How these measures represent mobility behaviors of individuals? Does human mobility follows any model or pattern? [16], [36], [59]. Is it possible to estimate the trajectory due to home-to-work commutes? Do the trajectories' patterns depend on the geographical position of individuals? [32] How different metropolitan areas exhibit distinct mobility patterns due to differences in geographic distributions of homes and jobs, transportation infrastructures, and other factors? [46] Is it possible to predict the next position of individuals having previous records of their trajectories? [16] [80] [79] [45]

The main focus of these approaches is spatial characteristics (measures) of movements and how they change in Human Mobility. At the large scale, when the behavior is modeled over a relatively long duration, human mobility can be described by three major components:

1. Trip distance or jump length distribution which is presented as $P(\Delta r)$. Brockman et al [15], analyzed a huge data set of records of bank notes circulation,

interpreting them as a proxy of human movements [27]. They showed that travel distances Δr of individuals follow a power-law distribution as:

$$P(\Delta r) \sim (\Delta r)^{(1+\beta)} \tag{2.1}$$

where $\beta < 2$. This fits the intuition that people usually move over short distances, whereas occasionally they take rather long trips. The distribution known as Levy Flight, was previously observed as an approximation of migration trajectories among different animal species. Studying data tracing mobile phone users, Gonzalez et al [16] complemented the previous finding with an exponential cutoff:

$$P(\Delta r) = (\Delta r + \Delta r_0)^{-\beta} \exp(\frac{\Delta r}{k}) \tag{2.2}$$

(with $\beta = 1.75 \pm 0.15$, $\Delta r_0 = 1.5$ km, and k a cutoff value varying in different experiments) and showed that individual truncated Levy trajectories coexist with population-based heterogeneity.

Gonzalez et al in [16] and Brockmann et al [15] showed a truncated power-law tendency in the distribution of jump length.

2. Radius of gyration of trajectories, a key quantity in human mobility trajectories, [84] is the root mean square distance of the trajectory's parts from its center of mass. If trajectory t is represented as $\overrightarrow{r_1^{(t)}}, ... \overrightarrow{r_i^{(t)}}, ... \overrightarrow{r_n^{(t)}}$ positions recorded for a trajectory, $\overrightarrow{r_{cm}^{(t)}} = \frac{1}{n} \sum_{i=1}^{n(t)} \overrightarrow{r_i^{(t)}}$ is the center of the mass of the trajectory. Then the gyration radius

$$\overrightarrow{r_g}(t) = \sqrt{\frac{1}{n(t)} \sum_{i=1}^{n(t)} (\overrightarrow{r_i^{(t)}} - \overrightarrow{r_{cm}^{(t)}})^2} \tag{2.3}$$

reflects the linear size occupied by each user's trajectory. Several studies have tried to model individuals trajectories around their radius of gyration. It was shown [16] that the distribution of the radius of gyration can be approximated by a truncated power-law:

$$P(r_g) = (r_g + r_g^0)^{\beta_r} \exp(r_g/k) \tag{2.4}$$

where $\beta r = 1.65 \pm 0.15$, $r_g^0 = 5.8$ km and $k = 350$ km. In other words, most people usually travel in close vicinity to their home location, while a few frequently make long journeys. Gonzalez et al [16] suggested using gyration radius as a characteristic travel distance for each individual.

Additionally, investigating statistical characteristics and patterns of human movements [36] [16] showed that the individual travel patterns collapse into a single spatial probability distribution, indicating that, despite the diversity of their travel history, humans follow simple reproducible patterns. Xiao et al in [84] simplified the human mobility model with three sequential activities (commuting to workplace, going to do leisure activities and returning home), and proved that the daily moving area of individuals is an ellipse, and they get an exact solution of the gyration radius. However, they used some basic assumptions which makes the model not usable for all types of trajectories (it's not strong enough). Besides trying to find spatial patterns in human mobility [34] [21], researches could find motifs in spatial network [11].

Some studies have tried to answer if there are different mobility behaviors among different groups of users [32], [6] , [86]. In China, [32] women and children were generally found to travel shorter distances than men. In another study, Xiao et al in [86] have studied the trajectories of individuals in different categories (student/working group/not working group). Although the power law property of jump length distribution was observed in their study, they concluded that individual traveling process in general cannot be characterized by the Levy-flight or truncated Levy-flight.

From the spatial point of view, human mobility has been studied in global , continent scale [10], country scale [10] [21] , regional scale [32] , city scale [45] [34] and much finer scales such as campus or building scale [40] [88]. As a result, human mobility occurs on a variety of length scales, ranging from short distances to long-range travel by air, and involves diverse methods of transportation (public transportation, roads, highways, trains, and air transportation). No comprehensive study that incorporates traffic on all spatial scales exists [67]. This would require the collection and compilation of data for various transportation networks into a multi-component data set; a difficult task particularly on an international scale [67] (e.g. [10]). Finding the proper scale for Mobility studies has been discussed in some studies [20],[21], [48]. The authors in [20] have discussed about the scale of spatial network in human mobility studies. They have investigated if there is an optimal spatial resolution for the analysis of Human Mobility. They built a multiresolution grid and mapped the trajectories with several complex networks, by connecting the different areas of region of interest. Then they analyzed the structural properties of these networks and derived a process to identify the optimal scale (cell size) for real world problems.

As another property of human mobility, gravity models have been investigated in some studies [10], [32], [36]. They assume the number of individuals T_{ij} that move between

location i and j per time unit is proportional to some power of the population of the source (m_i) and destination (n_j) location, and decays with the distance r_{ij} between them as:

$$T_{ij} = \frac{m_i^\alpha n_j^\beta}{f(r_{ij})} \qquad (2.5)$$

where α and β are adjustable exponents and $f(r_{ij})$ is a distance-dependent functional form. Gravity laws usually consider power or exponential laws for the behavior of $f(r_{ij})$. Occasionally T_{ij} is interpreted as the probability rate of individuals traveling from i to j, or an effective coupling between the two locations.

2.2.2 Temporal Dimension

Among Human Mobility studies, a considerable number of them have tried to investigate the periodic patterns of human mobility [21], [48] with extracting daily and weekly periodic patterns recognized in mobility data. Like the spatial dimension, the temporal dimension has been investigated in different temporal scales of human mobility. These scales can be defined as time intervals: from long-term such as monthly intervals to short-term such as hourly or even finer time intervals. The length of time interval in dynamic analysis should be chosen such that enough events are collected for any measures to be meaningful [52]. In other words, the time interval should be small enough to give meaningful results for our purpose. The importance of choosing proper time interval is a concern in both data collecting and analysis aspects. Regarding the temporal aspects in Human Mobility studies, there are certain questions that researches have tried to answer. One is to detect *frequently visited locations*. It was shown [16] that human trajectories indicate a high degree of temporal and spatial regularity, each individual being characterized by a time independent characteristic travel distance and a significant probability to return to a few highly frequented locations. Csaji et al in [21] showed that movement and location-related features are correlated with many other features. They have clustered users' most frequently visited locations to home and office and estimated the position of frequent locations based on a probabilistic inference framework.

Bagrow et al in [60] show that individual mobility is dominated by small groups of frequently visited, dynamically close locations, forming primary "habitats" capturing typical daily activity, along with subsidiary habitats representing additional travel.

Another purpose of focus on temporal aspects is to study the dynamics of Human Mobility and how it changes over time. Studies have tried to extract patterns to define mobility models based on them [11] [33]. These patterns could be found either by illustrating and analyzing daily mobility patterns [18] [21] or by analyzing hourly movement distribution [34], etc.

2.2.3   Social Dimension

The social aspect of Human Mobility is related to human interactions (e.g. cell phone conversations, text messages, e-mails etc.) that leave electronic traces and thus allow tracking. This tracking of human interactions helps to understand the temporal patterns of individual human interactions which is essential to managing information spreading and to tracking social contagion. Jiang et al in [47] have studied the temporal patterns of individual human interactions based on their calling data and the dynamics of calling patterns among cell phone users. They have investigated the communication patterns of cell phone users and after classifying them in different clusters, they have studied different properties of each cluster of users. In another study, Becker et al [6] have applied a clustering algorithm to CDR to investigate the groups of users where members of each group share the same patterns of cell phone communication, in particular patterns of calling and texting intensity over time. In their results, each group had a specific calling signature, which may be indicative of certain population types such as workers, commuters, and students.

A considerable amount of these approaches focus on studying dynamic network of Human Mobility. This dynamic network could be the inter-contact network of people who are moving to different places (the basic idea of *Opportunistic Networks* whose goal is to enable communication in disconnected environments [27]). The link in these networks illustrates a kind of relation between individuals. This relation could be defined as the period of time during which two individuals are in mutual specified range of distance or could be social contact among individuals (e.g.phone call) [40], [43]. For example in [40], the structural properties of contacts are presented by a weighted contact graph, where the weights express how frequently and how long a pair's nodes are in contact. In these types of networks, the relation between social contact and mobility patterns plays an important role in human mobility studies. These networks reflect the complex structure in people's movements: meeting strangers by chance, colleagues, friends and family by intention or familiar strangers because of similarity in their mobility patterns. The studies in these areas have tried to represent the

complex resulting patterns of who meets whom, how often and for how long, in a compact and tractable way. This allows quantifying structural properties beyond pairwise statistics such as inter-contact and contact time distributions. It is also important mentioning that these networks are defined based on interaction between individuals and consequently they are not interesting for studying individual trajectories. They are good to study social behaviors or group activity. Among researches which have investigated periodic behaviors from mobility data, Clause et al in [18] studied the temporal connectivity patterns using a small data set collected from a group of individuals. In order to investigate the periodicity of proximity (inter-contact) network, they have studied the adjacency of nodes in different time slots and measured the similarity between each two consecutive snapshots of network. They have also shown that the empirical distribution of proximity (inter-contact) time in their data set follows a heavy-tailed distribution. Their spectral analysis has shown a strong daily periodic behavior.

It was observed that the geographic distance plays an important role in the creation of new social connections: node degree and spatial distance can be combined in a gravitational attachment process that reproduces real traces. It was also observed that links arising because of triadic closure, where users form new ties with friends of existing friends, and because of common focus, where connections arise among users visiting the same place, appear to be mainly driven by social factors. The authors in [8] have described a new model of network growth that combines spatial and social factors and reproduces the social and spatial properties observed in their traces.

2.3   Spatial Networks in Human Mobility

Mobility studies have recently become popular in network science. The advantage of modeling the system as a graph is that we can infer the behavior of the dynamical system without studying the actual dynamics [39]. Such a modeling allows also estimating how much one part of the network influences another and how well the network is optimized with respect to the dynamical system. In Human Mobility studies, various networks have been defined (e.g. transportation network, road network, contact network, inter-contact network etc.) as dynamic or static depending on their behavior. A graph is a mathematical object consisting of a set of vertices and a set of edges defining the pairs of vertices that are interacting with each other [39]. Within

the scope of graph theory, mathematical measures such as centrality, connectedness, path length, diameter, degree and clique are playing key roles in network studies [57]. Among these measures, 'Centrality' has been significantly investigated in mobility studies. The following section serves as a brief outline of the centrality concept and of the state of the art related to it.

Using graph theory, there are several approaches that consider a particular class of networks which are embedded in the real space, i.e. networks whose nodes occupy a precise position. They are used to investigate the population flow, population density, etc. Base stations in cellular networks are instance of nodes for such networks. In the same way, voronoi diagram cells associated with the geographical positions or railway stations are some other occasions.

2.3.1 Centrality Measures

In addition to Human Mobility studies, the Centrality measure plays an important role in traffic flow studies. The centrality of a node determines the relative importance of a node within the graph. It can summarize the ability of each node to broadcast and receive information. The centrality measure is one of the mostly used parameters in network studies and thus, different types of centrality measures have been defined. According to [26], there is no centrality index that fits all applications and the same network may be meaningfully analyzed with different centrality indices depending on the question to be answered. The authors in [26] have reviewed different centrality measures, such as degree centrality, family of betweenness centrality indices, closeness centrality indices, feedback centrality. Prior to explaining the related studies, we describe below three classic centrality measures. Having graph $G = (V, E)$ with V as the set of $|V|$ nodes and E as the set of $|E|$ edges, A is the adjacency matrix and $a_{ij} = a_{ji}$ represents the link between node v_i and node v_j,

1. **Degree Centrality**- Degree centrality of a node is defined as the number of outgoing links from this node. The idea is that a node with more edges is considered as more important :

$$C_{Degree}(v_i) = \sum_{j=1}^{|V|} a_{ij} \qquad (2.6)$$

2. **Closeness Centrality**- measures the importance of a node by its geodesic distance to other nodes. The idea is that the closer a node is to other nodes,

the more important the node is. Closeness can be regarded as a measure of how long it will take information to spread from a given vertex to others in the network . Closeness centrality focuses on the extensivity of influence over the entire network.

$$C_{Closeness}(v_i) = \frac{1}{\sum_{j=1}^{|V|} d(v_i, v_j)} \quad (2.7)$$

where $d(v_i, v_j)$ is a geodesic distance between v_i and v_j.

3. **Betweenness Centrality**- Is equal to the number of shortest paths from all vertices to all others that pass through that node. A node with high betweenness centrality has a large influence on the transfer of items through the network, under the assumption that item transfer follows the shortest paths.

$$C_{Betweenees}(v_i) = \sum_{j \neq k \neq i} \frac{g_{jk}(v_i)}{g_{jk}} \quad (2.8)$$

where g_{jk} is the number of shortest paths between two nodes v_j and v_k, and $g_{jk}(v_i)$ is the number of shortest paths between the v_j and v_k that contain node v_i.

An important use of centrality measures is related to traffic flow in networks. The relation between congestion and centrality in traffic flow was studied by Petter Holme in [38]. His work investigates the relation between centrality assessed from the static network structure measured in simulations of some simple traffic flow models. He studied how the speed of the traffic flow is affected by the network structure (by tuning model parameters) and textcolorredfound that the relationship between the betweenness centrality and congestion in simple particle hopping models for traffic flow. Altshuler et al. in [9] studied the relationship between the centrality of a node and its expected traffic flow in a real transportation network. They used a dataset that covers the Israeli transportation network and showed the correlation between the traffic flow of nodes and their Betweenness centrality. They also showed that when some additional known properties of the links (specifically, time to travel through links) are taken into account, this correlation can be significantly increased which could be used to generate highly accurate approximations of the traffic flow in the network. Recent works in urban studies have shown significant differences between

cities in terms of metrics such as commute distances. The network centrality of metro systems in different countries has been studied applying the notion of betweenness centrality to 28 worldwide metro systems [25]. The share of betweenness was found to decrease with size following a power law distribution (with exponent 1 for the average node), but the share of nodes with high centrality measure decreases more slowly than that of nodes with low centrality measure. The betweenness of individual stations as nodes can be useful to locate stations where passengers can be redistributed to relieve pressure from overcrowded stations. *Edge Centrality* is another metric that has been used to study flow through the network [19].

Temporal centrality: Centrality measure plays an important role in dynamic networks as well as static networks. Recently, many studies have generalized this measure for dynamic networks ,[37], [53], [78], [76], [77]. The *average temporal path length* has been proposed in [76] and the characters of this temporal measure have been investigated and the new measure *temporal reachability* has been proposed based on average temporal path length in [77]. The concept of temporal closeness centrality is introduced in [52] as a generalization of closeness centrality.

In [53], the authors have defined a novel Centrality metric for dynamic networks and then have compared the results of dynamic and static Centrality measures for the paper citation network. In [78], the authors have presented a temporal centrality metric for the identification of key nodes in On-line Social Networks based on temporal shortest paths. They have discussed two *temporal betweenness centrality* and *temporal closeness centrality* in their study. Grindrod et al in [37], proposed a new centrality measure which can be computed at any point in time, with the main concern in different time-dependent scenarios where the population of nodes remains fixed.

2.3.2 Multimodal Transportation Networks and Complex Networks

As reported by the UN, currently 54% of the world's population lives in urban areas and is expected to increase to 66% by 2050. Similarly, the number of *megacities* (urban areas whose human population is larger than 10 million) has tripled since 1990 [61]. In the era where different transportation systems are cooperating together to ensure people transportation in metropolitan areas, a deep understanding of this cooperation is required for a successful urban planning. It is fundamental, therefore, to take into account different transportation layers rather than one single layer in mobility studies [71] in order to take into account all the transportation modes available

for a given urban area. By considering Multimodal transportation networks, novel insights about people mobility behaviors and mobility models over these networks can be revealed. Multimodal transportation network modeling has been studied in civil and transportation engineering literature [56],[54], but the analysis of the topological properties of networks is barely addressed and the different transportation modes are often treated separately [71]. Recently, multimodal transportation networks have attracted interest and attentions as complex networks and some studies [29] have modeled and investigated multiplex networks.

This section presents an outline of research in which multilayer networks (named multiplex) have been defined and modeled and their complexity analyzed. Although there are studies at the country scale [64], we mainly present the cases where multilayer transportation networks in urban and metropolitan areas have been considered.

In the transportation engineering field, Liu [54] has proposed an approach of modeling the multimodal network data with the objective of performing optimal path queries on it.

2.4 Mobility Data

One of the fundamental elements in Human Mobility studies is the data used for the investigations. Therefore data collection techniques that indicate the characteristics and features of data have become a principal issue in mobility studies. Generally, the spatial and temporal granularity (resolution) of the Mobility Data draw the overall picture of the possible probes that can bee carried out and are crucial for determining the scale of the study both from the spatial and temporal aspects. This section provides an outline of different mobility data reported in the state of the art on human mobility studies. The focus is on the properties and main characteristics of different data types rather than the techniques of data collecting. Specifically data collection cost, data accuracy and possible scale are considered in this overview.

Human mobility researchers have traditionally relied on expensive data collection methods, such as surveys and direct observation, to get a glimpse on the way people are moving. This high cost typically results in infrequent data collection or small sample sizes. For example, a national census produces a wealth of information on where millions of people live and work, but it is carried out only once every ten years [13]. Brockmann et al. [15] used the data of bank notes to study human traveling behavior. Later on, many other studies used GPS (Global Positioning System) to track

individuals or any moving objects [36] [16]. GPS provides accurate measurements of both position and speed in outdoor locations (fine granularity of the location data), but signal quality is reduced or completely lost in indoor environments. Moreover, phone users tend to keep GPS turned off when not in use to avoid battery drain. When the GPS signal is available, however, it tends to be a very good candidate for differentiating between dwelling and mobility [55]. Continuous scanning for WiFi APs has been used in context-aware computing to detect user mobility. This method is attractive because it can be performed on-line and in real-time, both desirable qualities for this class of applications [55].

In recent years, the emergence of information and communication technologies (ICTs), and substantial investments in wireless infrastructures have led to extensive use of Call Data Records (CDR) in human mobility studies. Each CDR contains the time a phone placed a voice call or received a text message, and the identity of the cellular antenna the phone was associated with at that time. When joined with information about the locations and directions of those antennas, CDRs can serve as infrequent samples of the approximate locations of the phone's owner. CDRs are an attractive source of location information for three main reasons: I) They are collected for all active cellular phones, which can generate millions of records. II) They are already being collected by operators, so that additional uses incur little marginal cost. III) They are continuously collected as each voice call and text message are completed, thus enabling timely analysis. In addition, CDRs may also be coupled to external data of customers such as age or gender which makes mobile phone CDRs an extremely rich and informative source of data for scientists. Blondel et al. in [14] have provided a survey on results obtained from extensive analysis on mobile phone datasets in different fields of studies from personal mobility and urban planning to security and privacy issues.

On the other hand, CDRs have two significant limitations: I) They are sparse in time because they are generated only when there is a phone call or text message for exchange. II) They are coarse in space because they record location only at the granularity of a cellular antenna (with average error of 175 meter [79] in dense areas up to couple of kilometers in rural areas). It is not obvious a priori whether CDRs provide enough information to characterize human mobility in any useful way [13]. As a solution, since CDRs rely on the calling frequency of individuals, high voice-call activity users are often chosen for conducting meaningful studies [21], which introduces a bias. This bias was investigated in [62] and the results revealed that although the voice-call process does well to sample significant locations, such as home and work, it may in

some cases incur biases in capturing the overall characteristics of individual human mobility [66]. The temporal sparsity problem of CDRs is solved by modifying the data collection sampling rate and tracking the users in fixed time intervals. Smoreda et al in [69] describe two different data collection methods from a cellular phone network: *active* and *passive* localization. Active localization provides a tool for recording positioning data on a survey sample over a long period of time. Passive localization, on the other hand, is based on phone network data which are automatically recorded for technical or billing purposes (CDRs).

Nowadays, thanks to technology advancements, a considerable proportion of people have smartphones. These phones are usually connected to the internet and for each of these connections, there is a signalization flow on the operator network. This flow carries the identifier of the antenna on which the mobile is connected. Being able to process this flow provides another precious source of mobility data. Since the **Cellular Signalization Data** can be collected with any preferred frequency, this data, compared to CDRs, does not suffer from temporal sparsity and hence is perfectly suitable to collect from a large group of users for traffic analysis and traffic monitoring purposes.

A set of techniques for data collection are used to capture GPRS Tunneling Protocol (GTP) messages from the Cellular Data Network. Packet inspection of GTP-C (GTP control plane) enables capturing users' localization information at a higher frequency than the usual CDR. The GTP is the tunneling protocol used to carry data traffic over the mobile network (from 2G to LTE) to internet. When a smartphone enables its internet connection (e.g. when it is turned on), a message is sent over the network asking for access. This message contains, among others, information the identity of the phone and the cell id covering the user. Once the session is established, update messages are sent carrying information like the bearer or the cell *id*. These messages are triggered when the user moves from a BTS to another or by resource allocation. Finally, when the mobile looses the signal or when it is turned off, a message closing the session is sent. With modern smartphone applications that emit and receive data on a regular basis (i.e. email, push notification), it is expected that the GTP tunnel for a given user remains constantly maintained, enabling us to sample the user position at each network event (handover and radio resource allocation) [72].

Table 2.1 presents a comparative summary of different data collection methods and features of each type. As shown in the table, cellular data collected from mobile phones have huge potential for extracting implicit knowledge of large population mobility behavior specifically in urban cities and metropolitan areas.

2.5 Mapping Algorithms

Trajectory mapping has been used for different purposes, such as routing applications, navigation systems, public transportation tracking and traffic monitoring. In human mobility studies, trajectories have been mostly defined as Origin-Destination (OD) and they are mapped over a desirable graph to produce an optimum path solution which is usually the shortest path between the Origin and Destination [33, 34, 36, 87]. The optimum path between two geospatial points is not necessarily the real path taken by the user. On the other hand, traffic monitoring applications, navigation and recommendation systems have been widely using GPS data to map individuals (as drivers) traces over road networks [22, 41, 44, 45, 58, 79, 80, 85]. As GPS provides precise localization data (with $\sim 5m$ error), these studies have sought to infer the real path over a road network given the noisy GPS observations, using different statistical approaches. Algorithms such as Expectation Maximization (EM) algorithms [45], Kalman Filter algorithm [41, 85] have been considered for the mapping objective and a considerable amount of studies have used Hidden Markov Models (HMM) in order to map imprecise data on the road network [22, 44, 58, 79, 80]. The main convenience of using a Hidden Markov Model is that it is robust to noise and sparseness. The following section presents an outline of Hidden Markov Model, a fundamental concept used in our work.

2.5.1 Hidden Markov Models & Viterbi Algorithm

A Hidden Markov Model is defined by five elements: *state space, set of possible observations, transition probabilities, emission probabilities and initial state distribution.* The Markov process which is hidden is determined by the current state and the *transition probability* matrix. We are only able to observe the noisy observations which are related to the (hidden) states of the markov process through the *emission probability*. Let us define the state space to have N hidden states labeled by i ($1 \leq i \leq N$). In a generic HMM, three main probability distributions are considered to define the model $\theta = (P_{ij}, e_i(O_t), P_i)$:

Methods	Advantages	Disadvantages
Survey & direct observations [80]	- Multi purposed use	- Expensive to collect data - Not accurate (usable as OD)
Wi-Fi localization [55] [80]	- Accuracy (∼40m error) - Energy usage ∼ 50% GPS	- Low coverage area - Providing access point is expensive
GPS localization [69], [55] [79]	- Highly precise (∼5m error) - Can distinguish bettween - transportation modes	- High battery (energy) usage - Expensive - No (low quality) signal in indoor and underground
Smart Cards [42] [75] [73] [74]	- Inexpensive collection	- Origin-Destination
Cellular network localization (passive) (Call Data Records)[13][79]	- Automatically generated	- Sparse in time - Needs filtering - Inaccuracy (∼ 175m error)
Cellular network localization (active) [69]	- More frequent than CDRs - Less costly than previous methods	- More costly than passive form - Arise the issue of large database
Cellular Signalization Data	- Inexpensive data collection - More frequent than CDRs	- Inaccuracy compared to GPS - Limited to smartphone users

TABLE 2.1: Comparative summary of different data collection techniques

- $P_{ij} = p(q_{t+1} = i | q_t = j)$ specifies the *'Markov property'* that is, given the value of q_t, the current state q_{t+1} is independent of all the states prior to t. This property is modeled by Transition probability.

- $e_i(a) = p(O_t | q_t = i)$ The emission probability specifies the relation between observations and hidden states. The larger the emission probability is given a state, the more likely this state is a match for the observed point.

- $P_i = p(q_1 = i)$ specifies initial conditions.

The earlier works of mapping algorithms using HMM have mostly used GPS localization data [22, 41, 45, 58, 79, 85] as observations to map the vehicle or user's GPS locations over road networks. The state space in these studies was usually the road transportation network, modeled either as a graph of nodes and edges (the nodes representing intersections and the edges representing road segments between the nodes) or a set of road segments in a digital representation of the area. The common approach for mapping algorithms is to use a set of labeled data to infer the parameters of the probabilistic models. In all of these studies, highly sampled GPS locations provide low noise observations. Gaussian functions [22, 58, 80] have been used to model conditional probability distribution for emission probability. Once the model is built, given sequences of observations, the supervised model performs the mapping by inferring the sequence of transportation network nodes (or road segments) with the maximum likelihood of generating the observation sequence.

This mapping is done by the 'Viterbi decoding algorithm'. In more details, assume the transportation network as a graph in which each rail station/ road intersection is a graph node. Let us define hidden states as graph nodes and noisy location data as sequence of observations (these observations do not belong to the graph node set). The Viterbi algorithm finds dynamically the most likely sequence of nodes that generate the observation sequence given the HMM model. The Viterbi algorithm definition is presented in the following section.

2.5.1.1 Viterbi Decoding Algorithm

Assume a Hidden Markov Model presented as $\theta = (P_{ij}, e_i(a), P_i)$ and defined to have N hidden Markov states labeled by $i(1 \leq i \leq N)$, and M possible observable for each states, labeled by $a(1 \leq a \leq M)$. The state transition probabilities are $P_{ij} = p(q_{t+1} = j | q_t = i), 1 \leq i, j \leq N$ (where q_t is the hidden state at time t), the

emission probability of observation at time t, O_t given state i is $e_i(O_t) = p(O_t|q_t = i)$, and the initial state probabilities are $P_i = p(q_1 = i)$.

Given a sequence of observations $O = O_1 O_2 ... O_T$, and an HMM $\theta = (P_{ij}, e_i(O_t), P_i)$, Viterbi algorithm finds the maximum probability state path $Q = q_1 q_2 ... q_T$ with a dynamic programming approach.

Let $v_i(t)$ be the probability of the most probable path ending in state i at time t, and generating the partial observation sequence $O = O_1 O_2 ... O_t$,

$$v_i(t) = \max_{q_1, q_2, ..., q_{t-1}} P(q_1 q_2 ... q_{t-1}, q_t = i, O_1 O_2 ... O_t | \theta) \tag{2.9}$$

and let w_i be the initial probabilities of the states i at time $t = 1$.

Then $v_j(t)$ can be calculated recursively using:

$$v_j(t) = e_j(O_t) \times \max_{1 \leq i \leq N} [v_i(t-1) \times P_{ij}] \tag{2.10}$$

together with initialization

$$v_i(1) = P_i \tag{2.11}$$

and termination

$$P^* = \max_{1 \leq i \leq N} [v_i(T)] \tag{2.12}$$

At the end we choose the highest probability endpoint, and then we backtrack from there to find the highest probability path.

Note that the maximally likely path is not the only possible optimal criterion, for example choosing the most likely state at any given time requires a different algorithm and can give a slightly different result. But the overall most likely path provided by the Viterbi algorithm provides an optimal state sequence for many purposes.

Fig. 2.2 illustrates how the Viterbi path is dynamically inferred.

The fundamental feature of mapping algorithms that have used HMM in previous researches is that the underlying network is usually the road network. Other transportation layers such as subway and train networks were not considered in such mapping algorithms. This is due to a couple of reasons: I) Collecting mobility data is
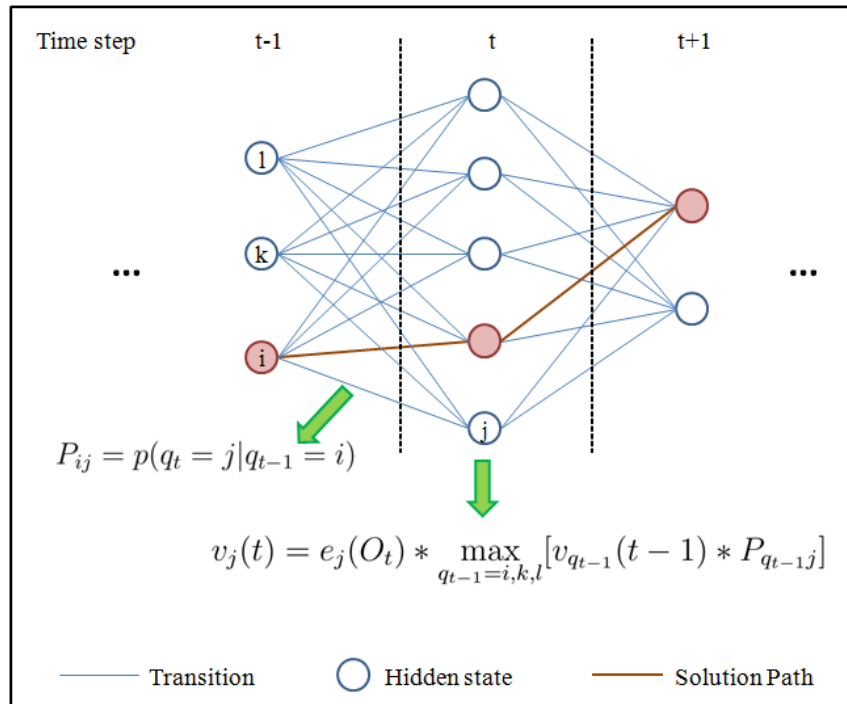
FIGURE 2.2: viterbi example

a highly demanding procedure specially if it is not limited to car drivers. II) Modeling and mapping individuals' movements over a transportation network containing different layers (called multimodal mobility) is much more complicated than modeling movements on a single layer road network. Thanks to the dramatic growth of smartphones, and use of cellular network data as mobility data, recent studies take advantage of this new type of mobility data to reduce the high energy consumption of GPS data collection techniques [80]. It is important to notice that replacing GPS data by cellular data for applications such as navigation systems is not feasible due to the highly spatial and temporal inaccuracy of cellular data.

2.6 Conclusion

In this chapter, an overview on literature of related works was presented. In the first part, basic concerns of Human Mobility studies and existing findings were presented. We described fundamental aspects of human mobility and summarized related studies and their scope. Network science has been deeply involved in mobility studies. We presented an overview of some researches who have taken advantage of network science in their investigations. We have provided details about the temporal and spatial

Related Studies	scale		Transportation Layer				Used Model				Data type		
	Regional	City	Road	Metro	Train	Air	EM	HMM	KF	CDRs	GPS	GSM	WiFi
Hu et al. 2003[41]		✓	✓					✓			✓		
Hummel 2006[44]		✓	✓					✓			✓		
Newson et al.2009[58]		✓	✓					✓			✓		
Thiagarajan et al.2009[80]		✓	✓					✓			✓		✓
Xu et al. 2010[85]		✓	✓						✓		✓		
Hunter et al. 2011[45]		✓	✓				✓				✓		
Thiagarajan et al.2011[79]		✓	✓					✓			✓		
Doyle et al.2011 [30]		✓	✓		✓								
C.Y.Goh et al.2012 [22]		✓	✓					✓		✓	✓		
Smoreda et al.2013[69]	✓	✓	✓		✓	✓						✓	

TABLE 2.2: Summary Table of Mapping Algorithms mentioned in the literature. The parameters for the comparison are scale of the study, transportation layers, used probabilistic model (EM: Expectation Maximization / HMM: Hidden Markov Model/ KF: Kalman Filter), and different data types. As table shows, trajectory mapping in the cities have considered only road transportation layer and have used mostly GPS data.

Related Studies	Scale			Study Baseline			Metrics			Data type		
	Country scale	Regional scale	City scale	Trace-based studies	Dynamic proximity networks	Flow on network	Centrality measure	Jump length distribution	Radius of gyration	GPS	GSM data	Wifi
Balcan et al.[10]	√											
Becker et al.[13]			√									
Yang et al. [84]				√				√	√			
Gonzalez et al.[16]		√						√	√		√	
Clauset et al. [18]					√							
Cs.Csajia et al. [21]	√			√					√		√	
Carske et al. [32]		√		√								
Giannotti et al.[34]			√	√						√		
Gonzalez et al.[36]		√		√								
P. Holme [38]						√	√					
Hunter et al.[45]			√	√		√	√			√		
Jiang et al.[47]					√							
Smoreda et al.[69]	√			√							√	
Thiagarajan et al. [79]			√	√							√	
Thiagarajan et al. [80]			√	√								√
Wang et al.[83]			√									

TABLE 2.3: Summary table

issues of human mobility, opportunistic networks and centrality measures studied in related fields.

To get a clear insight on specific features of mobility data, the second section was dedicated to describe different types of mobility data in related studies. It was mentioned that mobility data plays the important role of setting spatial and temporal constraints and scale for ongoing studies. We have seen that GPS data, despite its fine spatial accuracy, suffers from high energy usage and thus is not practical for large scale data collection due to the experiment cost. On the other hand, CDRs, in spite of their great scalability to a large number of people and to large spatial scales, lack the temporal granularity as they are sparse in time. We emphasized the importance of mobility data in providing good enough granularity and scalability both spatially and temporally. The third part of this chapter presents an outline of existing approaches

for trajectory mapping with an introduction to HMMs that forms the base of our mapping algorithm. It was mentioned that using HMM in mapping noisy locations of an individual trajectory over a transportation network was solely performed for GPS data. A novelty of this work is dealing with the challenge of utilizing network signalization data despite of their spatial inaccuracy for mapping over transportation networks in urban and metropolitan areas in order to obtain an inference of individuals real trajectory.

Chapter 3

Transportation Network Database and Mobility Datasets

3.1 Introduction

After a literature review on the main aspects of human mobility and providing a perception of the scope of the study and its challenges, this chapter provides an outline of the network database and real trajectory datasets collected to model the multimodal aspect of mobility in urban and metropolitan areas, which is the main focus of this thesis. To do this, using different resources of open data, the multimodal transportation network of Paris and its Region has been modeled and created, and the resulting database has been employed in this work.

In addition, to conduct experiments, we have asked a group of volunteers with the help of a french telecom operator, and we have collected their cellular trajectories along with the associated detailed GPS trajectories.

Succinctly, three types of data are used in this study:

1. In order to construct the multimodal transportation network database that contains all transportation modes (road/train/subway/tramway), geo-spatial data have been collected from different open data sources.After collecting open data from different sources, several data processing and transformation techniques have been conducted to build the multimodal transportation network database.
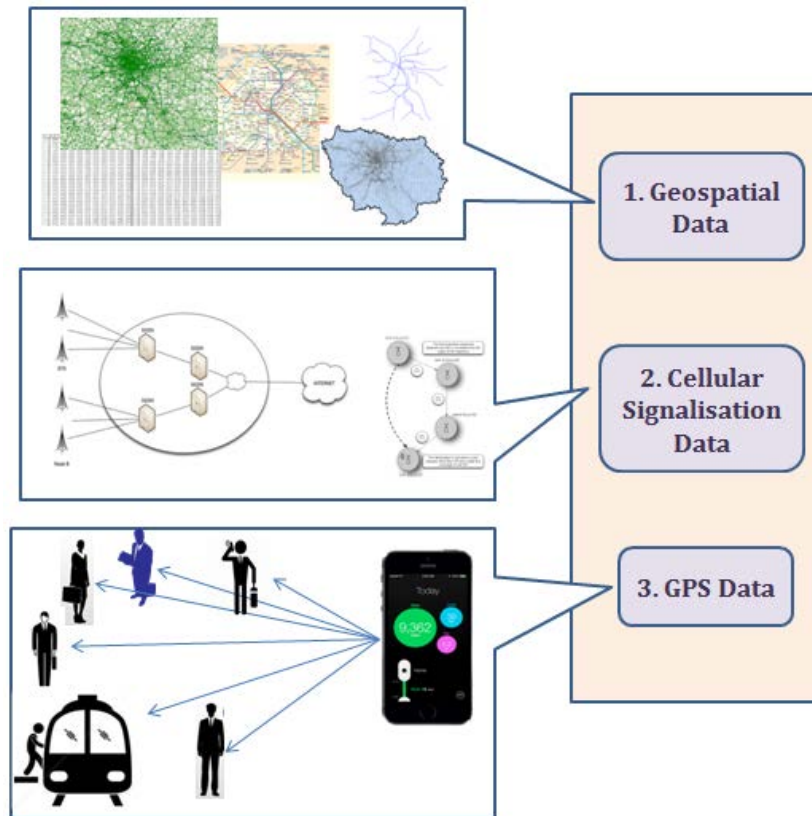
FIGURE 3.1: Three different data types that have been used in this PhD research and their resources. 1.Geospatial data: open data from different sources (IGN/OS-M/RATP) collected to model and build the database. 2.Cellular signalization data 3.GPS data collected from participants cellphones using 'Moves' application.

2. With the help of a french telecom operator, we have collected cellular signalization data of a group of smartphone users. We recruited these users for one month data collection experiment. The extracted real cellular trajectories were used for testing the mapping algorithm.

3. For the sake of validation of the proposed algorithm , GPS data are used as ground truth to assess the efficiency of the proposed mapping algorithm. The GPS data were collected in a parallel data collection experiment for the same group of users mentioned in the previous paragraph.

The variety of data resources that have been used to build the database and mobility datasets are illustrated in figure 3.1 to clarify the distinctions. The following sections describe the systematic procedures of data extraction, collection and processing to obtain these datasets.
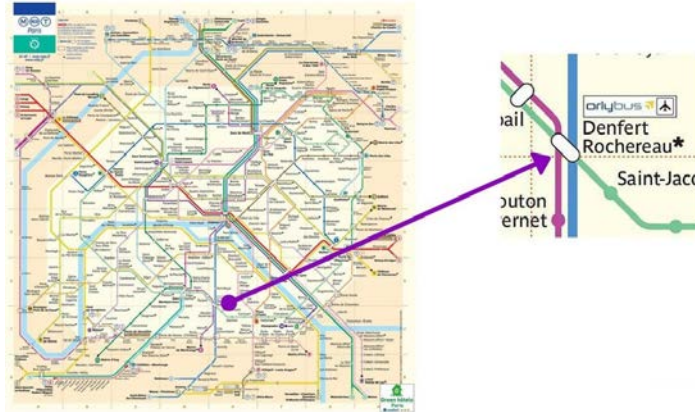
FIGURE 3.2: In station 'Denfert Rochereau' two metro lines and a train line meet

3.2   Multimodal Transportation Graph Databas

Currently, around 51% of the world population are living in cities and this percentage is expected to reach 70% by 2050[1], accordingly urban mobility is one of the main challenges in urban and metropolitan areas. Nowadays in cities and metropolitan areas a variety of transportation modes cooperate in order to perform the population mobility. Transportation modes such as subway, train, bike and bus are all cooperating with each other to ensure efficient traffic in the cities and help individuals to find a better and easier path to move from each origin to the preferred destinations. Studies on smart cities have been trying to improve and optimize this cooperation by detecting hubs and important locations as improving urban and transportation system regarding the demand.

The word *multimodal* refers to having or involving several modes, modalities, or maxima [2] or having multiple or many modes or instances [3]. *Multimodal transport* is the articulation between different modes of transport, in order to transfer more rapidly and effectively operations of materials and goods [4].

In the Human Mobility context, *multimodal* means having access to multiple modes in daily commutes. In this dissertation, we use the term *'multimodal trajectories'* to describe trajectories that were generated through different transportation modes (e.g. a trajectory that consists of a bus ride to a metro station and then a metro trip to reach the destination). The concept of multimodal trajectories is familiar in people's daily life: Fig. 3.2 represents the rail public transportation map of Paris region

---

[1] http://www.adlittle.com/downloads/tx_adlreports/ADL_Future_of_urban_mobility.pdf
[2] http://www.merriam-webster.com/dictionary/multimodal
[3] http://dictionary.reference.com/browse/multimodal
[4] http://www.slideshare.net/maxgalarza/multimodal-transport-3miridomemichellepedro
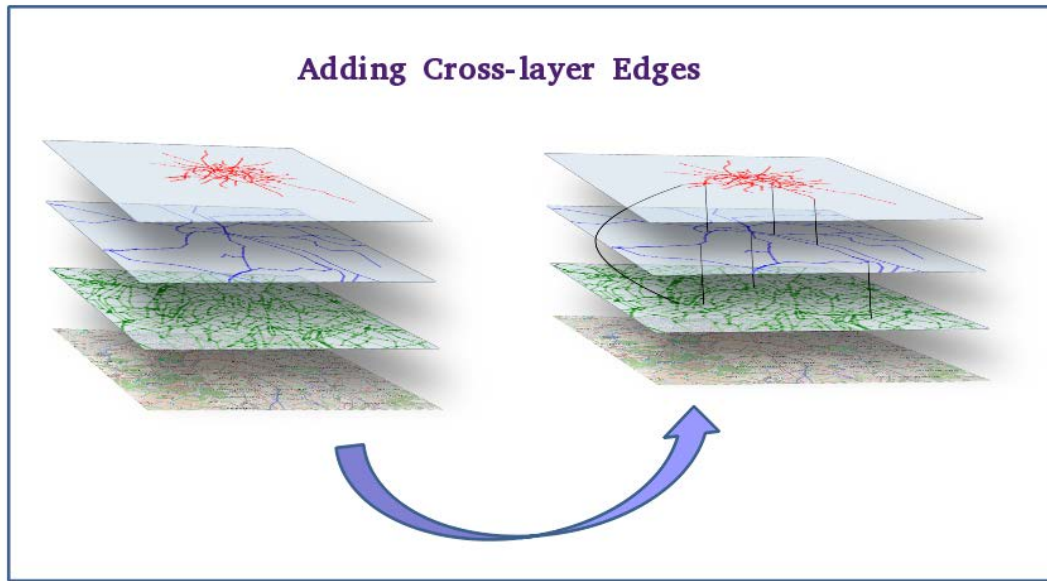
FIGURE 3.3: The Multilayer transportation network is obtained by defining cross-layer links between different transportation layers

(Ile-de-France) that is available in all subway and train stations of the Ile-de-France (Paris and its outskirts). Station 'Denfert Rochereau' is an instance station where two metro lines and one train line meet and people can change transportation modes between subway and train and contrariwise.

Nevertheless, to meet the objective of this research work, we are required to have a systematically designed multilayer transportation network in which different transportation layers are considered and subsequently, *'mode changing'* between different layers during a trajectory is feasible. We have modeled and built this network thanks to an extensive data collection and data processing procedure. In the next sections, we first present formal definitions of the multilayer transportation network and we then describe data collection and database modeling and building.

3.2.1 Multimodal Transportation Graph Representation

Before addressing the technical aspects of multimodal transportation network construction, this part describes the formal representation of the multimodal transportation network as a multilayer graph. The primary hypothesis is that each transportation layer is defined as a distinct layer. A proper description of the action of moving from one layer to another is the key challenge in multimodal transportation network

modeling and consequently in multimodal routing problems [54]. The multimodal transportation network is represented according to the following definition:

Definition 1. **Multilayer Transportation Graph**

The Multilayer Transportation Graph is characterized as $\mathbf{G} = (V, E, L, \Psi)$ in which set V represents the vertices of the graph, and Set E is the set of edges. Different possible layers are distinguished by set L; in our study, we have: $L = \{$road, train, subway$\}$. *Function* Ψ is embedded in graph definition and indicates the layer of each node $\Psi : V \to L$ in $\mathbf{G}$.

Definition 2. **Transportation Layer**

The Transportation Layer is denoted as $G^l = (V^l, E^l)$, where each G^l is a subset of $\mathbf{G}$. V^l is the node set of layer l and is represented as $V^l = \{v | v \in V, \Psi(v) = l\}$. Likewise, E^l is the edge set of layer l, where each edge connects two nodes both belonging to layer l : $E^l = \{< v_i, v_j > \in E, \Psi(v_i) = \Psi(v_j) = l\}$.
Each node v_i is characterized by its latitude and longitude (i.e., the geographical position $v_i = < lat, lon >_i$).

Definition 3. **Cross-Layer Edge**

The Multilayer Transportation Graph also contains Cross-Layer edges; set $E^{cl} \subset E$ includes the edges with pair of nodes not belonging to the same layer: $E^{cl} = \{< v_i, v_j > \in \mathbf{G} | \Psi(v_i) \neq \Psi(v_j)\}$. In other words, cross-layer edges enable the possibility of defining a path whose nodes can belong to different transportation layers.

The multilayer Transportation graph is represented by its *adjacency matrix* $W_{ij} \in \mathbb{R}^{|V| \times |V|}$. Fig. 3.3 illustrates how cross-layer links are added to different transportation layers to build a multimodal transportation network.
In the next section the procedure of data extraction for network construction is explained.

3.2.2   Data Extraction for Network Construction

To build the multilayer transportation graph $\mathbf{G}$, multiple geospatial datasets, namely the road network from the National Geographic Institute (IGN)[1] and the rail transport network (train and metro) from OpenStreetMap (OSM)[3] were aggregated. Each

node in **G** is either a road intersection, a rail station or a metro station. A key feature of the proposed multimodal transportation network is its modeling of transitions between different transport modes during a given trip. The intuition of building such a network was taken from [54] in which switching points were considered as the points where people could change their transportation modes. Cross-layer transition modeling is ensured by adding *Cross-Layer* appropriate edges between layers. In general, two main resources have been used to extract data for database creation:

Road Network - IGN, National Geographic information Institute[5] , has built a road graph data set which is called 'ROUTE 500'. ROUTE 500® is the road database describing 500 000 km of the classified road network (motorways, national, departmental) in France. The database format is 'Shapefile'. The nodes and edges were defined in two different tables. To construct the road network, we perform natural join operator between two tables. The join operator, combines two tables in a relational database to make the relations between connected nodes of the graph. In addition, a geographic pruning was executed to obtain the desire graph of Ile-de-France.

Edge File Features	Node File Features
- Edge ID (ID-RTE500)	- Node ID (ID-RTE500)
- Origin ID (ID-RTE500)	- Coordinates (lambert93)
- Destination ID (ID-RTE500)	- Type of intersection (simple
- Length (unite kilometer)	crossroad/traffic circle/...)
- Administrative class (highway/	
national/departmental/unknown)	
- Voaction (highway/local link/ ...)	
- Number of lanes (1/2/3/4...)	

TABLE 3.1: Data features for raw graph network extracted from IGN

Rail Network - The data for constructing the rail network was extracted from OSM (OpenStreetMap). OSM's conceptual data model is composed of three main elements: 'Nodes', 'Ways', 'Relations'. A node entity defines a specific point and is represented by its latitude and longitude and *id* number. In order to extract data, a set of parsing operations was performed on an XML file format.

---

[5]Institute National de L'Information Géographique

Edge Entity Features	Node Entity Features
- Edge ID (OSM-id) - Origin ID (OSM-id) - Destination ID (OSM-id) - Network type (subway, train, tramway, RER)	- Node ID (OSM-id) - Coordinates (WGS84)

TABLE 3.2: Data features for rail network extracted from OSM

3.2.3   Multimodal Transportation Network Database

3.2.3.1   Data Model

The conventional data model to represent transportation networks is a graph data model. In this work, we use a graph data model to define the transportation network as the set of nodes and edges that were formally presented in section 3.2.1.

3.2.3.2   Database Model

After defining the data model, the next step is to define a database model which specifies the logical structure of a database and fundamentally determines in which manner data can be stored, organized, and manipulated. It is important to notice that in our work, the *data model* is a 'graph model', but the *database model* is a 'document model'. In this work, we use **MongoDB** a document database system to implement the transportation network database. Every data element in MongoDB is stored in a JSON-style object called a document. An advantage of MongoDB is its flexible data structure: everything is stored as a document, which allows us to add or remove properties. A graph containing nodes and edges can fit properly in this structure. In addition, **MongoDB** offers a number of indexes and query mechanisms to handle geospatial information by supporting GeoJSON object types. GeoJSON is an open-source specification for the JSON-formatting of shapes in a coordinate space. It is a format for encoding a variety of geographic data structures. A location data point can be stored as GeoJSON object with this coordinate-axis order: longitude, latitude. The coordinate reference system for GeoJSON uses the WGS84 datum. Each GeoJSON document (or subdocument) is generally composed of two fields:

1. **Type** the shape being represented, which informs a GeoJSON reader how to interpret the "coordinates" field.

```
{
  "_id": {
      "$oid": "5453b63455474a33623186df"
  },
  "geometry": {
      "type": "Point",
      "coordinates":
          [ 2.07051454,48.866231]
  },

  "type": "Feature",

  "properties": {
      "database_ref": "IGN",
      "layer": "road",
      "type": "node",
      "database_id": "44588"
  }
}
```

```
{
  "_id": {
      "$oid": "54b954ba55474a0e08bd3f30"
  },
  "geometry": {
    "type": "LineString",
    "coordinates":
        [ [ 2.3146743, 48.8627572 ],
          [2.3146743, 48.8627572 ] ]
  },

  "properties": {
    "mongo_org_id": "5453b63455474a33623182d0",
    "layer": "crosslayer",
    "type": "edge",
    "mongo_dest_id": "5453b63455474a336231843e",
    "degreeDual": 29
  }
}
```

FIGURE 3.4: Left: A graph node stored as a 'Point' geometry object; right: a graph edge stored as a 'LineString' geometry object in the document database

2. **Coordinates** an array of points, the specific arrangement of which is determined by "type" field.

A geometry is a GeoJSON object where the type member's value is one of the following strings: "Point", "MultiPoint", "LineString", "MultiLineString", "Polygon", "MultiPolygon", or "GeometryCollection". Accordingly, all these objects are supported by MongoDB. A GeoJSON geometry object of any type other than "GeometryCollection" must have a member with the name "coordinates". The value of the coordinates member is always an array. The structure for the elements in this array is determined by the type of geometry. Consequently the simplest geometry can be represented as:

```
{
"type": "Point",
"coordinates": [long, lat]
 }
```

To implement the graph data model using GeoJSON format, each node is represented as a "Point" object type and each edge as "LineString". A set of common keys to store the properties of nodes and edges have been characterized. Fig. 3.4 presents two documents that describe node and edge of the graph. Subsequently, the *CrossLayer* edges are defined to make connections between each two nodes belonging to different transportation layers that are close enough to each other. We used a radius of 500 meters as the threshold of the closeness definition. In another similar work [71], for

(A) Road

(B) Train

(C) Subway

(D) Multilayer
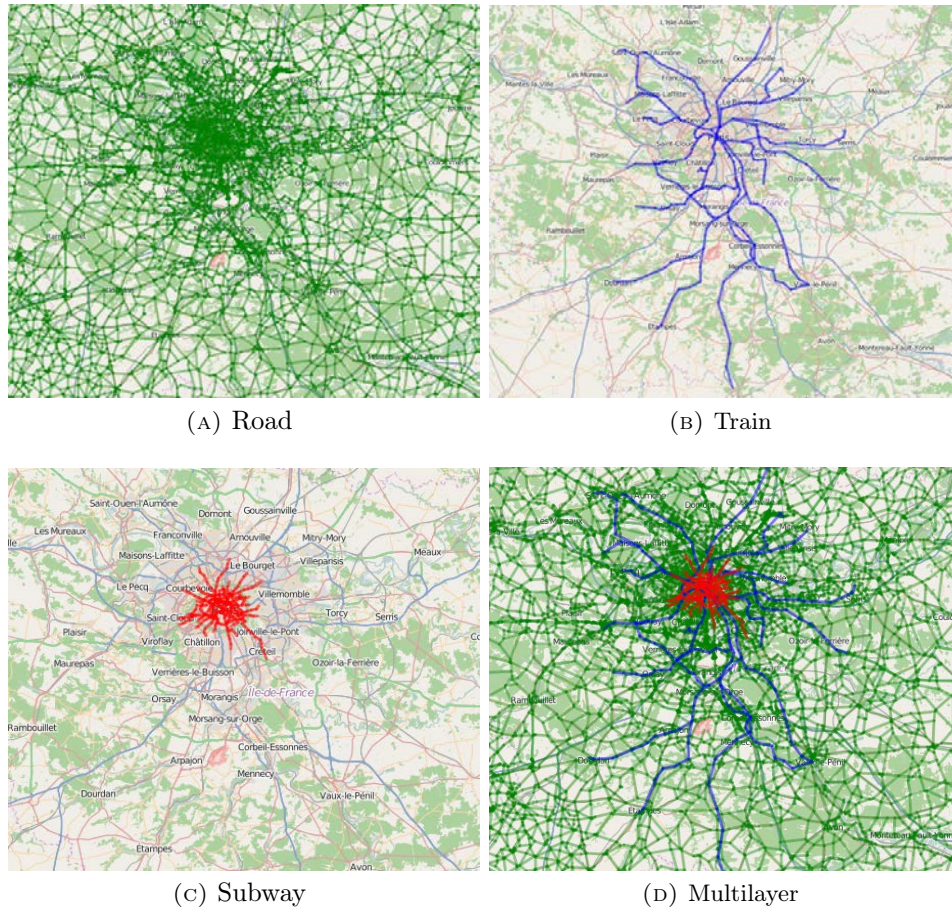
FIGURE 3.5: Different transportation layers and their expansion in Paris region

the simplification of the problem, each subway station is connected to its closest road intersection.

All the process of data integration (data cleaning, geographical pruning , etc.) were implemented using Python script, while graph formation and graph analysis were done by the help of the 'NetworkX' library.

3.2.4   Graph Statistics

This section is dedicated to inspection and examination of the multiomodal transportation network. The objective is to investigate the features and behavior of the multimodal graph **G**. We present a statistical analysis of multimodal transportation network to illustrate the fundamental properties of each transportation layer.

Although such a multilayer representation of the transportation network enables us to model and define trajectories using different transportation modes, it also increases the

complexity of the underlying network. Table 3.3 summarizes the topological features of different transportation layers. It clearly illustrates topological differences between each layer in the multilayer graph **G**. For example, the average length between two consecutive intersections is rather heterogeneous across different transportation layers. This heterogeneity is observed for other features as well.

The area of study is this research work, Ile-de-France (also known as "Paris Region") with the area of $12,012$ km^2, has a typical radiocentric urban structure that benefits from different public transportation networks. It is important to notice that coverage area of these transportation systems are dissimilar as is illustrated in Fig. 3.5. The subway layer illustrated in Fig. 3.5c covers fairly the central part of Paris region with the area of 105 km^2 and some part of inner ring with the coverage area of 657 km^2. The train layer is well expanded in the inner ring area and provides some coverage in the southern part of the outer ring area with $11,250$ km^2 coverage (Fig. 3.5b). There are areas which are not covered neither by rail transportation layer nor by subway transportation layer; these areas are visible in Fig. 3.5d.

Table 3.3 presents basic features of different transportation networks. As the table illustrates, the multilayer graph is essentially dominated by the road network.

Layer name	$|N|$	$|E|$	$<k>$	$<l>$ (km)	Diam^{topo}	$<SP>$	Reference
Subway	303	356	2.35	0.757	34	12.21	OSM
Train	299	303	2.027	3.07	47	16.54	OSM
Road	14798	22276	3.01	1.34	135	51.1	IGN
Multimodal	15342	26947	3.51	0.87	114	36.51	

TABLE 3.3: Different transportation layers and their main features: number of nodes $|N|$ and edges $|E|$, average node degree $<k>$, average edge length $<l>$, diameter and average shortest path $<sp>$ and their data references are indicated

3.3 Multimodal Cellular Trajectories Dataset

This section describes the cellular trajectory used in this study. For obtaining the trajectory dataset, we applied a new approach to collect cellular signalization data of smartphone users. As described in chapter 2, despite the spatial inaccuracy of cellular data, this method insures a constant sampling rate that enables us to obtain uniformly sampled cellular locations. Such a property cannot be insured with CDRs. This improvement in the temporal dimension enables us to extract sparse cellular trajectories of users that are more adequate for mapping than CDR trajectories. Fig. 3.6

is an example of cellular trajectories of a user collected during 100 days. As the figure shows, the cellular signalization data are capable to reflect the mobility of individuals. Table 3.4 illustrates four rows of the data table collected by this method. The raw data table contains userID, unix timestamp of the messaging time, the milliseconds of the time stamp (ms), type of "tunneling management message" (Msg type) and the geospatial coordinate of the antenna as 'latitude' and 'longitude'.

UserID	UNIX TIMESTAMP	ms	Msg Type	Latitude	Longitude
110003934	1363419350	63957	17	48.864901	2.409734
110003934	1363419401	697412	18	48.864929	2.409725
110003934	1363419401	495528	19	48.864967	2.409754
110003934	1363419744	497542	20	48.864054	2.409702

TABLE 3.4: subsample of raw cellular signalization data

The Cellular trajectory dataset that have been used in this work, has been collected from a group of smartphone users with the help of a french telecom company. The frequency of data sampling is 15 minutes and consequently, the extracted trajectories are called sparse cellular trajectories. To extract the cellular trajectories of users from given raw data, a set of data preprocessing techniques have been performed.
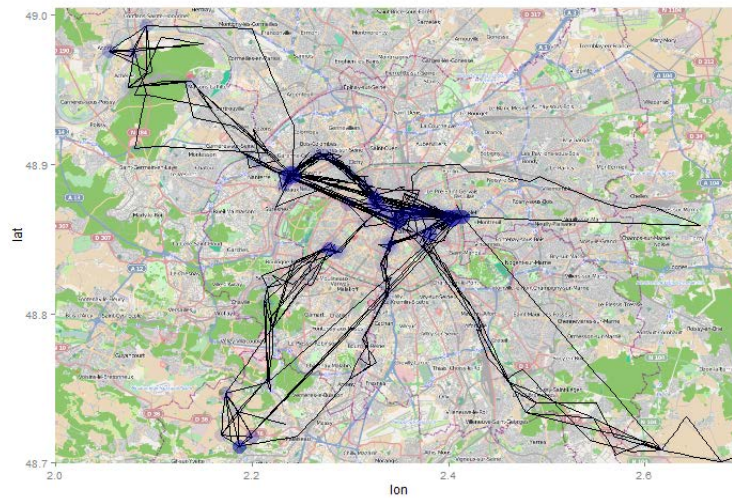
FIGURE 3.6: Cellular signalization data of a smartphone user during 100 days in Paris and vicinity. Blue circles are the most frequent visited places

First, we set a 'waiting time cutoff' as the maximum allowed time between two consecutive cell records in the same trajectory. A trajectory is started from the first movement (a change in cell position) and it ends when the difference between two

consecutive time stamps are more than value Δc where Δc (we set Δc=30 min). Each trajectory is a sequence of time stamped locations such as the time stamp difference for each two consecutive distinct locations is not bigger than Δc. This restriction means that if a user stays at the same location for more than Δc, the trajectory ends in that location. In this step, each trajectory is a sequence of time-stamped cell locations. However, not all the sequences are suitable for trajectory mapping. The radius of gyration defined in equation 2.3 is used to filter out the trajectories whose radius of gyration is smaller than a selected threshold D_{r_g}. Fig. 3.7 illustrates two trajectories with different scales of gyration radius. Given the spatial inaccuracy and the temporal sparsity of cellular data, we are interested in trajectories whose gyration radius is higher than a threshold D_{r_g} (e.g. 2 KM).

FIGURE 3.7: Two cellular trajectories with different radius of gyrations.

Definition. Cellular Trajectory

A cellular trajectory of a user is presented as a sequence of time-stamped locations $O = o_0 \rightarrow o_1... \rightarrow o_M$, where each time-stamped location $o_t =< c(t) >$ refers to the cell tower at time-stamp t the user is observed at.

3.4   Multimodal GPS Trajectories Dataset

This section presents an overview of the multimodal GPS trajectory dataset containing records of multimodal trajectories. A multimodal trajectory is defined as a trajectory involving several modes of transportation. The majority of mobility studies using GPS trajectories, have considered monomodal trajectories (e.g involving only the road transportation network) while in multimodal mobility studies, it is crucial to consider trajectories taking place using different transportation modes. To the best of our knowledge, there exists no real GPS dataset that covers individuals' trajectories over a multimodal transportation network. In this research study, to evaluate and

validate our proposed algorithms, we conducted a data collection experiment to collect fine-grained multimodal trajectory data that will serve as ground truth for sparse cellular trajectories.
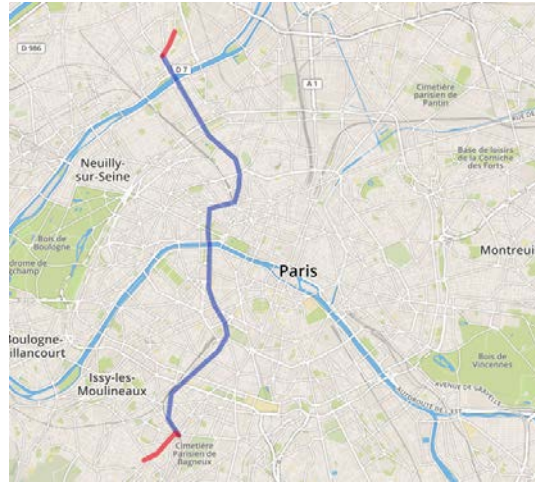
FIGURE 3.8: An example of multimodal trajectory, presented in different colors: red lines are the paths that the individual takes to walk to or from a metro station while the blue line is the trip path which is carried out by metro.

To collect the ground truth data, the recruited group were asked to install application 'Moves' [2]. The data captured by the application is classified in different categories 'Walking', 'Running', 'Cycling' and 'Transport'. With a series of interviews, the transportation mode of trajectories have been specified. Fig. 3.8 illustrates an example of multimodal trajectory in which an individual walks to the metro station (red line) and then walks from metro station to the final destination. As illustrated in the figure, a multimodal trajectory may consist of different sub-trajectories, each taking place on one specific transportation layer. By modeling and building the multimodal transportation network, it is possible to represent a multimodal trajectory as a sequence of nodes over the multimodal graph; such a case of study was not addressed before.

The collection of the GPS trajectories dataset was performed simultaneously with Cellular data collection for the same group of volunteers over the period of the sampling (Aug-Sept. 2014). The dataset covers 130 hours of walking and 470 hours of transportation which is not limited to road and contains multimodal trajectories. Figure 3.9 shows the coverage area of collected the GPS trajectory dataset. The trajectories are mapped over the multimodal transportation network containing road, train and metro layers. It is also important to notice that for underground trajectories there were missing data which were corrected manually after interviews with volunteers.
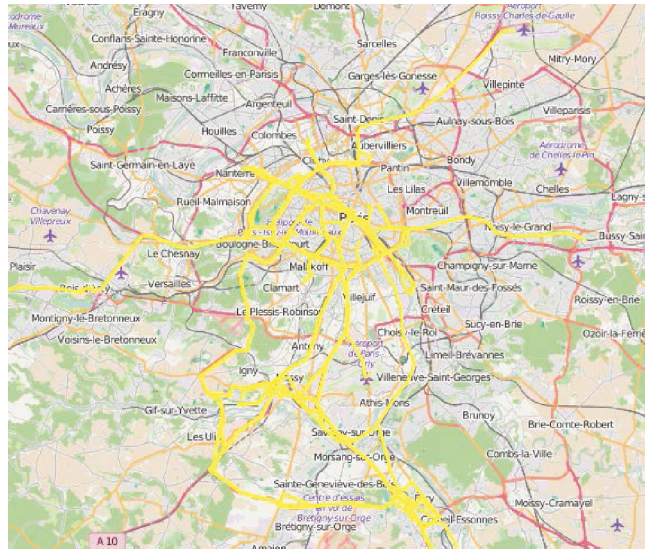
FIGURE 3.9: The coverage area of GPS data collected is shown in yellow on the map of Paris and region
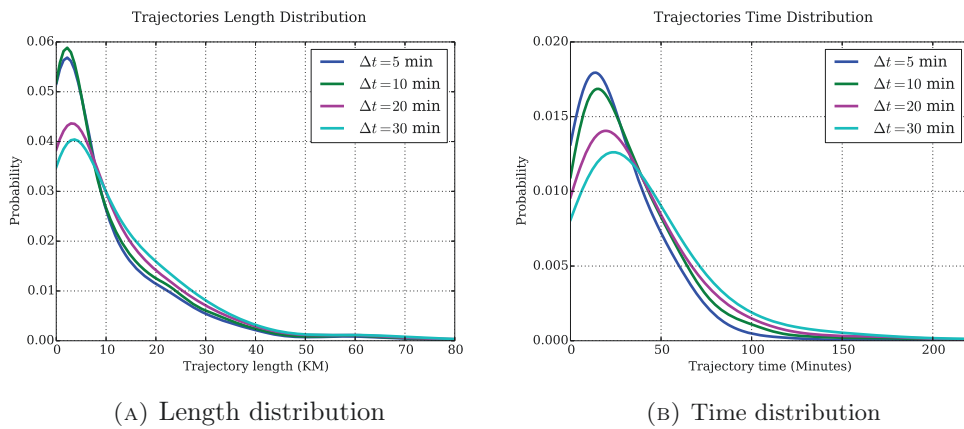
(A) Length distribution

(B) Time distribution

FIGURE 3.10: Distribution of trajectory lenth and trajectory time for a range of Δt waiting time cutoff are plitted

It is worth to mention that for GPS trajectory extraction, a 'waiting time cutoff' was used to separate different movement activities and to make distinction between them. Figure 3.10 presents some statistics on the multimodal trajectory dataset extracted from GPS collected data.

3.5   Conclusion

This chapter provided an overview of database modeling and building of cellular and GPS trajectories' extractions. The first part covered the steps carried out to build a

multilayer graph database. We described how the data model of the multimodal transportation network was defined as a graph of nodes and edges and how its database was implemented using a document oriented database system. The advantages of a document database system and specifically MongoDB is that it provides an efficient standard for storing and querying geospatial objects. Such a system is a proper choice for storing a multimodal graph in which nodes and edges have different properties but are all considered as geometry objects. The constructed database is related to Ile-de-France which is used in next chapters as the study area. The mutlimodal transportation networks of other areas could be constructed in the same way. The main advantage of the modeled transportation network is that it sets no constraint in multimodal trajectory representation. Accordingly, a multimodal trajectory involving different transportation layers is defined as a path over the multilayer transportation network. The nodes of the graph could belong to different transportation layers and the action of mode changing is duly represented as *cross-layer* edges.

In the second part of this chapter, the cellular signalization dataset and its characteristics are described. This section outlined the procedure to extract the users sparse cellular trajectories as sequences of time-stamped antenna locations.

Ultimately, the last part of this chapter introduced the multimodal GPS trajectory database and its features. The trajectories in this dataset can be defined as sequences of nodes where nodes are either road intersections or subway/train stations. That is, the multimodal transportation network database provides a geospatial reference that will be used in the rest of this work to represent the trajectories of individuals.

The multimodal transportation network and cellular trajectory dataset will be used in the following chapters to develop the mapping algorithm. For qualitative assessment, the GPS trajectory dataset will serve as labeled data to evaluate the accuracy of our proposed algorithms.

Chapter 4

Methodology: *CT-Mapper* Mapping Sparse Cellular Trajectories to Multimodal Transportation Network

4.1 Introduction

Macroscopic analysis of the traffic flow in large metropolitan areas is a challenging task. This is especially true when multiple transit authorities are in charge of different transport networks (road, train, subway). Due to the lack of a common source of information across these transit systems, it is often hard for city authorities to grasp a unified view of mobility patterns. In this context, mobile phone data have recently become an attractive source of information about mobility behavior. Thanks to the ubiquitous usage of mobile phones, mining mobile phone data becomes a promising way to understand multimodal human mobility [30, 63, 69] ranging from identifying a mobile user daily path to recording transportation usage (e.g., taking train, metro, bus, etc.) in a large metropolitan area. Traditional approaches of mobility studies used GPS to accurately sense spatial data with a localization error bound $\leq$ 50m. Although they ensure the collection of fine-grained mobility trajectories (as shown in Fig. 4.1b), GPS-based data collection has two main drawbacks: first, it causes high energy consumption, and second, it is constrained to a limited group of users (e.g. taxi

drivers [50] or a group of car drivers [34]). GPS sensing, therefore, is not suitable for collecting large-scale data from metropolitan area populations. By contrast, cellular data provided by network operators does not suffer from these issues, and has become recently, as a result, a new source of mobility information. Signaling information from mobile network operators (CDRs -Call Data Records-) has been used as a valuable source of mobility information for large scale population [4, 24, 69].

Localization of mobile phone users with antennas (i.e., cellular towers), nonetheless, provides only coarse-grained mobility trajectories at antenna level, with a varying localization error of hundred meters in densely populated cities, and within several kilometers in rural areas [69]. Given the resulting *cellular mobility trajectories* (i.e., a sequence of antenna *id*s) and the location of each antenna as shown in Figure 4.1c, it might be difficult to observe the road or metro station that the user passes by (as shown in Fig. 4.1a).

In order to collect cellular mobility trajectories using mobile phones, previous works [4, 24, 69] usually extracted the trajectories from Call Detailed Records (CDR), where the CDR of a user restores the antenna *id* and the time-stamp of each of his/her mobile calls. To understand human mobility, these works were mostly limited to aggregating the trajectories from a user's long-term CDR data in order to determine the frequently-visiting locations and the visiting time (e.g., the park he/she usually passes by during the 07:00–09:00 window of working days). As such, the techniques proposed by previous works are not suitable for estimating the precise mobility trajectories on the road/transportation network using the CDR cellular trajectories. Furthermore, one sample of CDR data (i.e., one call record) can be obtained only when the user places a call, making human mobility data between two consecutive calls irretrievable, especially when the time duration between the two calls is long (e.g., the inter-call mobility between the two calls in Fig. 4.1d). Thus, even though it has been studied widely, CDR is unlikely to be a good data source for the trajectory mapping problem. Considering the time sparsity drawbacks of CDRs, we use, in this work, a new passive capturing technique to efficiently extract the position of the base stations the mobile phone connects to. This technique analyzes the signaling channel of the data mobile network in order to extract base station locations. This way of capturing the mobility of users is scalable and provides a higher sampling rate than CDR-based sensing.

The sparse cellular trajectories are collected and provided upon the request of the experiment participants to the network operator. Considering *privacy issues* [51], the network operator localizes each mobile user using an antenna *id*, and further records

(A) Road Trajectory

(B) GPS Trajectory

(C) Cell Trajectory (Full)

(D) CDR Trajectory

(E) Sparse Cell Trajectory

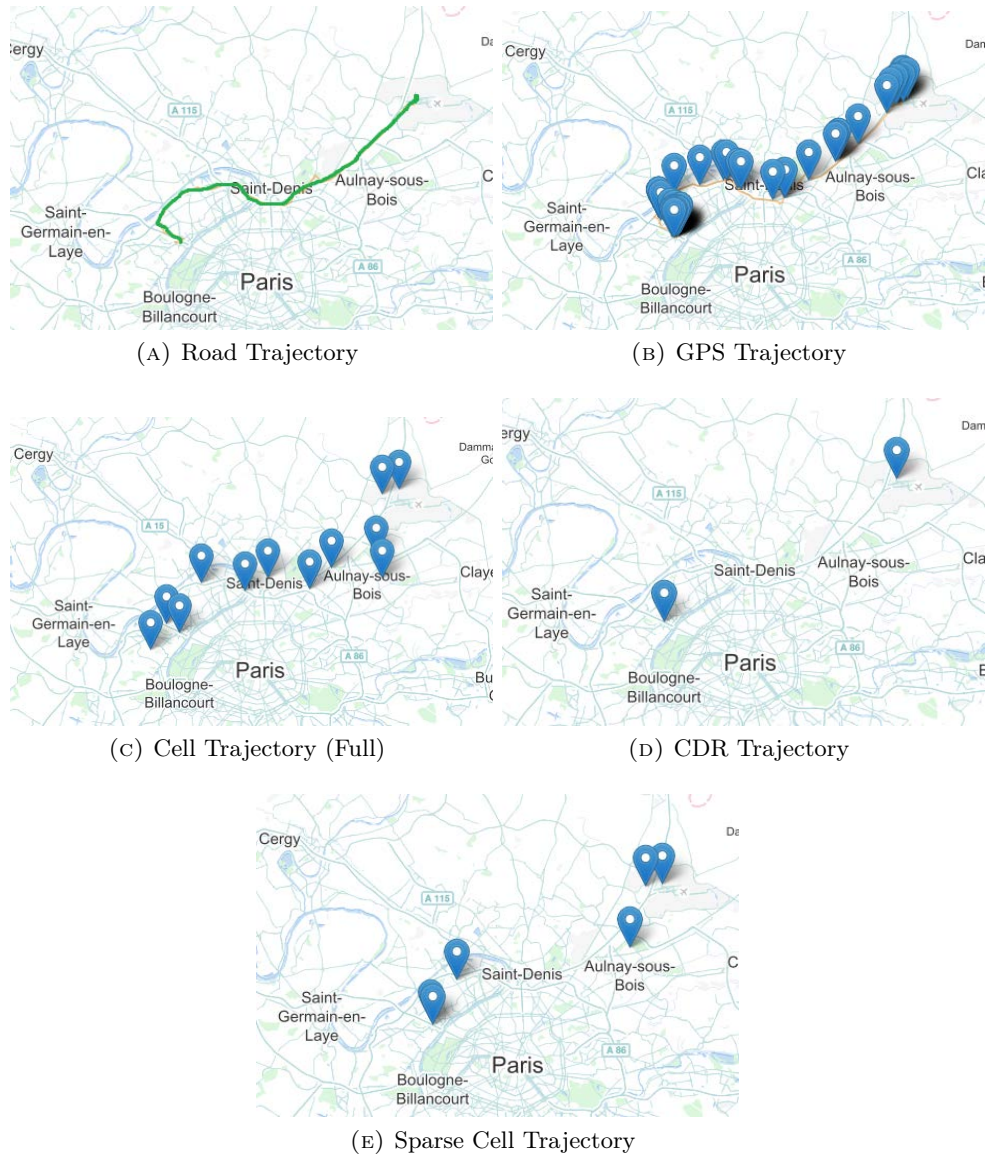FIGURE 4.1: A user's trip from Airport CDG to city center of Paris: The road trajectory consists of the sequence of roads that the user passes-by; The GPS trajectory is sampled in minute based frequency; The Cellular trajectory (Full) records each cell tower the user passes-by; The CDR trajectory reports the location of the user's each call during the trip; The Sparse Cellular trajectory is sampled every 15 minutes

each user's antenna *id* with time-stamp periodically (e.g., every 15 minutes in our study). Compared to the user's real trip (in Fig. 4.1a), the sparse cellular trajectory (in Fig. 4.1e) partially measures the user's mobility with coarse-grained localization. The objective of our work is to map each sparse cellular trajectory into the multimodal transportation network, in order to obtain the sequence of network nodes that the user passes by. For example, given the cellular trajectory shown in Fig. 4.1e and the transportation network of the Paris metropolitan area shown in Fig. 4.2, our goal is to recover the sequence of nodes of the real trip shown in Fig 4.1a.

The common approach for mapping cellular trajectories into the metropolitan transportation (usually road in the state of the art) network is to first collect a large amount of cellular trajectories and then to manually label each with the corresponding intersection sequence, an intersection being a graph node associated with a junction between two roads. The next phase is to train a *supervised mobility model* (e.g., HMM) using the labeled cellular trajectories, in order to build a probabilistic model mapping antenna *id* sequences to intersection sequences. After training, given a new user cellular trajectory, the supervised model predicts, as the mapping result, a sequence of intersections, having the maximal likelihood of generating the antenna *id* sequence. However, obtaining the labeled cellular trajectories to cover the road/transportation networks and all cellular towers of a metropolitan area is not practical, as it costs too much human efforts for trajectory collection and labeling. We propose, in this chapter, to solve the cellular trajectory mapping problem using an **unsupervised model**, that does not require collecting and labeling any trajectories.

Given the above examples and target research goals, the key issues in designing the unsupervised mobility model include:

1) *Given the antenna id sequence in a cellular trajectory, retrieve the sequence of road-/rail intersections that the user passes by given a **database** storing the **multimodal transportation network*** - The transportation network covering and connecting multiple types of transportation modes (e.g., rail, metro, highway , etc.) is named *multimodal transportation network* [54], in which each node is either a road intersection or a station of a rail transportation mode (i.e., subway, tramway and train), and each edge is a connection between intersections (e.g., the pathway connecting a metro station and a bus stop). Obviously, it is nontrivial to extract the precise user path from the multimodal transportation network using the antenna *id* sequences. The cellular trajectory might come from multiple transportation systems nearby each corresponding antenna and in different layers (underground, ground and trestle). To

overcome this issue, it is necessary to build a comprehensive database storing all the intersections of the multimodal transportation network, where we can accurately retrieve the surrounding intersections of each antenna. In this work, open data provided by OpenStreetMap (OSM) and the National Geographic Institute (IGN) are used to extract the multimodal transportation network of Ile-de-France (Paris and vicinity). This region is characterized by a high diversity of public transportation modes (subway, tramway, RER, train, bus) that have each particular specifications. Therefore, building a multimodal transportation network to study individuals' mobility requires a clear understanding of the multimodal network complexity. The multimodal transportation network is modeled in this work based on the concept of 'cross-layer' links that connect each two nodes where users can switch transportation modes.

2) *Given an observed cellular trajectory, compute the* **most-likely intersection sequence** *over the multimodal transportation network* - It is difficult to search the most-likely intersection sequence from the set of intersections, due to the following reason:

Likelihood Computation: In order to search the most-likely intersection sequence, given an observation sequence, we need to calculate the likelihood of each node given the cellular trajectory. While the traditional supervised HMM mobility model harnessing the statistics of labeled cellular trajectories (i.e. emission/transition probabilities) is usually used to estimate the likelihood, we propose an unsupervised HMM that does not leverage labeled data. Rather it proposes a method to calculate the likelihood using the *topological properties and other information of the transportation network*. In other words, the HMM parameters are automatically derived in an unsupervised way based on a priori knowledge of transportation network properties.

In summary, the main contributions of this work are:

- We propose to study the problem of mapping cellular trajectories to the *multimodal* transportation network, in order to obtain the precise mobility of the users. To the best of our knowledge, this is the first work addressing these issues. In particular, rather than mapping cellular trajectories using the supervised mapping algorithms with labeled mobility data, we propose to use an unsupervised mapping algorithm leveraging on topological properties of the transportation network, so as to eliminate the tedious human labeling efforts in building the mobility model.

- We propose an unsupervised trajectory mapping algorithm, namely *CT-Mapper*, which maps cellular location data over the multimodal transportation network. The multimodal transportation network database was built using different references of geospatial resources. The mapping algorithm is modeled by an HMM where the observations correspond to user cellular trajectories and the hidden states are associated with nodes of the multilayer graph which are either road intersections or subway/train stations. Transition probability and emission score were modeled based on topological properties of the transportation network and the spatial distribution of antenna base stations. Viterbi decoding algorithm helps reduce the complexity of finding the best match which might enable us to deploy our unsupervised mapping algorithm on large scale mobility data sets in order to estimate multimodal traffic in metropolitan areas.

The rest of this chapter is structured as follows: section 4.2 presents related work. Section 4.3 gives an overview of the proposed system. Section 4.4 presents the details of the unsupervised estimation of HMM parameters and explains how the two main probability distributions used for mapping are derived and the chapter ends by a discussion and a conclusion in section 4.5.

4.2 Related Work

4.2.1 General Human Mobility Models

A considerable amount of Human Mobility studies have been devoted to analyze trajectories of individuals based on their traces. Spatial characteristics such as center of the mass, radius of gyration and statistical characteristics revealed a number of scaling properties in human trajectories: Gonzalez et al in [16] and Brockmann et al [15] showed a truncated power-law tendency in the distribution of jump length. It was observed that most individuals travel only over a short distance, and there is only a few who travel regularly over hundred kilometers. Further studies [36] [16] showed that travel patterns collapse into a single spatial probability distribution, indicating that, despite the diversity of their travel history, humans follow simple reproducible patterns. In addition, statistical analysis confirms that individuals' movement follows spatio-temporal patterns [34] [33] [21] which can help defining mobility models. In all mentioned studies, multimodal mobility aspects were not taken into account. One objective, in this work, is to investigate the mobility patterns of trajectories through

the multimodal transportation network and to explore how these patterns are affected by the multiplicity of the layers of the network. Early mobility studies relied on expensive data collection methods, such as surveys and direct observation. Trajectories were mostly defined as Origin-Destination (OD), and were mapped over the desirable graph to retrieve an optimal path solution which is usually the shortest path between the Origin and Destination [33, 34, 36, 87]. Although recent studies have been trying to infer the traffic flow using additional traffic data [5], they still fail to retrieve the real path taken by individuals.

4.2.2 Mapping Algorithms

Along with mobility studies, applications such as navigation systems, traffic monitoring and public transportation tracking, used GPS data to track individuals or any moving object [22, 41, 45, 58, 79, 85]. A variety of statistical approaches such as Expectation Maximization (EM) [45], Kalman Filter [41, 85] and Hidden Markov Model (HMM) [22, 44, 58, 79, 80] were used to map 'noisy' sequential location data over transportation networks. Most of these mapping algorithms have used GPS data as they provide accurate location data with an error of about 50 meters. Moreover, using labeled data, supervised models were considered and trained to optimize model parameters in an automatic way. Once the models are trained, they are used to find the most likely path in the network assigned to sequences of 'noisy' location data. However, most of these mapping algorithms were developed to map noisy data over road networks without considering other mobility modes.

4.2.3 Human Mobility Modeling with CDR Cellular Trajectories

Recently, because of the expeditious growth of mobile phones, Call Data Records (CDR) have been providing great data sets for human mobility studies as they are collected continuously for all active cellular phones. CDRs, however, have two significant limitations: first, they are sparse in time because they are generated only when a phone engages in a voice call or text message exchange; and second, they are coarse in space and less precise than GPS location data, because they record location only at the granularity of a cellular antenna (with an average error of 175 meter in dense populated areas and up to 2 kilometers in less denser areas). Nonetheless, the fact that almost the entire population is already equipped with cell phones [69] allows for studying important aspects of individual mobility such as inferring transportation

modes. Cellular network data were, for instance, used to classify different transportation modes for long-distance travels [30, 69]. Thiagaran et al. in [79] used cellular signal data with combination of cellphone sensors to develop a supervised mapping algorithm in order to overcome the limitation of GPS data. While previous works have used cellular data to map long trajectories, this work proposes an unsupervised mapping algorithm that maps the sparse cellular trajectories over the multimodal transportation network in the Paris metropolitan area. This approach could be used for large scale smart-phone users for further studies in traffic estimation. Such a mapping is important for the development of smart cities and smart mobility. Studies of smart cities in the past were limited to analyzing multimodal transportation networks without considering large scale real mobility data. The main goal of multimodal mobility studies is to improve public transportation monitoring and to reduce traffic congestion [7, 54, 56] . Considering the aforementioned observations and the fact that the majority of trajectory mapping problems are developed for mono-modal transportation networks (specifically road networks), we believe that there is a gap in the literature. This study aims at bridging this gap by mapping cellular sparse data of smartphones over the multimodal transportation network in the Ile-de-France metropolitan area. The multimodal mapping results may help not only optimizing the multimodal transportation network, but also investigating the multimodal mobility behavior of individuals in metropolitan areas.

4.3   CT-Mapper System Overview

In this section, we first formulate the search problem of CT-Mapper, and introduce the datasets collected for mapping. We then analyze the computational complexity of the mapping problem over the collected datasets, and finally present the framework of CT-Mapper.

4.3.1   Problem Statement

In this section, we first formulate the problem be defining several key concepts used in our approach.

Definition 1. *Multilayer Transportation Graph* - Such a graph is represented as $\mathbf{G} = (V, E, L, \Psi)$ where V, E represent the vertices and the edges, L is the set of possible layers. In our study we focused on 3 layers: road, train and subway.

Aggregation of multi Layered Graph of public Transport
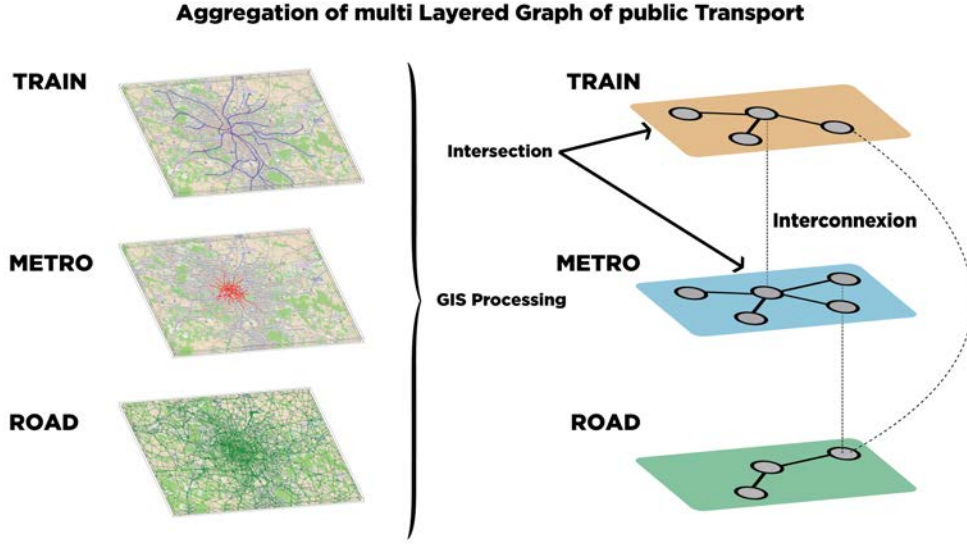
FIGURE 4.2: Multilayer representation of different transportation networks

Function Ψ indicates the layer of each node $\Psi : V \to L$ in **G**.

Transportation Layer $G^l = (V^l, E^l)$ is a subset of **G**, where $V^l = \{v | v \in V, \Psi(v) = l\}$ and $E^l = \{< v_i, v_j > \in E, \Psi(v_i) = \Psi(v_j) = l\}$. Each node v_i is characterized by its latitude and longitude (i.e., the geographical position $v_i = < lat, lon >_i$)

CrossLayer edge set $E^{cl} \subset E$ defines the edges with pairs of nodes not belonging to the same layer: $E^{cl} = \{< v_i, v_j > \in \mathbf{G} | \Psi(v_i) \neq \Psi(v_j)\}$

The multilayer Transportation graph is characterized by its *adjacency matrix* $W_{ij} \in \mathbb{R}^{|V| \times |V|}$. Fig. 4.2 illustrates how different transportation layers have been aggregated to build a multimodal transportation network.

Definition 2. *Cellular Network* - In this work, we characterize a cellular network as a set of cell towers $C = \{c_0, c_1, ...c_P\}$, where each cell tower $c_p = < lat, lon, r^{max} >_p$ is characterized by its latitude and longitude in the geographical coordinate system and by r^{max} which is the maximum radius of the voronoi cell the cell belongs to in the voronoi graph built from set C. Please note that the location of each cell tower does not coincide with the location of any intersection in the transportation network i.e., $\forall v_i \in V$, $\forall c_p \in C$, we have $< lat, lon >_p \neq < lat, lon >_i$.

Definition 3. *Sparse Cellular Trajectory* - Further we define a sparse cellular trajectory of a user as a sequence of time-stamped locations $O = o_0 \to o_1... \to o_M$, where each time-stamped location $o_t = < c(t) >$ refers to the cell tower at time-stamp t the user is observed at.
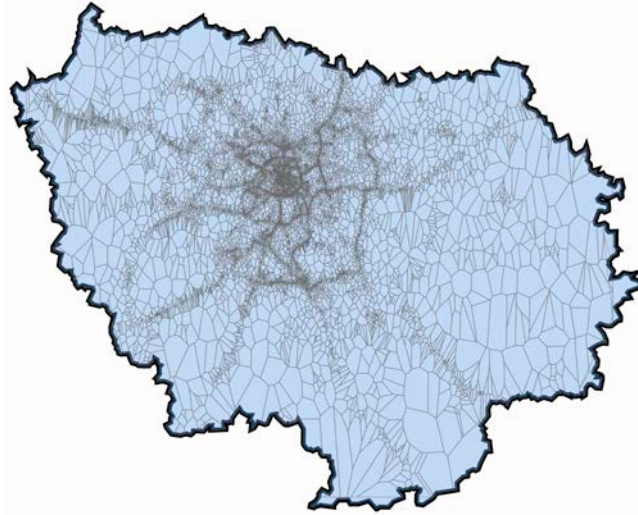
FIGURE 4.3: Voronoi tessellation of cellular antennas in Ile-de-France

Trajectory Mapping Problem - Given a transportation network **G**, cell tower network C, and a user sparse cellular trajectory O, our search problem is to *find a sequence of intersections* $v_0 \rightarrow v_1... \rightarrow v_q$ *which the user actually passes by on the transportation network.*

4.3.2 Data Collection and Datasets

Three types of data are used in this study: multimodal transportation network data, sparse cellular trajectory data, and GPS trajectory data. The multimodal transportation network data are used to build the multilayer network graph and the mobility model for the mapping algorithms. Cellular trajectories are used for testing while GPS trajectories are used as ground truth and not for training HMM parameters.

Sparse Cellular Trajectory Data - In this work we use a new type of cellular trajectory named Sparse Cellular Trajectory. A set of techniques for data collection are used to capture GPRS Tunneling Protocol (GTP) messages from the Cellular Data Network. Packet inspection of GTP-C (GTP control plane) enables us to capture users' localization information at higher frequency than the usual CDR. The GTP is the tunneling protocol used to carry data traffic over the mobile network (from 2G to LTE) to internet. When a smartphone enables its internet connection (e.g. when it is turned on), a message is sent over the network asking for access. This message contains among other things the identity of the phone and the cell id covering the user. Once the session is established, update messages are sent carrying information

like the bearer or the cell *id.* These messages are triggered when the user moves from a BTS to another or by resource allocation. Finally, when the mobile looses the signal or is turned off, a message closing the session is sent. With modern smartphone applications that emit and receive data on a regular basis (i.e. email, push notification), it is expected that the GTP tunnel for a given user remains constantly maintained, enabling us to sample the user position at each network event (handover and radio resource allocation).

GPS Trajectory Data - To evaluate the accuracy of our proposed mapping algorithm, GPS data were used as ground truth. A group of participants were asked to install the "Moves" smartphone application [2] to record their GPS locations. The GPS locations provided by "Moves" were analyzed to extract real trajectories of participants.

4.3.3 Computational Complexity of the Mapping Problem in the Collected Datasets

Layer name	$|N|$	$|E|$	$<k>$	$<l>$ (KM)	Reference
Subway	303	356	2.35	0.757	OSM
Train	241	244	2.025	3.07	OSM
Road	14798	22276	3.01	1.34	IGN

TABLE 4.1: Different transportation networks with four main features: number of nodes ($|N|$), number of edges ($|E|$), average degree ($<k>$) and average edge length ($<l>$)

The underlying transportation network used in this study is the multimodal transportation network of Ile-de-France which is modeled by several separated graph layers corresponding each to a different transportation mode, interconnected together into a multilayer graph **G**. To build this graph, multiple geospatial datasets, namely the road network from the National Geographic Institute (IGN)[1] and the rail transport network (train and metro) from OpenStreetMap (OSM)[3] were aggregated. Each node in **G** is either a road intersection, a rail station or a metro station. A key feature of the proposed multimodal transportation network is its modeling of transitions between different transport modes during a given trip. Cross-layer transition modeling are ensured by adding *CrossLayer* appropriate edges between layers.

To quantitatively assess network complexity, we use entropy measure to characterize the ease/difficulty of navigation in a network using "the search information" developed

in [70], and in [65].

Eq. (4.1) defines the probability for a random walker starting at node s with degree k_s to reach node t through the shortest path SP_{st}. Consequently, in eq. (4.2) we define the search entropy of a graph as the sum over all shortest paths $\{SP_{st}\}$ from node s to node t in G averaged over all possible pair of nodes (s, t) in graph G. As a result, by computing the average entropy of all the possible paths in G, we can express the relative complexity (S_{avg}) of finding a given path in a given graph G.
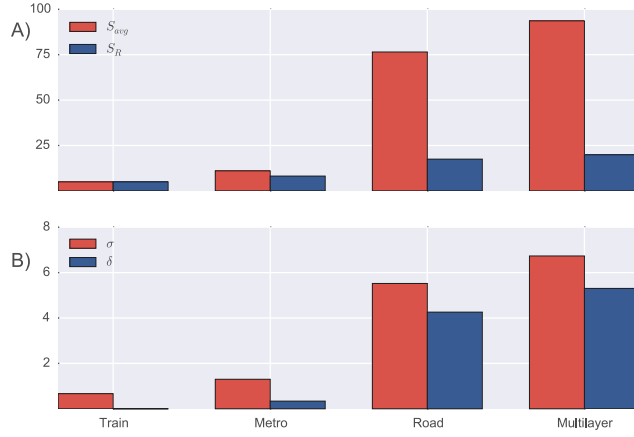
FIGURE 4.4: Graph Entropy: (A) absolute value of the average entropy of the graph where S_{avg} is the entropy of the real graph and S_R is the entropy of the random graph with similar characteristics, (B) is the relative of the average graphs entropy of the paths in the subgraph of the metro, train,road

$$P[SP_{st}] = \frac{1}{k_s} \prod_{j \in SP_{st}} \frac{1}{k_j - 1} \tag{4.1}$$

$$S_{avg} = \frac{1}{N(N-1)} \sum_{s=1}^{N} \sum_{t=1}^{N} -\log_2 \sum_{\{SP_{st}\}} P[SP_{st}] \tag{4.2}$$

In figure 4.4a we plot the average entropy of each layer of the multimodal transportation graph of Ile-de-France along with the average entropy of the interconnected multilayer network. We observe that the average entropy is higher in the multilayer transportation network than in each of the layers taken separately. Figure 4.4b also shows the average path entropy relative to the size of the graph (σ). As it shows clearly, the complexity of the multilayer graph is higher than each of its layers taken separately, regardless of its size. We define $\sigma = S/\log_2(N)$ as the average graph

path's entropy relative to its size and $\delta = (S_{avg} - S_R)/\log_2(N)$ to describe how a graph compares with its random counterpart in terms of its node degree, irrespective of the network size.

As a conclusion, the search complexity of finding the right path in the multilayer transportation graph increases compared with a single layer graph. This is due to two effects: firstly when different layers are combined together in a multilayer graph, the number of degenerate paths (paths of the same length) increase and so the overall complexity. Secondly, when we build the multilayer transportation network, we add multiple interconnections between each two layers, and we thus increase the degree of nodes that are at the junctions of two layers. It is also important to notice the clear increase of path complexity between different layers (train, metro, road). The aggregation of layers increases the number of rail degenerated paths from about one or two to several. The number of degenerated path increases as well but rather slowly with respect to the large number of paths already existing before aggregation.

These effects combined increase the search complexity of a given path in the multi-layer transportation network and increase, therefore, the difficulty of finding a correct mapping of the sparse trajectories on the graph. This phenomenon explains why in multimodal transportation systems using an algorithm that tries to find the best match of a user trajectory (cellular trajectory) over the transport network will usually fails, due to the presence of many degenerate paths.

4.3.4 Framework and Overall Design

Given the multimodal transportation network $\mathbf{G}$ and the cellular network C, we define an algorithm that outputs the most likely path or sequence of intersections given the sequence associated with a user sparse cellular trajectory O. In order to infer the accurate sequence of intersections from the given sparse cellular trajectory, we propose a *two-phase* unsupervised mapping algorithm: in the **first phase**, the algorithm searches a sequence of intersections, namely the *skeleton sequence*, where each two consecutive intersections are not necessarily adjacent (shown in Fig. 4.5c). For this objective we developed an unsupervised Hidden Markov Model inference algorithm that accommodates the sparsity of observations (15 minutes). The hidden states in the HMM are the multimodal graph nodes corresponding to road intersections or metro/train stations. The transition probability in our model takes care of sparsity of observations by permitting transitions between nonadjacent nodes as explained in

sec.4.4.A . For each observation, a set of hidden states are selected as the candidate states in order to minimize the complexity of search in the graph. Given a sequence of sparse cellular observations, our HMM model outputs the most likely sequence over the multilayer network (there are cases of only 3 or 4 observation points).

Then, in the **second phase**, (shown in Fig. 4.5d) the algorithm traverses the skeleton sequence and outputs a sequence of adjacent intersections by completing the sequence (shown in Fig. 4.5e). Please note that the skeleton sequence searched in the first phase is with equal-length to the given sparse cellular trajectory O, while the intersection sequence outputted in the second phase would be longer than O. Given the frequency of 15 minutes for observations, it is clear that a user would pass through more than one intersection between each 2 consecutive observation points, (e.g. when commuting with metro, it takes around 3 minutes to move between each 2 stations).

Skeleton Sequence Search - Given the sparse cellular trajectory $o_0 \rightarrow o_1, ... \rightarrow o_M$, this phase returns the skeleton sequence of the intersections as $v_0 \rightarrow v_1, ... \rightarrow v_M$. The algorithm is first initialized by $Pr_{t_0}(v_i) = P(o_0|v_i)$ for the candidate intersections v_i corresponding to the first time-stamped location o_0, with $Pr_{t_0}(v_i)$ denoting the probability of a user to be located at intersection/node (v_i) at time t_0. Then for each candidate state corresponding to cell tower o_t, the probability of a user being in v_j at time t and generating $o_0 \rightarrow o_1, ... \rightarrow o_t$ is calculated by Eq. 4.3;

$$Pr_t(v_j) = P(o_t|v_j) \times \max_{\forall \ v_i}[Pr_{t-1}(v_i) \times Tr(v_i, v_j)] \tag{4.3}$$

where $P(o_t|v_j)$ is the probability of a user connecting to cell tower of o_t when he/she is in the intersection v_j and $Tr(v_i, v_j)$ is the transition probability of moving from node v_i to node v_j. The parent node is also stored using Eq. 4.4;

$$Par(v_j) = \arg \max_{\forall \ v_i}[Pr_{t-1}(v_i) \times Tr(v_i, v_j)] \tag{4.4}$$

At the end, we find $\overset{*}{v}_M = \arg \max_{\forall v_M} Pr_t(v_M)$ Then a backtracking iteration using Eq. 4.5

$$\overset{*}{v}_{b-1} = Par(\overset{*}{v}_b) \quad \text{for} \quad b = [M, ..., 2, 1] \tag{4.5}$$

retrieves the most likely intersection sequence $\overset{*}{v}_0 \rightarrow \overset{*}{v}_1, ... \rightarrow \overset{*}{v}_M$ which produces the most likely path for the sparse cellular trajectory $o_0 \rightarrow o_1, ... \rightarrow o_M$. Sequence $\overset{*}{v}_0 \rightarrow \overset{*}{v}_1, ... \rightarrow \overset{*}{v}_M$ serves as input for the next phase to retrieve the adjacent sequence of intersections for the given sparse cellular trajectory.

Adjacent Sequence Completion - Given the skeleton sequence $\overset{*}{v}_0 \to \overset{*}{v}_1 ... \to \overset{*}{v}_M$, for each pair of consecutive intersections $\overset{*}{v}_i, \overset{*}{v}_{i+1}$ that are not adjacent in multilayer **G**, the algorithm searches the optimal sequence of intersections $v_{i_1} \to v_{i_2} ... \to v_{i_k}$ and inserts the newly-searched sequence between the two intersections $\overset{*}{v}_i, \overset{*}{v}_{i+1}$ as:

$$\overset{*}{v}_i \to \underbrace{v_{i_1} \to v_{i_2} ... \to v_{i_k}}_{\substack{\Uparrow \\ \text{Recovered path}}} \to \overset{*}{v}_{i+1} \tag{4.6}$$

as the complete adjacent sequence. Please note that each two consecutive nodes in the newly obtained sub-sequence are adjacent in multilayer graph **G**. In the next section, we will introduce the computation of probabilities used in our framework.

4.4 Core Algorithms

In the previous section we described the general algorithm of mapping cellular trajectories over the multimodal transportation network. The two main probability distributions used in the mapping algorithm, are the HMM transition and emission scores that are estimated in an unsupervised way. This section explains in detail how the two scores are defined and estimated.

4.4.1 Transition Probability

The transition probability $Tr(v_i, v_j)$ in our mapping algorithm specifies the probability of an individual's moving from hidden state v_i at time $t - 1$ to hidden state v_j at time t. The transition probability is inferred from the underlying network, i.e. the multilayer transportation network in which each transportation layer has its specific characteristics and properties. Table I shows some graph topological properties such as the node degree distribution and the physical edge length distribution in different layers of the multimodal transportation network. It is crucial to notice that relying on the topological properties of network layers without considering their differences, leads to a biased mapping algorithm in which the observations tend to be mapped over a specific transportation layer. In addition, taking into account the sparseness

(A) Cellular trajectory

(B) CT-Mapper's input + Real trajectory

(C) Phase I (Input & output)

(D) Phase II input

(E) Phase II input and output

(F) CT-Mapper's input + Final output

FIGURE 4.5: An illustration of different phases of mapping algorithm. The Blue line in the Fig. 5(a) is the real GPS trajectory of a user and given a sequence of 5 antenna base stations with the frequency of 15 min, the mapping algorithm can retrieve the pink line in Fig.5(e)

of cellular observations, it is a key to authorize transitions between nonadjacent intersections. We propose a transition probability of moving from intersection v_i to the intersection v_j that is a function of 2 given factors:

1) Edge type and average speed over each edge: each physical edge in the multilayer graph **G** belongs to a layer. Moreover, only the road layer contains different types of edges (such as highway, principal, local, etc.). We define matrix W where each element of the matrix represents a weight between two nodes if there exists an interconnection between them. The weight of each link is defined as the inverse of average speed that one could have over the corresponding edge. Table 4.2 represents the weight according to average speed over the edges of graph **G**.

$$W_{ij} = \begin{cases} w_{ij} & \text{if } v_i, v_j \text{ are adjacent in } \mathbf{G} \\ 0 & \text{otherwise.} \end{cases} \tag{4.7}$$

value of w_{ij}	Condition
1/10	$\Psi(v_i) \neq \Psi(v_j)$
1/100	$\Psi(v_i) = \Psi(v_j) = \text{train}$
1/80	$\Psi(v_i) = \Psi(v_j) = \text{metro}$
1/90	$\Psi(v_i) = \Psi(v_j) = \text{road (highway)}$
1/60	$\Psi(v_i) = \Psi(v_j) = \text{road (principale)}$
1/40	$\Psi(v_i) = \Psi(v_j) = \text{road (regional)}$
1/30	$\Psi(v_i) = \Psi(v_j) = \text{road (local)}$

TABLE 4.2: Edge classification and weights for multilayer transportation network **G**.

2) Edge length: involving edge length in the transition probability, indirectly considers higher probability for the nodes close to each than that for farther ones.
The transition probability between two intersections v_i and v_j is defined as the inverse of the shortest path cost between v_i and v_j:

$$Tr(v_i, v_j) = \left(\sum_{\forall \ (mn) \ \in \ SP_{v_i v_j}} w_{mn} \times d(v_m, v_n) \right)^{-1} \tag{4.8}$$

where (mn) is an edge between v_m and v_n belonging to $SP_{v_i v_j}$, the shortest path between two nodes v_i and v_j in graph **G**. The shortest path cost of $SP_{v_i v_j}$ is the sum of distances over each edge (mn) belonging to $SP_{v_i v_j}$, weighted by w_{mn}. $d(v_m, v_n)$ is

the euclidean distance between each two nodes v_m and v_n.

In earlier studies, the transition probability was quantified based on topological properties of the underlying network which was mainly a road graph. In [58, 80], the transportation network was represented as road segments and transitions were assumed to occur between adjacent road segments. The authors in [44, 80] considered equal transition probabilities between nodes in the same road segment or nodes between road segments which are adjacent with an intersection. The transition probability in [79] is defined based on the Manhattan distance between the grid cells of the road network. The objective of our proposed transition probability model is to minimize the bias of the mapping algorithm for layers with different topological properties.

4.4.2 Emission Probability

In HMM, at each time step t, there exists an observation o_t which in our study is characterized as $c_t = < lon, lat, r_t^{max} >_t$. The emission score reflects the notion that it is more likely that a particular observation point is observed from a nearby intersection than an intersection farther away [80]. For studies in which GPS data were used as observations [22, 58, 80], the emission probability score is modeled by a normal distribution that is a function of the euclidean distance between the observation point and the hidden state, and with a standard deviation estimated from sensor errors.

In this work, cellular antenna locations serve as observations; Since there is no labeled data available to estimate cellular sensor errors, we build the voronoi tessellation of cellular antennas in the area of study. In the voronoi network of cellular antennas, each cellular antenna C_i is characterized by radius r_i which is the maximum distance of the cellular antenna from the corresponding voronoi cell vertices. Our emission score is defined as a decreasing function of the distance between the antenna location and the hidden node (intersection):

$$Pr(o_t|v_j) \propto \begin{cases} 1.0 & \text{if} : d_{tj} \leq r_t^{max} \\ \left(\dfrac{r_t^{max}}{d_{tj}}\right)^{\beta} & \text{if} : r_t^{max} \leq d_{tj} \leq \tau \\ 0 & \text{otherwise.} \end{cases} \tag{4.9}$$

where $d_{tj} = d(o_t, v_j)$ is the euclidean distance between o_t and intersection v_j, and τ is a threshold corresponding to the maximum distance that a cell phone can be hit

by a cellular antenna. τ enforces the constraint that only intersections in the radius of τ from the cellular antenna could be considered as candidate states (nodes).

4.5   Discussion & Conclusion

This chapter covers the body of our proposed methodology, an unsupervised mapping algorithm *(CT-Mapper)* designed and developed to map sparse cellular trajectories over a multimodal transportation network. The unsupervised mapping algorithm is designed using Hidden Markov Model properties and Viterbi decoding algorithm was employed to infer the most likely path of the individuals given wholly sparse cellular trajectory. The mapping algorithm is designed in a way that it takes into account changing between different transportation layers. We modeled and built the multi-layer transportation network database including subway, train and road layers for the Ile-de-France metropolitan area. The multilayer transportation network enables the mapping algorithm to retrieve the trajectories involved with more than one transportation layer. Investigating the complexity of the multilayer transportation graph, a transition probability model leveraging the transportation layer type and topological properties was estimated and used in the unsupervised HMM-based mapping algorithm. The emission probability is formed with respect to the noisy cellular observations. In addition, since investigating the behavior of noisy cellular observations to infer the emission probability model is a highly data dependent task, a smoothed emission score is derived to quantify the emission score.

The *CT-Mapper* is designed to map the sparse cellular trajectories over the multilayer transportation network in two phases: The first phase infers the most likely sequence of the nodes given only sparse cellular observations (e.g. sampled each 15 minutes) and returns the skeleton sequence as the result. Eventually, the second phase retrieves the complete path on the multilayer transportation network given the skeleton sequence and returns the most likely path associated to the cellular trajectory. The main strength of this approach is that all the steps are designed and performed in an unsupervised way as no labeled data are required to train the model. Subsequently, we can deploy the algorithm in large scale without manual intervention associated with human labeling. Moreover, by injecting new knowledge from either transportation systems or geospatial properties of the cellular antenna, the algorithm performance can further be improved. To the best of our knowledge, this is the first attempt to

infer multimodal trajectories of individuals over a multimodal transportation network given only their sparse cellular data in metropolitan areas.

Along the same lines, We expect that using a dynamic weight matrix, which is compatible with the traffic model at different times of the day, is likely to enhance the mapping results. This issue will be investigated in future studies. Furthermore, The improvement of accuracy measures of our mapping algorithm by minimizing bias mainly emanating from the multimodality of the transportation network is of great importance which shall be discussed in future contributions. Finally, investigating the possibility of using the proposed mapping algorithm at near real-time (NRT) for traffic monitoring is another direction of further contributions.

Chapter 5

Mode Classification with LCT-Mapper

5.1 Introduction

The particular advantage of studying individual trajectories over a multimodal transportation network is to investigate the multimodal mobility behavior of people in cities and urban areas. Due to the challenges of access to real, fine grain multimodal mobility data, any insight that can shed light on these issues is extremely precious. Investigating multimodal mobility behavior is important from different aspects: In urban planning, it helps improving the public transportation systems. In smart cities, it can assist in detecting the major mode changing hub nodes which can lead to improving public transportation access and facilities. Human mobility studies are interested in exploring individuals behavior in using different transportation layers. Last but not least, it helps investigating, monitoring and predicting congestion in urban areas. However, in order to investigate large scale multimodal mobility behaviors, it is essential to have a mechanism to obtain and perceive multimodal trajectories of individuals. It would have involved detecting the usage of transportation modes so that we would be able to distinguish the mode changes points. Transportation mode inference has recently become an important issue because it can reveal valuable insights about peoples behavior. In civil and transportation engineering fields, an extensive study of a travel survey provided valuable information about the usage of different transportation modes [56]. We have been inspired by this work to adapt some definitions regarding transportation mode for our current study. It should be noted

that not many studies could investigate the transportation mode detection problem without having access to fine-grain data in metropolitan areas. Wang et al. [81] proposed a model that uses CDRs to infer the percentage of travelers using a given transportation mode. They used travel time distribution and clustered travelers in different subgroups according to their travel time. Concerning individual trajectories, researches have tried to classify transportation modes for long range trajectories [69] [30]. The approaches above using cellular data show that inferring the transportation mode for urban mobility and in metropolitan areas still remains a challenge.

In Chapter 4, we proposed *CT-Mapper* as a solution to infer the real trajectory of smart phone users based on their sparse cellular trajectories. Since *CT-Mapper* is an unsupervised estimation algorithm and does not need labeled data to infer the parameters, it can be easily adapted for a large amount of data to infer population trajectories. Nevertheless, it has some limitations in mode detection. As described in 4, *CT-Mapper* maps the sparse cellular trajectory over the multimodal transportation network. Therefore, an inferred path can contain nodes from different transportation network and correspondingly, deducing the transportation mode from a set of nodes belonging to different layers is not always straightforward.The multilayer network modeling exponentially increases the number of paths between a given source and destination. Subsequently for a given trajectory, one can find several paths that might be extremely similar. This complexity imposed by aggregating different transportation networks, makes mapping more difficult. This chapter is focused on this issue with the objective of proposing a solution for the problem of mode detection. We present a solution in which we reduce the mode changing complexity by representing the multimodal transportation networks in two main class-layers. Concretely, we propose **LCT-Mapper** (Layered CT-Mapper) with the supplementary objective of uncovering if the user is on rail class-layer or he/she is on the road class-layer.

LCT-Mapper is built on with a transportation mode detection procedure augmenting the unsupervised mapping algorithm. We first represent the multimodal transportation network in two separated class-layers, namely *Rail class-layer* and *Road class-layer*. Then, the mapping algorithm is performed separately on each class-layer and the result is the most likely path of the users on each class-layer associated to the given cellular trajectory. Subsequently, the algorithm uses a classifier to choose the best path and infer the real class-layer corresponding to the observation sequence. *LCT-Mapper* provides a direct interpretation for the mode detection problem. This interpretation is acquired by avoiding multiple changes between different transportation layers which causes errors in mode detection for *CT-Mapper*. To do this, we
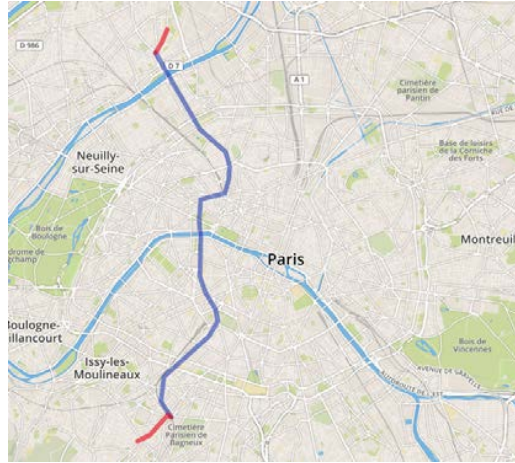
FIGURE 5.1: Instance of a trajectory in multimodal transportation network in Paris and vicinity. An individual walks from origin to metro station and from metro station to final destination (red lines) . This trajectory in mode detection problem is considered as unimodal trajectory which is metro (blue line)

cluster the multimodal transportation network into two class-layers in which we allow mode changing only between specific transportation layers. Domenico et al. in a recent study [28] showed that a multiplex can be reduced to a proper proportion in order to reduce the complexity. Inspired by this work, we reduce the multiplex of [road+train+subway & tram] to two main clusters: rail and road networks.

In this study, we define the *'Main mode'* of a trajectory as the transportation mode that covers the largest portion of the trajectory. **Our objective, then, is to infer the main transportation mode given a user sparse cellular trajectory.** It is worth noticing that walking is almost always part of a trajectory. This is obvious when individuals walk to and from stop stations of the public transport system, but using the car also requires walking to and from the parking place, although the involved distances might be short. Walking can thus be considered as a universal component at the start and the end of any trajectory, and is therefore not considered as a separate mode in the definition of a multimodal trip. Individuals who walk to the bus stop, ride the bus, and walk from the stop to their destination thus make a unimodal trajectory.

Figure 5.1 illustrates an example of real trajectory in multimodal transportation network in Paris and region separated by different colors each associated to one specific mode. The beginning and end of the trajectory consists of walking to and from the

| Mode type | Mode | Transportation Network | |
		Functional type	Carrier type
Private	Walking	Pedestrain-allowed	**Road**
	Car driving	Private car-allowed	
	Bicycle riding	Bicycle-allowed	
	Motorbike	Motorbike-allowed	
	Taxi	Taxi allowed	
Public	Bus taking	Bus line	**Railway**
	Underground train	Underground line	
	Suburban train	Suburban line	
	Tram train	Tram line	

TABLE 5.1: Transportation Modes and Networks [54]

subway station. This trajectory is considered unimodal and the objective is to infer the *main mode* which in this example is subway.

The rest of this chapter is organized as follows: section 5.2 presents the mapping algorithm framework with emphasis on the novel additional mode classifier component of *LCT-Mapper*. Subsequently, section 6.5 provides the evaluation results to assess the efficiency of our proposed approach compared to previous models and under different circumstances. Then we discuss the obtained results and conclude the chapter.
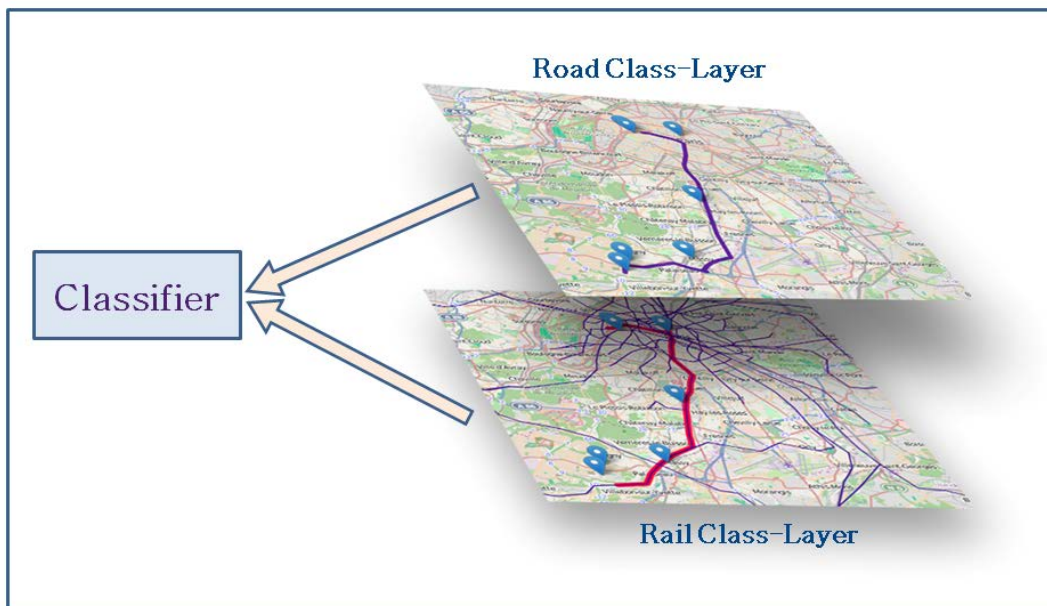

FIGURE 5.2: Mapping Cellular trajectory over 2 class-layers with a classifier to chose the best match among the two likely path

5.2 LCT-Mapper System Overview

This section starts with problem statement in which we formulate the objective addressed in the previous section. Then, we present the framework of LCT-Mapper with emphasis on the supplementary element of the mapping algorithm which is the class-layer classifier. Since LCT-Mapper is the ameliorated version of CT-Mapper, for the common components of the algorithm, we refer to chapter 4 where CT-Mapper has been elaborated in details.

5.2.1 Problem Statement

This section contains basic mathematical definitions that are required to formulate the problem.

Definition 1. Multilayer Transportation Graph - We define graph $\mathbf{G} = (V, E, L, \Psi)$ in which V, E are the vertices and the edges of the graph. L is the set of all considered layers (road, train, subway, tramway). Function Ψ indicates the layer of each node by mapping each node to a layer. $\Psi : V \rightarrow L$ in $\mathbf{G}$.

Definition 2. Class-layer Graph - We define the Class-layer graphs G_{Road} and G_{Rail} as road class-layer and rail class-layer where:

$$G_{Road} \subset \mathbf{G}, \text{ and } \forall \ v_i \ \in \ G_{Road}, \ \Psi(v_i) = \{\text{Road}\}$$

$$G_{Rail} \subset \mathbf{G}, \text{ and } \forall \ v_j \ \in \ G_{Rail}, \ \Psi(v_j) = \{\text{train}|\text{subway}|\text{tram}\}$$

Each class-layer is a connected component, a subset of multimodal transportation graph $\mathbf{G}$. In other words, we split the multimodal transportation network into two main class-layers.

Definition 3. Cellular Network - As described in section 4.3.1, the cellular network is defined as the set of cell towers $C = \{c_0, c_1, ...c_P\}$, where each cell tower $c_p = < lat, lon, r^{max} >_p$ is characterized by its latitude and longitude in the geographical coordinate system and by r^{max} that is the maximum distance of the center of the voronoi cell from its corners. Please note that the location of each cell tower usually does not coincide with the location of any intersection in the transportation network i.e., $\forall v_i \in V$, $\forall c_p \in C$, we have $< lat, lon >_p \ \neq \ < lat, lon >_i$.

Definition 3. Sparse Cellular Trajectory As defined in chapter 4, a sparse cellular trajectory of a user is defined as $O = o_0 \rightarrow o_1 ... \rightarrow o_M$ and each time-stamped location $o_t = < c(t) >$ refers to the specific antenna cell at time-stamp t.

Trajectory Mapping and Mode Classification Problem - Given the transportation network containing two class-layers G $= \{G_{Road}, G_{Rail}\}$, the cellular network C, and a user sparse cellular trajectory O, the search problem is to find a sequence of intersections $v_0 \rightarrow v_1 ... \rightarrow v_q$ as the most likely path and the associated transportation mode associated with the retrieved path.

5.2.2   Algorithm Framework

The fundamental features of LCT-Mapper that enables it to outperform CT-Mapper are:

I) To split the multimodal transportation network into class-layers.

II) Applying a classifier to determine the best match among the two likely paths each associated to a class-layer.

Given the transportation network $G = \{G_{road}, G_{Rail}\}$, the cellular network C and a user sparse cellular trajectory O, the mapping algorithm determines the most likely path over each of the two class-layer G_{road} and G_{Rail}. As mentioned, the core of mapping algorithm in LCT-Mapper is implemented as the same manner of CT-mapper. This core algorithm explained in section 4.3.4, is designed in two main phases:

Skeleton Sequence Search - In the first phase, the Viterbi decoding algorithm is applied to find the most likely sequence of nodes separately for each class-layer . Given the cellular trajectory $o_0 \rightarrow o_1, ... \rightarrow o_M$, the result for this phase is two separated sequences:

1) Road class-layer skeleton sequence $v_0 \rightarrow v_1, ... \rightarrow v_M$ where $\forall v_i, \Psi(v_i) = \{Road\}$

2) Rail class-layer skeleton sequence $v'_0 \rightarrow v'_1, ... \rightarrow v'_M$ where $\forall v'_i, \Psi(v'_i) = \{Rail\}$

Notice that in this step, there are trajectories for which the rail class-layer skeleton sequence is empty {}. This case happens when the trajectory takes place in an area which is not covered by the rail class-layer. (As pointed out in chapter 3, the area of study in our work is Paris an vicinity and we showed that not all the area is covered by the rail transportation layer.

Adjacent Sequence Completion - The two class-layer skeleton sequences serve as the input of the second phase to obtain the complete sequence of nodes where each two consecutive nodes in the sequence are adjacent in their associated class-layer. Given the skeleton sequence $\overset{*}{v}_0 \rightarrow \overset{*}{v}_1... \rightarrow \overset{*}{v}_M$, for each pair of consecutive intersections $\overset{*}{v}_i, \overset{*}{v}_{i+1}$ that are not adjacent in class-layer G_{Road}, the algorithm searches the optimal sequence of intersections $v_{i_1} \rightarrow v_{i_2}... \rightarrow v_{i_k}$ and inserts the newly-searched sequence between the two intersections $\overset{*}{v}_i, \overset{*}{v}_{i+1}$ as:

$$\overset{*}{v}_i \rightarrow \underbrace{v_{i_1} \rightarrow v_{i_2}... \rightarrow v_{i_k}}_{\substack{\Uparrow \\ \text{Recovered path}}} \rightarrow \overset{*}{v}_{i+1} \tag{5.1}$$

as the complete adjacent sequence. Please note that each two consecutive nodes in the newly obtained sub-sequence are adjacent in multiplex G_{Road}. It is important to notice that the same procedure is performed for both class-layers. Consequently, at the end of this step, the results are two sequences of adjacent nodes, one associated to G_{Road} and one for G_{Rail}.

The two inferred paths as illustrated in figure 5.2 serve as the input of the **Class-Layer Classifier** which selects the best match for the given cellular trajectory among the most likely paths. In the following section it is explained how the Class-Layer Classifier performs.

5.2.2.1 Class-Layer Classifier

As mentioned, the foremost improvement of *LCT-Mapper* is the classifier to determine the correct class-layer for a given cellular observation. Accordingly, the parameters of the classifier play a key role in algorithm performance. The classifier takes as input the two likely paths that each one is the result of mapping algorithm on the class-layer G_{Road} or G_{Rail}.

Definition - We define p_{road} as the likely path on G_{Road} and p_{rail} as the likely path on G_{Rail}, we also define l_{road} as the length of the likely path p_{road} on the G_{Road}. Accordingly, l_{rail} will be the length of p_{rail} on the G_{Rail}.

Classification Problem - Given two likely paths p_{road} and p_{rail} with l_{road} and l_{rail} as their lengths, and cellular trajectory O, the classifier selects one of the paths as the best match for the cellular trajectory O.

In designing the classifier, there are several parameters that can be considered in the classification problem, such as stretch factor [17] and similarity between cellular trajectory and obtained skeleton similarity. Following, we elaborate on these parameters and how they can be employed in the classifier.

- **Stretch Factor**. The stretch factor is defined as the ratio of the actual distance traversed on a given trajectory to that of the shortest distance between the origin and destination [31]. Using the mathematical definition of stretch factor [68] in class-layer selection, the classifier selects the class-layer which its associated likely path has smaller stretch factor:

$$L = \arg \min_{\forall \ i \in class-layer} \frac{d_{p_i}(x,y)}{d_{G_i}(x,y)} \tag{5.2}$$

$d_{p_i}(x,y)$ is the length of the most likely path between x and y inferred by the mapping algorithm on class-layer G_i and $d_{G_i}(x,y)$ is the length of shortest path between x and y over class-layer i.

- **Similarity Scores** - The second approach to select the best match among the two class-layers is to compare the two most likely paths with the cellular trajectory. For the comparison, we propose two different metrics:

  1. Root Mean Square Error (RMSE) for a set of points is the square root of the average of squared differences between each two compared points.

$$RMSE = \sqrt{\frac{1}{n} \sum_{i=1}^{n} (x_i - \hat{x}_i)^2 + (y_i - \hat{y}_i)^2} \tag{5.3}$$

  Using RMSE for class-layer selection means that the most likely path with minimum RMSE between skeleton points and cellular observation is selected as the best match:

$$L = \arg \min_{\forall \ i \in class-layer} RSME \tag{5.4}$$

  2. Path length similarity - Using length similarity between the most likely path and cellular observation, the class-layer whose most likely path has

closer length to the cellular trajectory length is selected as the best match.

$$L = \arg \min_{\forall \ i \in class-layer} |l_c - l_{r_i}| \tag{5.5}$$

The classifier then returns the selected class-layer as the best match and sets its associated most likely path as the inferred most likely path.

5.3 Discussion

The previous section outlined the framework of the classifier and listed the potential parameters that classifier can use for classification task. These parameters are probed independently, nevertheless all can be employed in an aggregation function to derive a fuzzy classifier that also assigns a degree of certainty to the final result.

Our proposed approach presented in *LCT-Mapper* can raise a question that what about the precision and information lost that result endures. It is worth to recall that cellular signalization data used in this study, offer a novel level of temporal and spatial granularity which is not as accurate as fine-grain mobility data such as GPS location data. Besides, sampling rate of 15 minutes for cellular observation, prevents us from fine-grain investigation to extract detailed sub-trajectories of an individual during a trajectory.

In addition, taking into consideration the temporal sparsity of cellular trajectories with the spatial resolution of antenna level, it is fair that differentiating between private cars and taxis or identifying the mode change from riding a bus to walking to or from a point is problematic. However deriving an approach that distinguishes the main transportation mode between (road, train and metro) is an outstanding attainment.

5.4 Conclusion

In this chapter we proposed *LCT-Mapper* by improving the mapping algorithm proposed in *CT-Mapper* to detect the main transportation mode of trajectories with a fair accuracy. This refinement obtained by separating the multimodal transportation network into two class-layers and designing a classifier which distinguishes the best match among the two most likely inferred paths.

Splitting the multiplex transportation network into two class-layers, namely *Road* and *Rail* class-layers, reduces the complexity of multiplex network. Moreover, this approach enables us to obtain a straightforward solution for the mode detection problem. Nevertheless, this separation imposes a specific limitation into the mapping problem which can be mentioned as disadvantage of this approach. Since the classifier selects one of the two class-layers, loosing some precision in mapping is unavoidable. This can be accepted as a satisfactory compromise given the limited spatial resolution of the cellular data.

It is expected that this method provided efficient solution for the problem of trajectories' main mode inference. In the next chapter, the results of this algorithm are evaluated and will be compared with the result of *CT-Mapper* in both, trajectory mapping and trajectory mode detection. In case of a fair trade-off between the two objectives, meaning the mapping algorithm from one side and the mode inference problem from another side, this methodology with respect to the unsupervision of all the steps, can be considered as a precious approach to analyze the cellular mobility data in large scale.

Considering the spatial resolution of cellular observations along with the temporal sparsity of data [which in our study is not as sparse as CDRs but less frequent than GPS track (1-2 minutes)] induces a novel level of spatial scale for efficient study of trajectories. This novel scale in current study was obtained by partitioning the multimodal transportation network into 'Road' and 'Rail' class-layers. This approach leads to an efficient solution for sparse cellular trajectory mapping by restricting the mode changing actions.

Chapter 6

Algorithms Validation

6.1 Introduction

In this chapter, we present the experiments carried out to validate our proposed model, and we provide analysis tools to assess the model's effectiveness in reaching the stated objectives.

In the previous two chapters, two mapping algorithms, the so-called *CT-Mapper* and *LCT-Mapper*, were proposed to map cellular trajectories over the multimodal transportation network and to infer the main transportation mode of users. As stated previously, the two proposed methods are based on unsupervised inference models in which no labeled data are used for training the models. As described in chapter 3, two datasets have been collected for the sake of evaluation and validation:

1. Cellular sparse trajectories, provided by French telecom company, from a group of volunteers during 1 month. This dataset was obtained by sampling the cellular location of users with a frequency of 15 minutes. The test dataset contains 80 trajectories (section 3.2)

2. GPS data for the participants have been collected to serve as ground truth for the evaluation procedure. (section 3.3)

Figure 6.1 illustrates an example of the result provided by the *CT-Mapper* mapping algorithm (colored in orange) along with the GPS trajectory that is colored in blue. Although visualization of the mapping results may be seen as an approach to evaluate the overall quality of mapping algorithms, quantitative measures are required

in order to objectively assess the performance of the latter. For a comprehensive assessment of the performance of mapping algorithms, we use a set of metrics, namely, sequence similarity score, Recall, Precision and F-measure. Furthermore, to evaluate both phases of the mapping algorithm, we evaluate separately two results : skeleton sequence similarity and complete sequence similarity. The next section provides a brief description of these measures. Subsequently, we present the result of computing different metrics for our obtained results. In order to establish validity of our proposed algorithm, we also derive a baseline algorithm and an extensive set of comparison have been performed between baseline model and our proposed models using evaluation metrics.

Before explaining the evaluation metrics, some description regarding the experiments is necessary.
- The result of the mapping algorithm for each trajectory is a path on the multimodal transportation network.
- To obtain the ground truth, collected GPS data have been mapped over the same multimodal transportation network.
- Despite the fact that GPS fine-grained data and cellular sparse trajectoreis are mapped over the same transportation network, comparing fain-grained GPS data with result of noisy cellular data mapping without considering any authorized error, raises some critics. Correspondingly, we use (Root Mean Square Errors) as a measure to use as threshold to find the match points. Following, we briefly explain how we employed different accuracy measures for evaluation and validation purpose.

6.2 Metrics For Performance Evaluation

6.2.1 Root Mean Square Error

Root Mean Square (RMS) Error is the difference between the desirable point (ground truth) and the inferred point. Mathematically the RMS error is:

$$\text{RMS error} = \sqrt{(x - \hat{x})^2 + (y - \hat{y})^2} \tag{6.1}$$

where (x, y) is the ground truth coordinates and $(\hat{x}, \hat{y})$ is the output coordinate. Similarly, the Root Mean Square Error (RMSE) for a set of points presented in equation 6.2 is the square root of the average of squared differences between collected
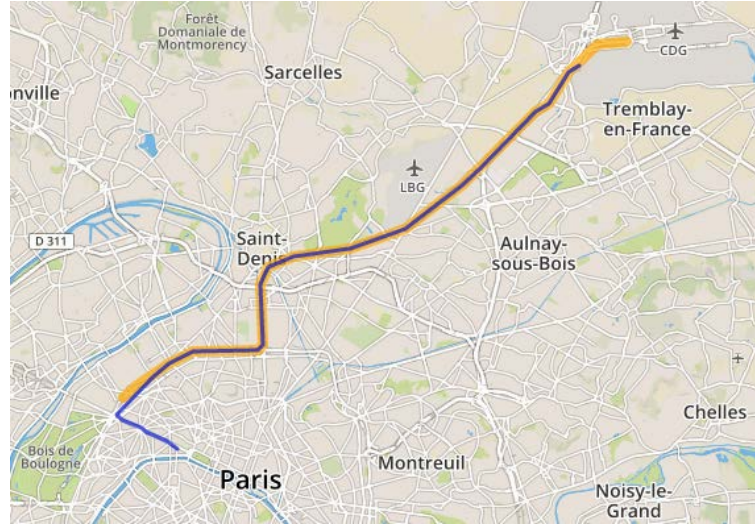
FIGURE 6.1: CT-Mapper's result in orange and GPS trajectory is the blue line.
The two trajectories are compared using different evaluation metrics.

coordinates and coordinates from an independent source of higher accuracy ("ground truth") for identical locations.

$$RMSE = \sqrt{\frac{1}{n} \sum_{i=1}^{n} (x_i - \hat{x}_i)^2 + (y_i - \hat{y}_i)^2} \qquad (6.2)$$

It is a frequently used measure of the differences between values (Sample and population values) predicted by a model or an estimator and the values actually observed. The use of RMSE makes a general purpose error metric for numerical predictions. Compared to the similar Mean Absolute Error, RMSE amplifies and severely punishes large errors.

In our evaluation, the RMS error has been used for two purposes:

1. The first one is to quantify the overall distance between the algorithm result and the real GPS trajectory as ground truth. Figure 6.2 illustrates an example of two trajectories, where the red line is the real trajectory and the blue line is the algorithm result. Considering the different points (marked in blue and red markers), the RMS error is calculated using equation 6.2.

2. The second purpose is to use RMS error to detect matches between 2 points using threshold ϵ. In this case, if the RMS error between two points is smaller
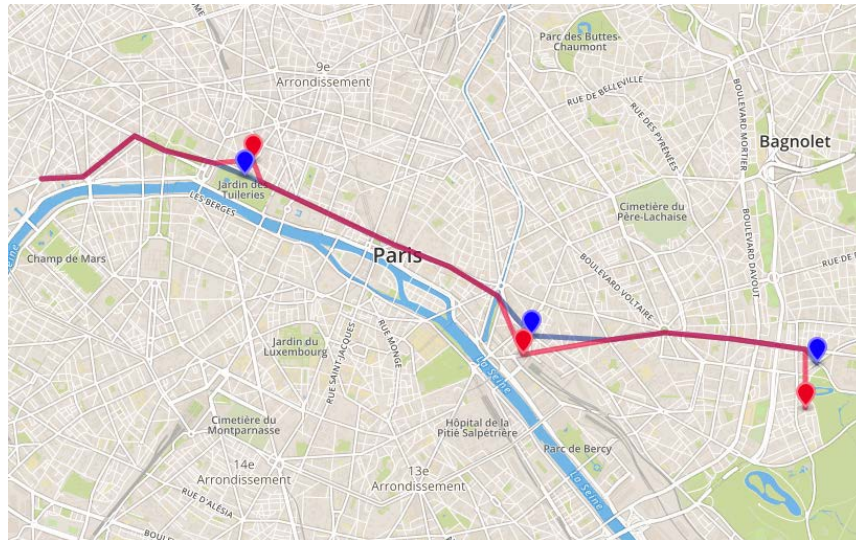
FIGURE 6.2: Example of using RMSE for comparing two trajectories

than ϵ, we consider the inferred point as a match (using equation 6.1). Figure 6.3 shows an example illustrating an error between the inferred path and the real path. If the RMS error between two points is smaller than ϵ, the inferred point will be considered as a match; otherwise, it will be a miss-match for the source point.

6.2.2 Edit Based Similarity Score

In order to evaluate the proposed mapping algorithm, we need to assess how similar are the Cellular trajectory mapping result to the ground truth *GPS trajectories.* Similarity score $sim(x, y)$ quantifies the similarity between x, y where x and y are two sequences. It is important to take into consideration that the two sequences are not necessarily from the same length. Thus, we use Edit distance [23] which is so named because it can also be thought of as the minimum number of edits (insertions, deletions, and substitutions) needed to transform one sequence into the other. The flexibility of Edit Distance is that it is possible to give different cost to different types of edits and it can be employed to compare sequences of two different length. In addition it is computed optimally based on dynamic programming algorithm.

Edit Distance or Levenshtein distance: The basic form, where each edit has cost 1, is a dynamic programming algorithm that computes the distance between 2 strings x and y). However in our case, we do not have strings of letters, but locations, so we
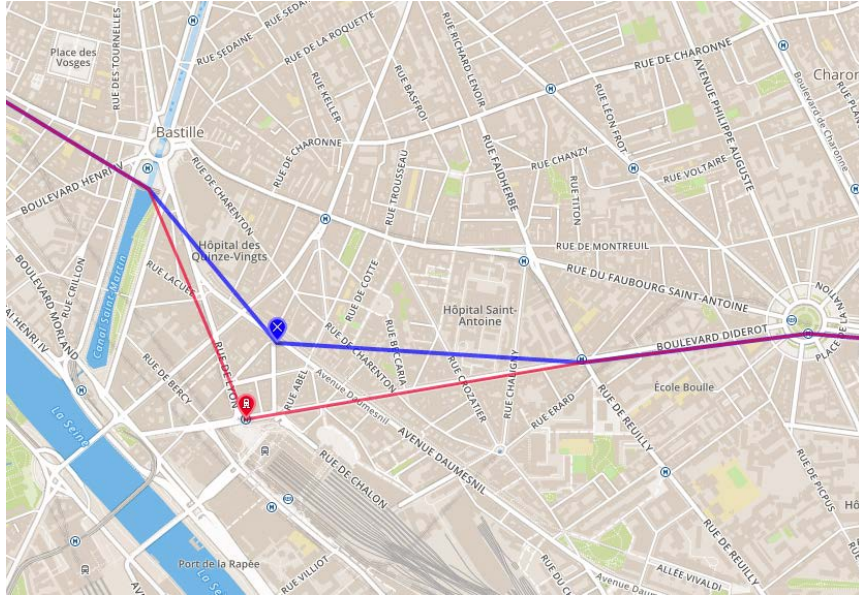
FIGURE 6.3: example of how RMSE can be used as a threshold, the red marker showes the ground truth and the blue marker is the inferred point. the RMS error between two points is 263 meters; it means that for threashold smaller than 263 meters the blu point is miss match and othervise it is a match for the point indentified with red marker

define the costs as distance between locations. This algorithm in [82] is mentioned as Edit distance with Real Penalty (ERP). Consequently, instead of 1, we use $cost = d(x[i], y[j])$ where d is the euclidean distance between location $x[i]$ and $y[j]$. Since the algorithm uses euclidean distance, the result is a metric measure. The modified algorithm is:

1. Initialize matrix $M_{(|x|+1)(|y|+1)}$

2. Fill matrix: $M_{i,0} = d(x[i], y[1])$ and $M_{0,j} = d(x[1], y[j])$

3. Recursion:

$$M_{i,j} = \begin{cases} M_{i-1,j-1} & \text{if } x[i] = y[j] \\ cost + \min(M_{i-1,j}, M_{i,j-1}, M_{i-1,j-1}) & \text{else} \end{cases}$$

4. Distance: $Dist(x, y) = M_{|x|,|y|}$

- Edit Similarity: $1 - \dfrac{Dist(x,y)}{max(|x|,|y|)}$

In conventional approach, each mismatch costs 1. In modified case, the cost of mismatch for (x,y), is $d(x,y)$ where d is the geographic distance between x and y.

6.2.3 Recall and Precision

Precision and Recall are the basic measures used for evaluating the results. Precision is the fraction of retrieved instances that are relevant. Recall (also known as sensitivity) is the fraction of relevant instances that are retrieved. Both precision and recall are based on an understanding and measure of relevance. In simple terms, high precision means that an algorithm returned substantially more relevant results than irrelevant, while high recall means that an algorithm returned most of the relevant results. When we talk about trajectories, one option is obtaining recall and precision using parameter 'length':

$$\text{Precision} = \frac{\text{Overlapped path length}}{\text{Result path length}} \tag{6.3}$$

$$\text{Recall} = \frac{\text{Overlapped path length}}{\text{Real path length}} \tag{6.4}$$

One issue with these measures however, is that the result is given by one absolute value for recall and precision, that take into account perfect local matches. For example, in figure 6.1, although given only 5 cellular observation, the obtained result looks fair enough, but the recall and precision obtained with equations 6.4 and 6.3 are 67% and 64% . Since the ground truth dataset comes from higher resolution, it is reasonable to consider a permitted error in our evaluation. Accordingly, in order to be capable of allowing an error for evaluation, we use the nodes of the graph for relevance measure rather that the length of the trajectory. In other words, if we define a trajectory as a sequence of nodes over the transportation graph, the aforementioned metrics can be represented as:

$$\text{Precision} = \frac{\text{Number of common (matched) nodes}}{\text{Number of result nodes}} \tag{6.5}$$

$$\text{Recall} = \frac{\text{Number of common (matched) nodes}}{\text{Number of real path nodes}} \tag{6.6}$$

With this formulation, a given allowed error can be considered in calculating match and mismatch between each two nodes.

6.2.4 F-Measure

the F_1 score (also F-score or F-measure) is a measure of a test's accuracy. It considers both the precision p and the recall r of the test to compute the score: p is the number of correct positive results divided by the number of all positive results, and r is the number of correct positive results divided by the number of positive results that should have been returned. The F_1 score can be interpreted as a weighted average of the precision and recall. the F_1 score reaches its best value at 1 and worst at 0. The traditional F-measure or balanced F-score (F_1 score) is the harmonic mean of precision and recall:

$$F_1 = 2.\frac{\text{precision. recall}}{\text{precision+recall}} \tag{6.7}$$

6.3 Dataset for Evaluation

In order to evaluate our proposed algorithms, GPS data are used as ground truth. We collected the cellular trajectories of 10 volunteer participants during one month (Aug-Sept 2014) with their corresponding GPS data. The GPS data were collected with the help of the application "Moves" [2] which was installed on participants' smartphones. The captured data were the sampled phone positions during user's movements as well as its activities classified in four different categories: 'Walking', 'Running', 'Cycling' and 'Transport'. Based on this dataset, a set of prepossessing steps were performed in order to extract trajectories mapped over the transport networks. Furthermore, trajectories whose lengths are shorter than 5 kilometers were filtered out from the database. Given the low sampling rate of cellular data (a data point every 15 minutes), it is not realistic to seek recovering a trajectory that lasts less than this threshold. The effect of this filter on the dataset distribution could be observed in Fig. 6.4a and Fig. 6.4b.

(A) Trajectory Time Distribution
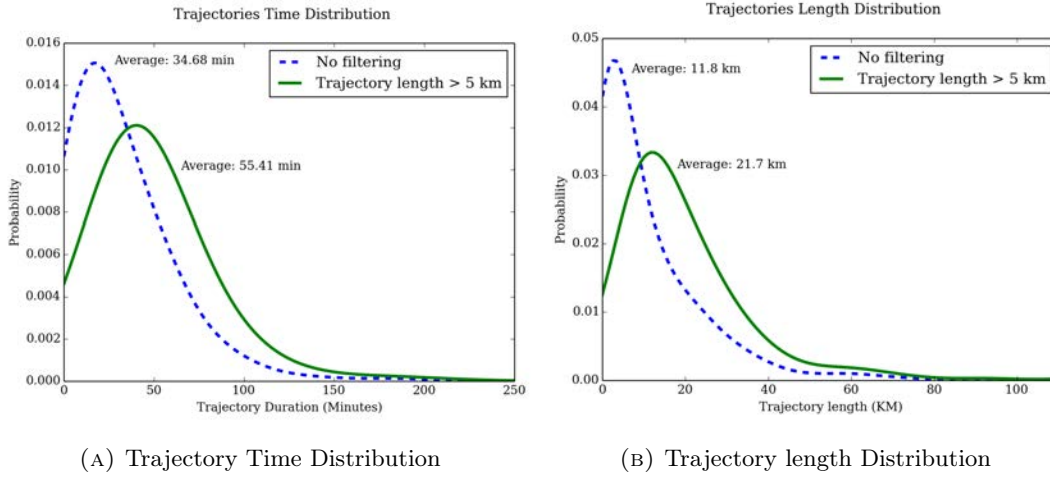
(B) Trajectory length Distribution

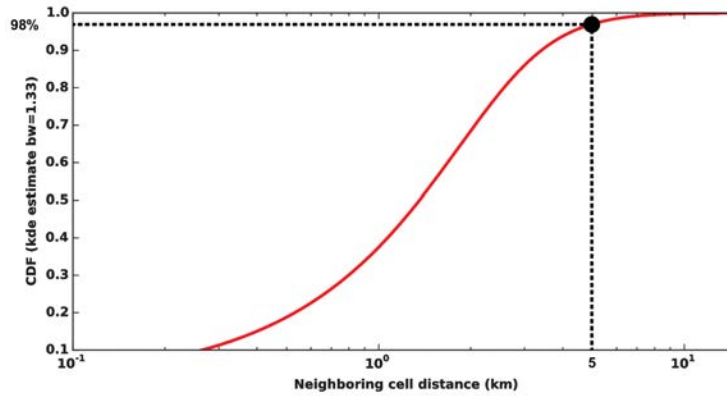FIGURE 6.4: Time distribution and distance distribution

FIGURE 6.5: Neighboring cell distance distribution

The spatial accuracy needed in order to distinguish a real mobility from noise depends on the distance between two base stations. In order to filter out irrelevant movements, we filtered out all the trajectories under the threshold x_{th} such that $P_r(X < x_{th}) = q$ where $P_r(X)$ is the distribution of distance between neighboring antennas. For $q = 0.97$, as Fig. 6.5 shows, all the neighboring distances are less than 5 kilometers.

As a conclusion, we built a dataset of 80 cellular trajectories (sequences of base stations) with their corresponding GPS paths mapped over a multilayer graph **G**. The multilayer transportation network contains around 16000 nodes and 26000 edges. The users trajectories covered a total distance of 2200 kilometers. The average number of observation points in each cellular trajectory is 5.55 and the average length of a trajectory is 26.5 kilometers.
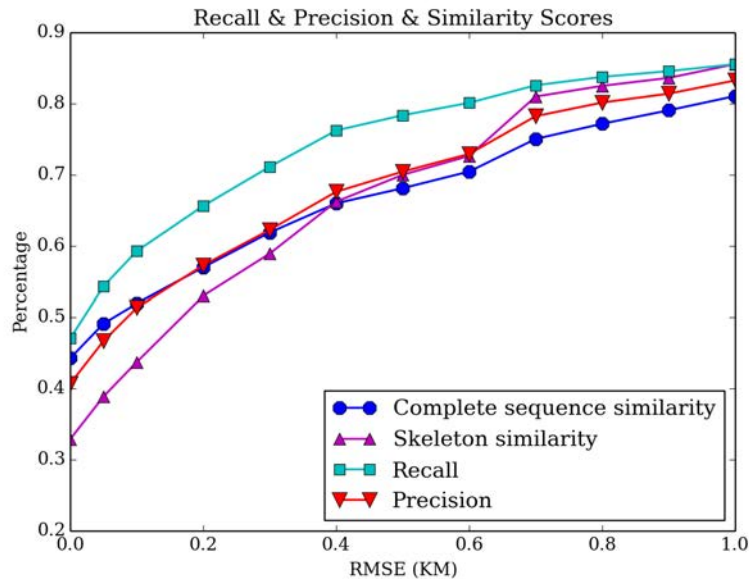
FIGURE 6.6: CT-Mapper Result Evaluation

6.4 CT-Mapper Evaluation

6.4.1 Algorithm Performance

To evaluate our algorithm, the aforementioned labeled dataset was used for test and evaluation. We performed *CT-Mapper* to map the cellular trajectories and to compare the result with GPS ground truth. It is important to notice that this comparison is performed between two trajectories which do not have necessarily the same length. Figure 6.1 illustrates the example in which the result of the *CT-Mapper* mapping algorithm (in orange) is plotted along with the GPS trajectory (in blue). To compare sequences of different lengths, we used the Edit distance between two sequences, consisting of the minimum number of single-location edits (i.e. insertions, deletions or substitutions) required to change one trajectory into the other. A short recall that the *CT-Mapper* was designed in two phases, with skeleton sequence as the result of phase one and complete sequence as the result of phase two. We evaluate both phases of the algorithm by calculating the edit-based similarity scores for each step. To have a comprehensive insight, we also calculate the average recall and precision of the mapping results. Owing to the considerable spatial noise of cellular observations, we used the RMSE (Root Mean Square Error) to identify the matched points between retrieved locations and real trajectory locations. For example, an error of

0.1 kilometers indicates that for each node in the output sequence, the node is considered as a match point if it is within a 0.1 kilometer radius of its corresponding real location. We calculated the four mentioned accuracy results (precision, recall, skeleton and complete sequence similarity score) for a range of fixed allowed RMSE on the obtained mapping results. The similarity scores are the complementary of the edit distance scores. Fig. 6.6 represents the result of this evaluation. As Fig. 6.6 shows, with allowed RMSE of 200 meters, more than 50% of skeleton and complete trajectories can be retrieved.

This is remarkable given the sparsity of the coarse grain cellular antenna positions with respect to real user trajectory (average of 5.5 observations per trajectory in the dataset while the average length is 26.5 *km*). It is important to mention that as the frequency of cellular data collection is 15 minutes, higher performance is expected for *CT-Mapper* when the sampling is carried out at higher frequency, . The average similarity score, for a RMSE of 1 kilometer, raises to 80%. In addition, *CT-Mapper* reaches a recall and a precision of around 80% when a RMSE of 1 kilometer is allowed. In addition to the metrics mentioned above, we compute the edit distance error not as the number of required edits, but by considering the euclidean distance as the cost of each required edit. The average of edit distances for all trajectories in the dataset is 0.79 kilometer.

6.4.2 Comparison with Baseline

The purpose of the baseline run is to establish the validity of the proposed model with specified parameters. As already mentioned, in the literature there exists no similar mapping solution that is as comprehensive as *CT-Mapper* and that considers a multilayer transportation network. Accordingly, to derive a baseline model , we keep the same framework of the mapping algorithm and attempt to validate the parameters of the algorithm by setting baseline parameters. To do this, one approach is to use the parameters of models that have been proposed for the mapping algorithm with modifications to adapt to current transportation network. **Baseline 1** is a simple model that snaps each observation to the nearest node in the network to find the skeleton and for the second phase, uses least-cost paths between them to retrieve the full path. The result of this baseline model is compared with *CT-Mapper* in Fig.6.7.

To evaluate our transition probability model based on the transportation network properties presented in eq.(4.8), we derive **Baseline 2**, an HMM based baseline model
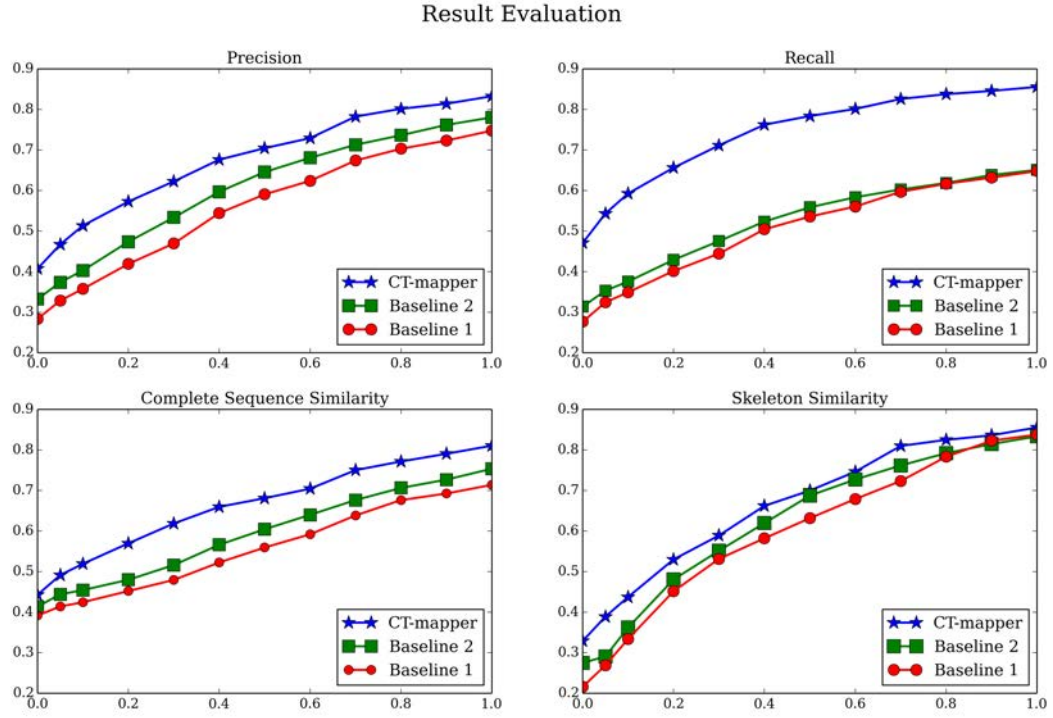
FIGURE 6.7: Up-left: Precision, up-right: Recall, bottom-left is Edit-based similarity scores and bottom-left is the skeleton similarity score

associated with the naive assumption consisting of setting equal probabilities for all outgoing transitions from each node (including self node transition). Under such a model, the transition probability between two nodes v_i and v_j is represented as:

$$Tr(v_i, v_j) = \left(k_i * \prod_{n \in Q} k_n \right)^{-1} \tag{6.8}$$

where $Q = SP_{v_i v_j} - \{v_i, v_j\}$ and k_i is the degree of v_i. This basic assumption considers all the multilayer network edges on equal footing irrespective of their layer transportation properties. Using this transition probability model, we build an HMM in the same way as *CT-Mapper* was developed. We use this model as a baseline algorithm and run it on the test dataset to compare the results with *CT-Mapper*. We calculate all four performance measures for the baseline algorithm. Fig. 6.7 compares the performances of the two models. As the figures show, there is up to 20% improvement in recall using our proposed transition probability model. Also, the average edit distance of the baseline algorithm result was 1.04 kilometer which proves that *CT-Mapper* performs significantly better compared to the baseline algorithm.

Fig. 6.8 shows the distribution of edit distance for both the baseline algorithm and *CT-Mapper*.
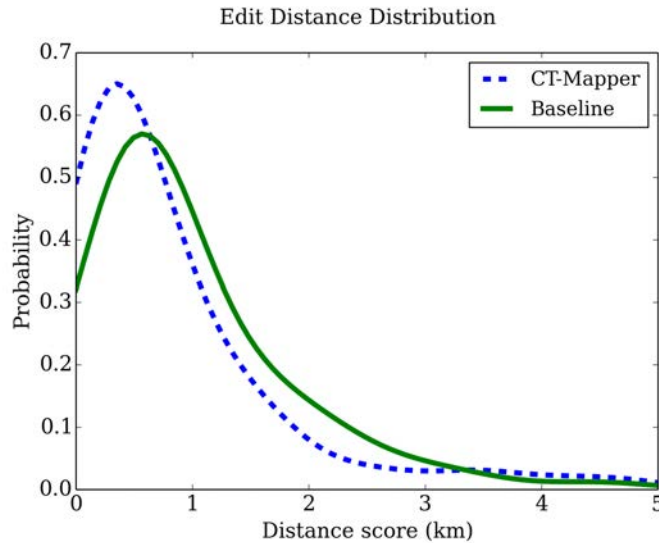

FIGURE 6.8: Sequence Edist Distance

6.4.3 Multimodality Analysis

In the next step of assessing our mapping algorithm, we investigate the accuracy of the mapping algorithm in transportation layer detection. As mentioned in section 4.8, the complexity of multimodal mapping significantly increases owing to the considerable topological differences between transportation layers. Since the multilayer transportation network provides the possibility of layer changing in any single trajectory, the result of mapping algorithm happens to be mapped on different transportation layers and some times the optimum path produced by mapping algorithm is splitted on different transportation layers. Accordingly, to analyze the performance of *CT-Mapper* in mapping on the correct layer, we calculate the recall and precision for correct layer detection for each layer. The overall recall and precision for the whole network is computed as the average of recall and precision for each layer, by counting the number of correct layer detected and we show this value for different transportation layer. Fig. 6.9 shows these measures compared with the baseline algorithm. It is important to notice that since each assumption considers specific aspect of network's topological properties, they might introduce a bias in the mapping problem that can impair the result compared to the baseline. As it is shown in fig. 6.9, the overall recall

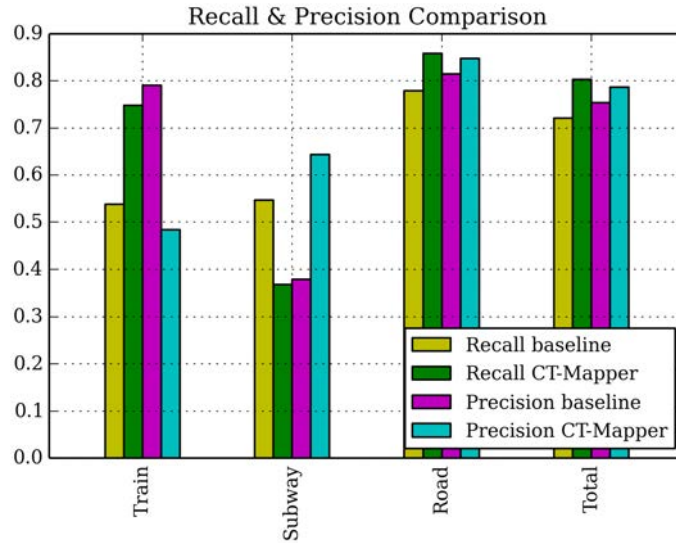and precision of correct layer detection is improved in *CT-Mapper* compared to the baseline algorithm.

FIGURE 6.9: Recall and precision in layer detection

6.5 LCT-Mapper Evaluation

The mapping algorithm with LCT-Mapper has been performed on our data set and different accuracy measures have been computed to evaluate the efficiency of *LCT-Mapper* compared to CT-Mapper and the baseline algorithm. We have investigated different parameters for the classifier.

6.5.1 Algorithm Performance

The first measure that we compute for the sake of evaluation is the average RMSE of trajectories for the obtained results. Figure 6.10 compares the error distribution of *LCT-Mapper* compared with *CT-Mapper* and the baseline model. While the average value of RMSE for *CT-Mapper* was 0.79 kilometer, it was reduced to 0.66 kilometer in *LCT-Mapper*. To assess the efficiency of *LCT-Mapper*, several experiments have been conducted to compute different evaluation metrics. Figure 6.11 illustrates all the metrics (recall, precision, F-measure, skeleton and complete sequence similarity) that have been computed with respect to a range of allowed values of RMSE. In order

to have a better perception of the improvement of *LCT-Mapper* compared to *CT-Mapper*, we provide an extensive comparative set of experiments to clearly assess the efficiency of *LCT-Mapper*.
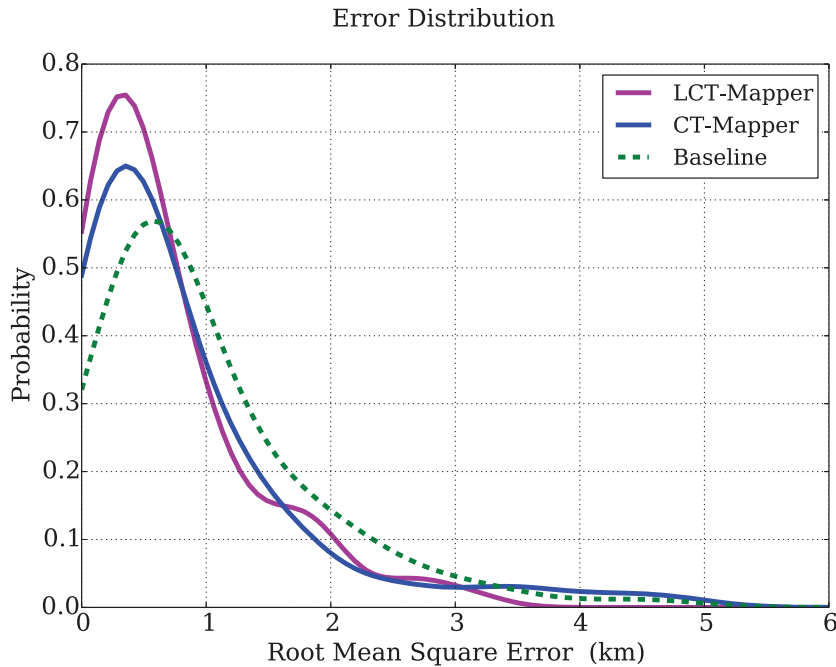

FIGURE 6.10: Root Mean Square Error (RMSE) Distribition

6.5.2 Comparison with Baseline and CT-Mapper

This section provides more comprehensive results by comparing different models: we compare the result of *LCT-Mapper* with *CT-Mapper* and the baseline model. Moreover, as mentioned in the previous section, the unsupervised classification can decide based on different measures; We conduct a set of experiments for different parameters of classifier to clearly determine the efficiency of *LCT-Mapper* under each condition. As stated in the previous section, to plainly compare the performance of mapping algorithm, the similarity score is computed for both phases results. Figures 6.12 and 6.13 illustrate the skeleton and complete sequence similarity scores of the *LCT-Mapper* result obtained from different classification models. In all the evaluations, we consider the value of RMSE as threshold to accept a match between the result point and the ground truth. Following, figures 6.14, 6.15 and 6.16 represent the precision, recall and the F-measure of the results computed to compare different mapping algorithms with respect to a range of allowed RMSE.
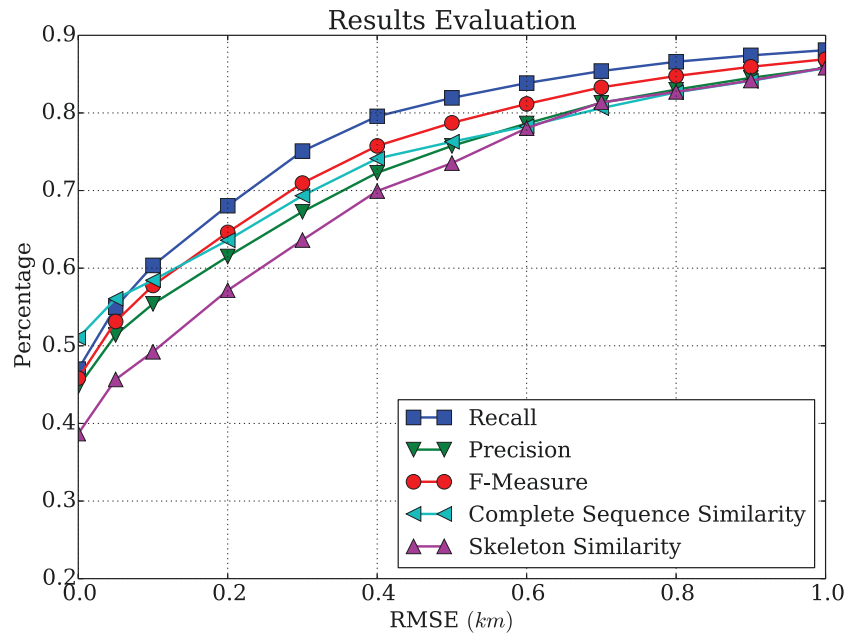
FIGURE 6.11: Different evaluation metrics have been caculated for LCT-Mapper with respect to a range of allowed RMSE

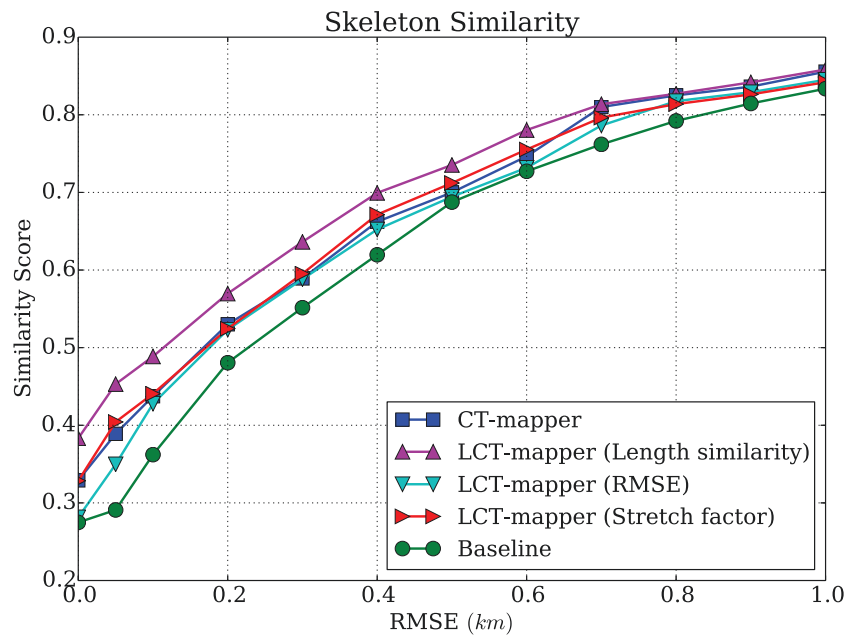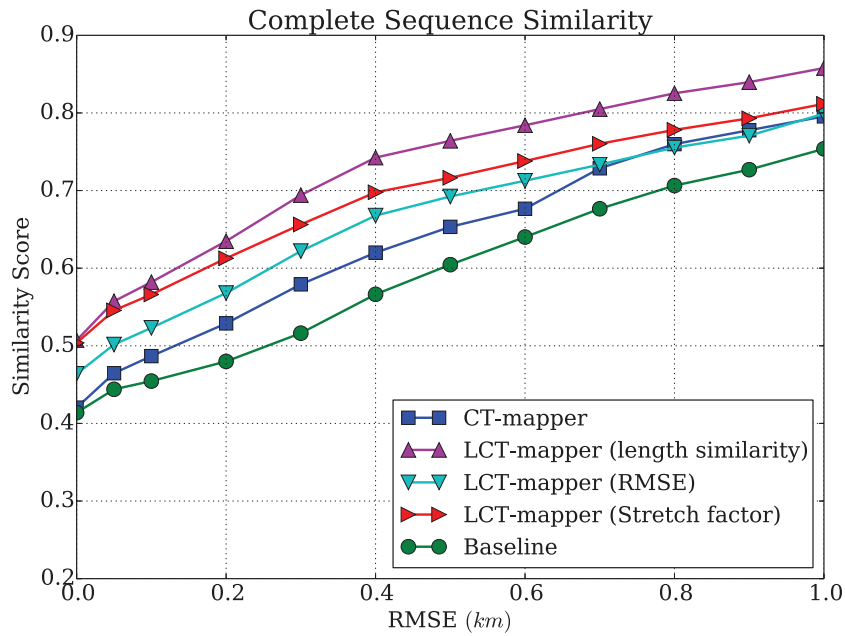FIGURE 6.12: Skeleton similarity LCT-Mapper compared to baseline and CT-Mapper

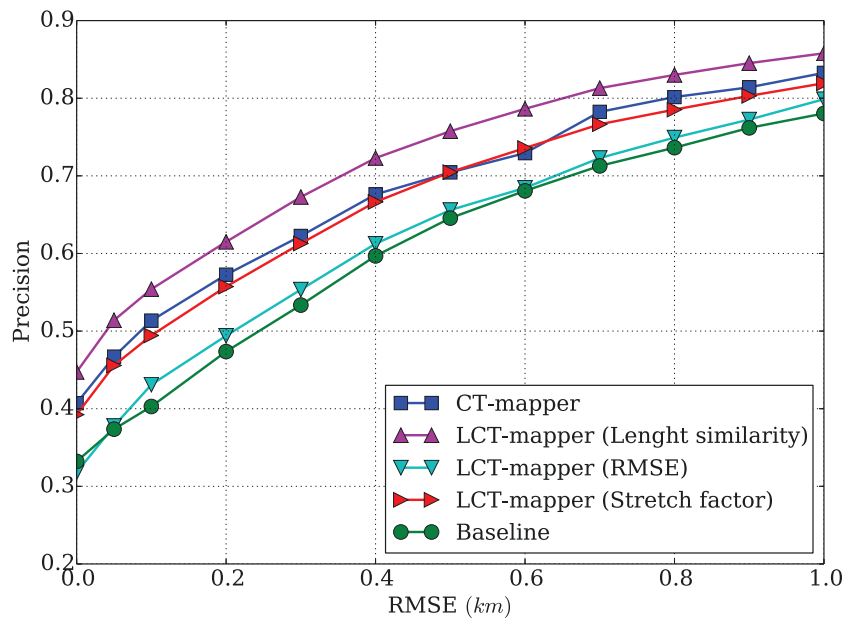FIGURE 6.13: Complete sequence similarity LCT-Mapper compared to baseline and CT-Mapper

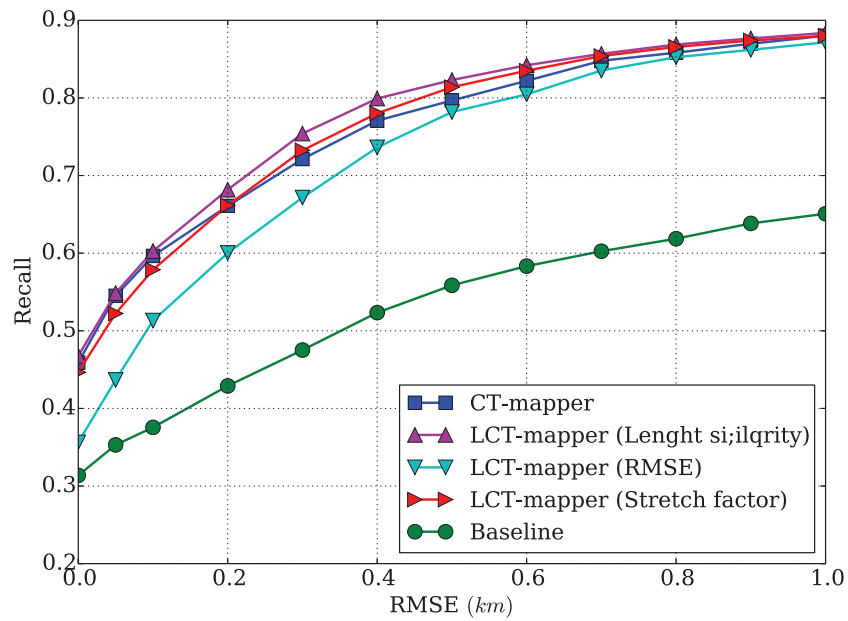FIGURE 6.14: Precision calculated for LCT-Mapper compared with CT-Mapper and baseline

FIGURE 6.15: Recall calculated for LCT-Mapper compared with CT-Mapper and baseline
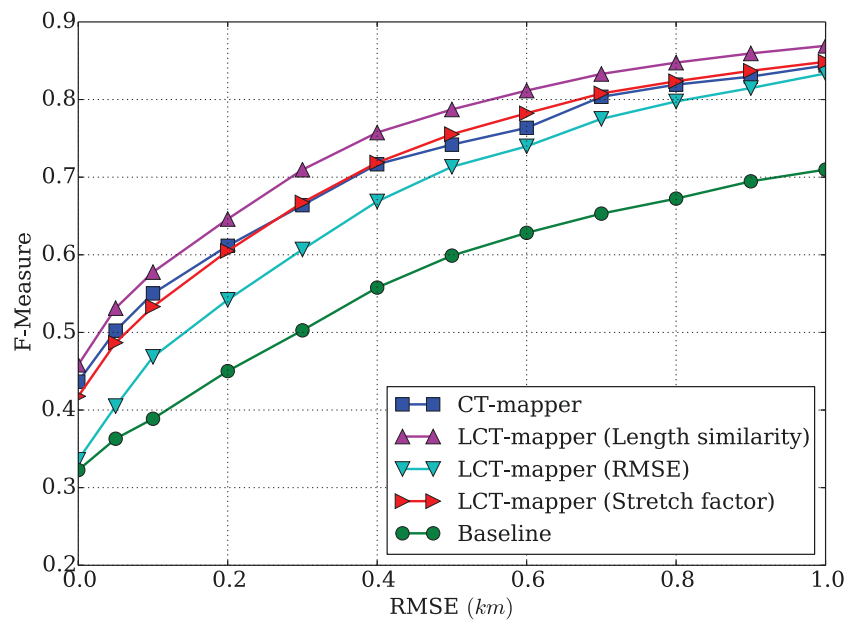

FIGURE 6.16: F-measure calculated for LCT-mapper compared to CT-Mapper and baseline

As the figures illustrate, among the three analyzed factors, the length similarity performs better that stretch factor and RMSE measure, and then stretch factor stays in the second place. The plots show that *'length similarity'* yet simple but effective measure for the class-layer classifier performs better than *CT-Mapper* from different aspects.

6.5.3 Mode Classification

In this section we analyze the efficiency of *LCT-Mapper* in mode detection. This task in *LCT-Mapper* is straightforward by designing the classifier which infers the class-layer that individuals have taken during their real trajectories. The result of classifier is either *'Road'* class-layer or *'Rail'*. We computed recall and precision of this classifier using different parameters for the classifier. As figure 6.17 illustrates, the unsupervised classifier can infer the class-layer associated to the main trajectory mode with 0.83 percentage of accuracy. This performance is a significant achievement considering that the overall mapping phases and classifier are conducted without using any labeled data.
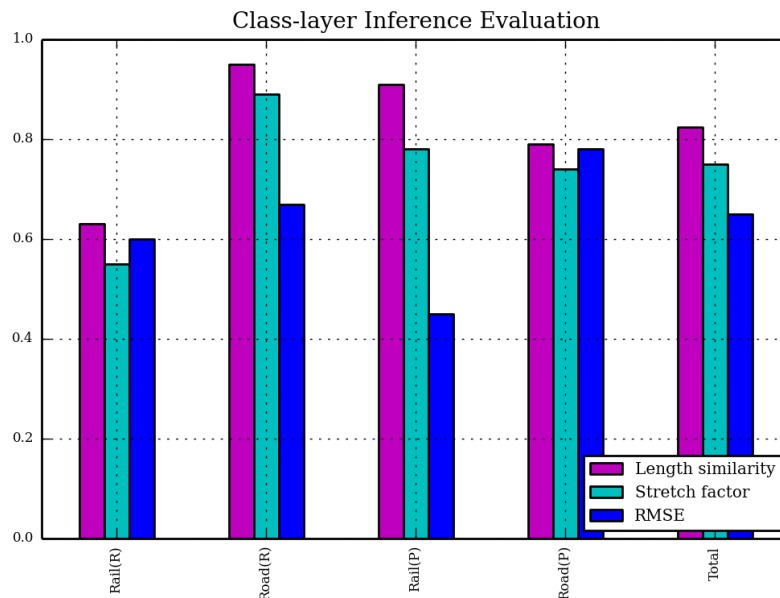

FIGURE 6.17: The performance of classifier in class-layer inference have been computed by two measures: Recall (R) and Precision (P) for both class-layers Rail and Raod. The Right column shows the overal accuracy of classifier that was obtained using different factors

6.6 Discussion & Conclusion

In this chapter we provide an extensive range of evaluations to evaluate and validate the two algorithms *CT-Mapper* and *LCT-Mapper* proposed in the previous chapters. We carried experiments on a test dataset of 80 real multimodal trajectories collected from 10 participants during one month (Aug-Sept 2014) to evaluate our algorithms. Considering the sparsity of cellular observations (with a frequency of 15 minutes), the percentage of retrieved paths of smartphone users is notable. To validate our transition probability model, we compared it with a baseline algorithm that does not take into account the transportation properties of each layer and the results show up to 20% of accuracy improvement of the first over the second. This shows that our transition model better accommodates the complexity of the multimodal transportation network. Since for average speed over the edges only static values are considered, it is expected that using a dynamic weight matrix which is compatible with the traffic model at different times of the day, is likely to enhance further the mapping results.

The accuracy of results obtained from different alternative parameters of *LCT-Mapper* were computed and compared to *CT-Mapper* and to the baseline model. As discussed previously, in spite of loosing some precision in cases where mode changing occurs between the two distinct class-layers, separating the transportation layers in two main class-layers allows *LCT-Mapper* to improve the overall transportation mode detection performance. This result confirms that given limited spatial resolution, a good compromise can be reached by trading off lost of precise multimodal trajectory inference against a better main transportation mode detection. The results also shed light on the complexity of multimodal transportation behaviors of people in metropolitan areas by raising questions such as: is there in reality any preference in mode changing behavior of people? Can we conclude from our obtained results whether people tend to change modes within class-layers rather than between them? These questions deserve more investigations to be conducted in future works. The classifier of *LCT-Mapper* infers the main mode of the trajectories with around 83% accuracy. This achievement is considerable given the fact that no labeled data were used to train the model. Moreover, this performance is expected to be improved by injecting new knowledge from either transportation systems or cellular sensors behaviors.

Chapter 7

Conclusion

This PhD research provides a novel solution to the high demanding problem of multimodal mobility analysis of large populations in metropolitan areas. It proposes an unsupervised mapping algorithm that maps sparse cellular trajectories over the multimodal transportation network of the considered metropolitan area. We then adapt this algorithm to propose a new solution for transportation mode detection.

This chapter summarizes the contributions of the thesis and points out its strengths as well as its limitations. Finally, the opportunities that our research creates for further works are presented.

7.1 Contributions

According to the objective defined in this thesis, we proposed a mapping algorithm that maps sparse cellular data, associated with signalization data of smart phones, over the multimodal transportation network of the considered metropolitan area. The mapping algorithm is able to estimate the real trajectories of smart phone users over different layers of the transportation network. To the extent of our knowledge, this is the first attempt that considers a multimodal transportation network in an urban area and that employs wholly noisy cellular data for the mapping algorithm.

We have used different sources of open data to create the multimodal transportation network and to model the unsupervised mapping algorithm. The multimodal transportation network database is available and is running in a MongoDB server. This network covers the city of Paris metropolitan area (Ile-de-France), and will allow for conducting large scale experiments when sufficient mobility data are available.

We developed CT-Mapper, an inference algorithm that maps sparse cellular trajectories of smart phone users over the multimodal transportation network. CT-Mapper is an unsupervised algorithm: in terms of parameter estimation and also the main algorithm, no labeled data have been used. To the best of our knowledge, this is the first attempt to use an entirely unsupervised algorithm for this purpose.

To validate *CT-Mapper*, a dataset of real multimodal trajectories has been used. We have asked a group of volunteers and with the help of a French network operator, we have obtained the cellular signalization data of these individuals for a period of one month (Aug. - Sept. 2014). In parallel, another experiment has been run to collect the associated GPS data, so that it could be used as ground truth in the evaluation and validation phases.

Since there exists no similar algorithm for mapping noisy cellular data over a multimodal transportation network, we derived a baseline model by using basic assumptions of studies mentioned in the literature. Then, extensive experiments were performed to evaluate the performance of *CT-Mapper* compared to the baseline algorithm.

We also proposed *LCT-Mapper* that, in addition to mapping sparse cellular trajectories over the transportation network, infers the main transportation mode of trajectories. *LCT-Mapper* is more effective than *CT-Mapper* in real trajectory inference and it performs transportation mode classification with 85% of accuracy. *LCT-Mapper* is also suitable for large scale experiments as inference can be performed in parallel for many trajectories at a time.

Comparing the mapping results between *CT-Mapper* and *LCT-Mapper*, it was observed that despite its expected loss of mapping precision, the *LCT-Mapper* was shown to be superior to *CT-Mapper* in terms of transportation mode detection. It confirms the correctness of the compromise we make between spatial resolution and accuracy of mapping algorithm. Nevertheless, this observation deserves further investigations in future studies.

7.2 Limitations

To meet the objective of this thesis, we made several choices in terms of the methodology we applied and the usage of the data related to the research context. Despite the satisfactory results that we obtained, there are some limitations as follow:

- **Cellular Mobility Data -** Network operators are strict about using mobility data of users and specifically regarding their privacy. The privacy issue brought barriers for data collection for large scale identified users. As a result, we ended up with a small data set.

- **Data Sampling Rate -** In this study, sparse cellular trajectories with the frequency of 15 minutes were collected. In case of using cellular data with higher frequency (e.g. 5 minutes), considering the noisiness of the cellular data, obtaining higher accuracy can be expected.

- **Trajectory Length Constraints -** A direct consequence of temporal sparsity of cellular trajectories, is the constraints that it imposes on the study as short trajectories cannot be analyzed with our proposed mapping algorithm. Assuming the frequency of 15 minutes for data sampling, an individual in a car or on a train, can be relocated for distances more than 5 or 10 kilometers in a period between two consecutive time stamps. As a result this approach may not correctly retrieve short trajectories. We believe that a higher frequency of cellular data sampling can relax this constraint.

- **Noisy cellular data** - The behavior of cellular observations are not well investigated and unlike GPS localization data type, no model have been defined for cellular localization error. Since inferring the emission score from real data is highly data-dependent, we expect that emission score for the mapping algorithm can be improved with a bigger data set for cellular data.

7.3 Future Directions

Following the limitations mentioned in the previous section, we consider some directions as perspectives for this study:

- This work can be improved by using labeled data sets to improve the emission and transition scores. Since manual labeling is a strenuous task, we are interested in approaches that provide labeled data which does not require this heavy task. To do this, we offer a solution to motivate individuals to get involved in the process of data labeling. This motivation to contribution has to bring some

value to users and we believe a mobile application can be proposed to provide such a value.

- In this PhD study, we modeled and developed a tool that employed cellular mobility data, which is suitable for large scale experiments. In case of having access to a large data set of cellular mobility data, treating such a large amount of data requires developing parallel computing. Similarly, in case of using streaming data for traffic monitoring purposes, providing a near real time monitoring system dealing with streaming data becomes fundamental.

- Moreover, the thesis creates opportunities for further researches and works by raising the following questions:

  - Do people have specific preferences in using different transportation networks?
  - Are these behaviors observable from individuals inferred trajectories?
  - Can the multimodal mobility behavior of individuals help define the multimodal mobility models?

  The answers to these questions shed light on many issues regarding the multimodal mobility behavior of user in metropolitan areas. They also help future urban planning organizations to design and provide high performance traffic plans and also to efficiently develop the transportation infrastructures .

- In terms of algorithm improvement, the need for more investigation in multimodal transportation networks was one of the reasons behind my scientific visit at Alephsys Lab at the "Universitat Rovira i Virgili" of Tarragona whose activity is focused on investigating complex networks.

Thesis Contributions

- **Journal Paper**:

  F. Asgari, A. Sultan, H. Xiong, V. Gauthier, M. El-Yacoubi. *"CT-Mapper: Mapping Sparse Cellular Trajectories to Multimodal Transportation Network"*. Submitted to Computer Communications Journal.

- **Patent**:

  V. Gautheri, F. Asgari, A. Sultan, M. El Yacoubi. *"Procédé D'estimation de Trajectoires Utilisant des Données Mobiles"*. Patent number: 1562736. France. Deposed December 18, 2015

Bibliography

[1] Institut géographique national. http://www.professionnels.ign.fr/.

[2] Moves. https://www.moves-app.com/.

[3] Openstreetmap project. http://www.OpenStreetMap.org/.

[4] Detecting mobility patterns in mobile phone data from the ivory coast. *Data for Challenge D4D 2013*, 2013.

[5] A. Abadi, T. Rajabioun, and P. A.Ioannou. Traffic flow prediction for road transportation networks with limited traffic data. *IEEE TRANSACTIONS ON INTELLIGENT TRANSPORTATION SYSTEMS*, 16(2):653–662, April 2015.

[6] R. A.Becker, R. Caceres, K. Hanson, J. M. Loh, and S. U. et al. Clustering anonymized mobile call detail records to find usage groups. 2011.

[7] A. Aguiar, F. M. C. Nunes, M. J. F. Silva, P. A. Silva, and D. Elias. Leveraging electronic ticketing to provide personalized navigation in a public transport network. *IEEE TRANSACTIONS ON INTELLIGENT TRANSPORTATION SYSTEMS*, 13(1):213–220, March 2012.

[8] M. Allamanis, S. Scellato, and C. Mascolo. Evolution of a location-based online social network: Analysis and models. *IMC '12 Proceedings of the 2012 ACM conference on Internet measurement conference*, pages 145–158, 2012.

[9] Y. Altshuler, R. Puzis, Y. Elovici, S. Bekhor, and A. Sandy. Augmented betweenness centrality for mobility prediction in transportation networks. *International Workshop on Finding Patterns of Human Behaviors in NEtworks and MObility Data*, pages 1–12, September 2011.

[10] D. Balcan, V. Colizza, B. Goncalves, H. Hu, and J. J. et al. Multiscale mobility networks and the spatial spreading of infectious diseases. *PNAS*, 106(51):21484–21489, 2009.

[11] M. Barthelemy. Spatial networks. *arXiv:1010.0302*, 2010. Available online: http://arxiv.org/pdf/1010.0302v2.pdf.

[12] R. C. Basole. The value and impact of mobile information and communication technologies. *Proceedings of the IFAC Symposium, Atlanta, GA.*, 2004.

[13] R. Becker, R. Cáceres, K. Hanson, S. Isaacman, J. M. Loh, M. Martonosi, J. Rowland, S. Urbanek, A. Varshavsky, and C. Volinsky. Human mobility characterization from cellular network data. *Communications of the ACM*, 56(1):74–82, January 2013.

[14] V. D. Blondel, A. Decuyper, and G. Krings. A survey of results on mobile phone datasets analysis. Feb 2015. DOI: 10.1140/epjds/s13688-015-0046-0.

[15] D. Brockmann, L. Hufnage, and T. Geisel. The scaling laws of human travel. *Nature*, 439, January 2006.

[16] M. C.Gonzale, C. A.Hidalgo, and A.-L. Barabasi. Understanding individual human mobility patterns. *Nature*, 453, June 2008.

[17] S.-W. Cheng, C. Knauer, S. Langerman, and M. Smid. Approximating the average stretch factor of geometric graphs. *Journal of Computeational Geometry JoCG*, 3(1):132–153, 2012.

[18] A. Clauset and N. Eagle. Persistance and peridicity in a dynamic proximity network. *DIMACS workshop on Computational Methods for Dynamic Interaction Neworks*, 2007.

[19] R. Cohen and S. Havlin. *COMPLEX NETWORKS Structure, Robustness and Function*. CAMBRIDGE University Press, 2010.

[20] M. Coscia, S. Rinzivillo, and D. P. Fosca Giannotti. Optimal spatial resolution for the analysis of human mobility. *IEEE/ACM International Conference on Advances in Social Network Analysis and Mining*, 2012. DOI:10.1109/ASONAM.2012.50.

[21] B. Cs.Csajia, A. Browetc, V. Traagc, J.-C. Delvennec, E. Huensc, P. V. Doorenc, Z. Smoredae, and V. D. Blondelc. Exploring the mobility of mobile phone users. *Statistical Mechanics and its Applications*, 392:1459–1473, November 2012.

[22] C.Y.Goh, J. Dauwels, N. Mitrovic, M. T. Asif, A. Oran, and P. Jaillet. Online map-matching based on hidden markov model for real-time traffic sensing application. *Intelligent Transportation Systems (ITSC)*, pages 776–781, Sept. 2012. DOI: 10.1109/ITSC.2012.6338627.

[23] S. Dasgupta, C. Papadimitriou, and U. Vazirani. *Algorithms*, chapter 6, pages 169–199. McGraw-Hill, 2006.

[24] V. D.Blondel, M. Esch, C. Chan, F. Clerot, P. Deville, E. Huens, F. Morlot, Z. Smoreda, and C. Ziemlicki. Data for development: The d4d challenge on mobile phone data. 2012.

[25] S. Derrible. Network centrality of metro systems. *PlosONE*, 7(7), July 2012.

[26] L. P. S. R. D. T.-P. Dirk Koschutzki, Katharina Anna Lehmann and O. Zlotowski. *Chapter 3:Centrality Indices*. Springer-Verlag Berlin Heidelberg, 2005.

[27] M. C. Dmytro Karamshuk, Chiara Boldrini and A. Passarella. Human mobility models for opportunistic networks. *Communications Magazine, IEEE*, 49:157–165, 2011.

[28] M. D. Domenico, V. Nicosia, A. Arenas1, and V. Latora. Structural reducibility of multilayer networks. *Nat. Commun.*, 6:6864, 2015. doi: 10.1038/ncomms7864.

[29] M. D. Domenico, A. Sole-Ribalta, E. Cozzo, M. Kivela, Y. Moreno, M. A. Porter, S. Gomez, and A. Arenas. Mathematical formulation of multilayer networks. *Physical Review*, 3, 2013. DOI: 10.1103/PhysRevX.3.041022.

[30] J. Doyle, P. Hung, D. Kelly, S. McLoone, and R. Farrell. Utilising mobile phone billing records for travel mode discovery. *22nd IET Irish Signals and Systems Conference, ISSC*, June 2011.

[31] R. Ganti, M. Srivatsa, A. Ranganathan, and J. Han. Inferring human mobility patterns from taxicab location traces. *UbiComp '13 Proceedings of the 2013 ACM international joint conference on Pervasive and ubiquitous computing*, pages 459–468, 2013. http://dx.doi.org/10.1145/2493432.2493466.

[32] T. Garske, H. Yu, and Z. P. et al. Travel patterns in china. *PLoS ONE*, 6(2), Feb 2011. 10.1371/journal.pone.0016364.

[33] F. Giannoti, M. Nanni, F. Pinelli, and D. Pedreschi. Trajectory pattern mining. *Proceedings of the 13th ACM SIGKDD international conference on Knowledge discovery and data mining*, pages 330–339, 2007.

[34] F. Giannotti, M. Nanni, and D. Pedreschi. Unveiling the complexity of human mobility by querying and mining massive trajectory data. *The international Journal on Very Large Data Bases*, July 2011.

[35] F. Giannotti, L. Pappalardo, D. Pedreschi, and D. Wang. A complexity science perspective on human mobility, 2012. Available online in http://www.dashunwang.com/pdf/2012-mobilityBook.pdf.

[36] M. C. Gonzalez, F. Simini, and A. M. andAlbert Laszlo Barabasi. A universal model for mobility and migration patterns. *Nsture*, 484:96–100, 2012.

[37] P. Grindrod, M. C. Parsons, D. J. Higham, and E. Estrada. Communicability across evolving networks. *Physical Review*, 83:046120, 2011.

[38] P. Holme. Congestion and centrality in traffic flow on complex network. *Advances in Complex Systems*, 06:163–176, June 2003. DOI: 10.1142/S0219525903000803.

[39] P. Holme and J. Saramaki. Temporal networks. *Physics Reports*, 519:97–125, October 2012.

[40] T. Hossmann, T. Spyropoulos, and F. Legendre. A complex network analysis of human mobility. *3rd IEEE International Workshop on Network Science for Communication Networks*, April 2011.

[41] C. Hu, W. Chen, Y. Chen, and D. Liu. Adaptive kalman filtering for vehicle navigation. *Journal of Global Positioning Systems*, 2(1):42–47, 2003.

[42] X. Huang and J. Tan. Understanding spatio-temporal mobility patterns for seniors, child/student and adult using smart card data. *ISPRS - International Archives of the Photogrammetry, Remote Sensing and Spatial Information Sciences*, XL-1:167–172, 2014.

[43] P. Hui and J. Crowcrof. Human mobility models and opportunistic communication system design. *Mathematical, Physical and Engineering Sciences*, 336(1872):2005–2016, 2008.

[44] B. Hummel. Map matching for vehicle guidance, in dynamic and mobile gis: Investigating changes in space and time. 2006.

[45] T. Hunter, T. Moldovan, M. Zaharia, S. Merzgui, J. Ma, M. J. Franklin, P. Abbeel, and A. M. Bayen. Scaling the mobile millennium system in the cloud. *Proceedings of the 2nd ACM Symposium on Cloud Computing - SOCC '11*, pages 1–8, 2011.

[46] S. Isaacman, R. Becker, R. Caceres, and M. M. et al. Human mobility modeling at metropolitan scales. *MobiSys*, June 2012.

[47] Z.-Q. Jiang, W.-J. Xie, M.-X. Li, and B. P. et al. Calling patterns in human communication dynamics. *PNAS*, 110(5):1600–1605, January 2013.

[48] H.-H. Jo, M. Karasai, J. Karikiski, and K. Kaski. Spatiotemporal correlation of handset-based service usages. *EPJ Data Science*, 1(10), 2012.

[49] M. Kakihara and C. Sorensen. Expanding the 'mobility' concept. *SlGGROUP Bulletin*, 22(3), 2001.

[50] C. Kang, S. Sobolevsky, Y. Liu, and C. Ratti. Exploring human movements in singapore: A comparative analysis based on mobile phone and taxicab usages. *Proceedings of the 2nd ACM SIGKDD International Workshop on Urban Computing*, Audust 2013. doi:10.1145/2505821.2505826.

[51] J. Krumm. Inference attacks on location tracks. *Proceedings of the 5th international conference on Pervasive computing*, pages 127–143, 2007.

[52] R. Kumar and J. Saramaki. Path lengths, correlations, and centrality in temporal networks. *Phys. Rev. E 84*, 2011.

[53] K. Lerman, R. Ghosh, and J. H. Kang. Centrality metric for dynamic networks. *MLG '10 Proceedings of the Eighth Workshop on Mining and Learning with Graphs*, pages 70–77, 2010.

[54] L. Liu. *Data Model and Algorithms for Multimodal Route Planning with Transportation Networks*. PhD thesis, Technical University of Munich (TUM), January 2011.

[55] M. Y. Mun, D. Estrin, J. Burke, and M. Hansen. Parsimonious mobility classification using gsm and wifi traces. *HotEmNets'08, ACM*, January 2008.

[56] R. V. Nes. *Design of multimodal transport networks : a hierarchical approach*. PhD thesis, Technical University of Delft (DUP), January 2002.

[57] M. E. J. Newman. The structure and function of complex networks. 2003.

[58] P. Newson and J. Krumm. Hidden markov map matching through noise and sparseness. *Proceedings of the 17th ACM SIGSPATIAL International Conference on Advances in Geographic Information Systems*, pages 336–343, 2009. DOI: 10.1145/1653771.1653818.

[59] A. Noulas, alvatore Scellato, R. Lambiotte, M. Pontil, and C. Mascolo. A tale of many cities: Universal patterns in human urban mobility. *PLoS ONE*, 7(5), May 2012. doi:10.1371/journal.pone.0037027.

[60] J. P.Bagrow and Y.-R. Lin. Mesoscopic structure and social aspects of human mobility. *PLoS ONE*, July 2012. DOI: 10.1371/journal.pone.0037676.

[61] U. N. W. U. Prospects. Worlds population increasingly urban with more than half living in urban areas. https://www.un.org/development/desa/en/news/population/world-urbanization-prospects.html, 2014. [access: 10 Jul. 2015].

[62] G. Ranjan, H. Zang, Z.-L. Zhang, and J. Bolot. Are call detail records biased for sampling human mobility? *ACM SIGMOBILE Mobile Computing and Communications Review*, pages 33–44, July 2012. doi:10.1145/2412096.2412101.

[63] S. Reddy, M. Mum, and J. Burke. Using mobile phones to determine transportation modes. *ACM Transactions on Sensor Networks*, 6(2), February 2010. DOI 10.1145/1689239.1689243.

[64] M. B. Ricardo Galloti. The multilayer temporal network of public transportat in great britain. 2015. cea-01119006.

[65] M. Rosvall, A. Trusina, P. Minnhagen, and K. Sneppen. Networks and cities: An information perspective. *Phys. Rev. Lett.*, 94:028701, Jan 2005.

[66] D. Schulz, S. Bothe, and C. Korner. Human mobility from gsm data - a valid alternative to gps? *Proceeding paper at Nokia Mobile Data Challenge*, June 2012.

[67] H. G. Schuster and D. Brockmann. *Reviews of Nonlinear Dynamics and Complexity,*. John Wiley & Sons, July 2010. ISBN: 978-3-527-40729-3.

[68] Siu-erman and M. Smid. Space-efficiency for routing schemes of stretch factor three. *Journal of Parralel and Distributed Computing*, 61:679–687, 2001.

[69] Z. Smoreda, A.-M. Olteanu-Raimond, and T. Couronne. Spatiotemporal data from mobile phones for personal mobility assessment. *International conference on transport survey Methods: Scoping the Future while Staying on Track*, pages 745–767, 2013.

[70] K. Sneppen, A. Trusina, and M. Rosvall. Hide-and-seek on complex networks. *EPL (Europhysics Letters)*, 69(5):853, 2005.

[71] E. Strano, S. Shai, S. Dobson, and M. Barthelemy. Multiplex networks in metropolitan areas: generic features and local effects. *The Royal Socierty Interface*, September 2015. DOI: 10.1098/rsif.2015.0651.

[72] A. Sultan, F. Benbadis, V. Gauthier, and H. Afifi. Mobile data network analysis platform. *HotPlanet, 6th International Workshop on Hot Topics in Planet-Scale Measurement*, 2015.

[73] L. Sun, K. W. Axhausen, D.-H. Lee, and X. Huang. Understanding metropolitan patterns of daily encounters. *PNAS*, 110(34):13334–13779, Aug. 2013. DOI: 10.1073/pnas.1306440110.

[74] L. Sun, D.-H. L. A. Erath, and X. Huang. Using smart card data to extract passenger's spatio-temporal density and train's trajectory of mrt system. *Urb-Comp '12 Proceedings of the ACM SIGKDD International Workshop on Urban Computing*, pages 142–148, 2012. DOI: 10.1145/2346496.2346519.

[75] L. Sun, J. G. Jin, K. W. Axhausen1, D.-H. Lee, and M. Cebrian. Quantifying long-term evolution of intra-urban spatial interactions. *The Royal Society Interface*, 12 (102), 2014. DOI: 10.1098/rsif.2014.1089.

[76] J. Tang, M. Musolesi, C. Mascolo, and V. Latora. Temporal distance metrics for social network analysis. *in Proceedings of the 2nd ACM SIGCOMM Workshop in online Social Networks (WOSN09)*, 2009.

[77] J. Tang, M. Musolesi, C. Mascolo, and V. Latora. Characterising temporal distance and reachability in mobile and online social networks. *ACM SIGCOMM Computer Communication Review*, pages 118–124, 2010.

[78] J. Tang, M. Musolesi, C. Mascolo, V. Latora, and V. Nicosia. Analysing information flows and key mediators through temporal centrality metrics. *In Proceedings of 3rd Workshop on Social Network Systems (SNS)*, April 2010.

[79] A. Thiagarajan, L. Ravindranath, H. Balakrishnan, S. Madden, and L. Girod. Accurate, low-energy trajectory mapping for mobile devices. *NSDI'11 Proceedings of the 8th USENIX conference on Networked systems design and implementation*, 2011.

[80] A. Thiagarajan, L. Ravindranath, K. LaCurts, S. Toledo, and J. Eriksson. Vtrack: Accurate, energy-aware road traffic delay estimation using mobile phones. *SenSys 09*, November 2009.

[81] H. Wang, F. Calabrese, G. D. Lorenzo, and C. Ratti. Transportation mode inference from anonymized and aggregated mobile phone call detail records. *13th International IEEE Anual Conference on Intelligent Transportation Systems*, 2010.

[82] H. Wang, H. Su, K. Zheng, S. Sadiq, and X. Zhou. An effective study on trajectory similarity measures. *Proceeding of the Twenty-Fourth Australasian Database Conference (ADC)*, 2013.

[83] P. Wang, T. Hunter, A. M. Bayen, K. Schechtner, and M. C. González. Understanding road usage patterns in urban areas. *Scientific Reports*, 2(101), December 2012. doi:10.1038/srep01001.

[84] Y. Xiao-Yang, H. Xiao-Pu, Z. Tao, and W. Bing-Hong. Exact solution of gyration radius of an individual's trajectory for a simplified human regular mobility model. *Chiniese Physics Letter*, 28(12):120506–1, 2011.

[85] H. Xu, H. Liu, C.-W. Tan, and Y. Bao. Development and application of a kalman filter and gps error correction approach for improved map matching. *Journal of Intelligent Transportation Systems*, 14(1):27–36, 2010.

[86] X.-Y. Yan, X.-P. Han, B.-H. Wang, and T. Zhou. Diversity of individual mobility patterns and emergence of aggregated scaling laws. *Scientific Reports*, 3, September 2013. doi:10.1038/srep02678.

[87] J. Yuan, Y. Zheng, and X. Xie. Discovering region of different functions in a city using human mobility and pois. *ACM KDD '12*, pages 186–194, 2012.

[88] M. Zhao, L. Mason, and W. Wang. Empirical study on human mobility for mobile wireless networks. *Military Communications Conference. MILCOM 2008. IEEE*, November 2008.